Universitatea Transilvania din Brașov

INTERDISCIPLINARY DOCTORAL SCHOOL

Faculty of Electrical Engineering and Computer Science

Ing. Vlad COJANU

Monitoring and control of performance indicators in the urban drinking water supply system

Monitorizarea și controlul indicatorilor de performanță din sistemul urban de alimentare cu apă potabilă

SUMMARY

Scientific Supervisor:

Prof. dr. ing. Elena HELEREA

BRAȘOV, 2025

Acknowledgements

First and foremost, I would like to express my profound gratitude to my PhD supervisor, Professor Elena HELEREA, PhD, for her perseverance, professionalism, and outstanding competence demonstrated throughout the entire period of research and writing of this doctoral thesis. I am sincerely thankful for her patience, scientific rigor, and continuous guidance provided in all stages: from the development of the conceptual framework and the conduct of experiments, to the writing and dissemination of the results. Her academic rigor, interdisciplinary vision, and extensive experience in engineering have been an essential support in the development of this work. Her rigorous approach and encouragement of an interdisciplinary scientific methodology have significantly contributed to my intellectual and professional progress.

I extend my special thanks to the members of the scientific advisory committee: Professor Gheorghe MANOLEA, PhD, Professor Aurel FRATU, PhD, Professor Paul BORZA, PhD, and Senior Lecturer Marius Daniel CALIN, PhD, for their valuable scientific suggestions, constructive feedback, and willingness to support the improvement of this thesis entitled *"Monitoring and Control of Performance Indicators in Urban Potable Water Supply Systems."* Their critical insights and recommendations have contributed substantially to the consolidation of the methodological and experimental foundation of the research.

I also express my sincere appreciation to all those who supported the implementation of the measurement campaigns, which were essential to this research. I thank the economic operators in the water and wastewater sector for their institutional openness and professional collaboration, the technical and operating personnel for their logistical support and field availability, as well as my colleagues from the Faculty of Electrical Engineering and Computer Science and from other faculties of the Transilvania University of Brașov, for their assistance in configuring, installing, and monitoring the experimental systems. The contributions of these collaborators were indispensable for the collection and validation of the data necessary to strengthen the experimental basis of this work.

I equally thank all co-authors involved in the scientific papers published during the doctoral period. Their valuable contributions supported the collective effort to disseminate the results and had a direct impact on the quality and visibility of the undertaken research.

Finally, I express my deepest gratitude to my family for their unconditional emotional support, understanding, patience, and constant encouragement, even during difficult moments or in the face of inherent research challenges. Without their moral and emotional support, this endeavor could not have been brought to completion.

The doctoral research represented a complex experience, characterized by significant scientific challenges as well as by profound intellectual fulfillment. It has been a formative process of professional maturation through which I acquired in-depth knowledge and established lasting academic collaborations. To all those who have contributed directly or indirectly to the realization of this thesis, I extend my sincere thanks and deepest appreciation.

Vlad COJANU

CONTENT

1. Introduction

1.1. Rationale and Justification of the Thesis

In the context of accelerated urbanization, increasing pressure on natural resources, and climate change, urban drinking water supply systems must ensure reliability, sustainability, and energy efficiency. These systems represent critical infrastructure, essential for public health and the coherent functioning of the urban environment.

The energy transition and the principles of sustainable development require a reconceptualization of how such systems are managed, with a focus on integrating renewable sources, digitization, and optimizing resource consumption. Monitoring performance indicators becomes a central tool in this process, particularly in evaluating the water–energy nexus.

Pumping systems, as the largest energy consumers within water supply infrastructures, require accurate assessments of their energy intensity and operational efficiency. Analyzing these parameters enables functional optimization and cost reduction.

This research project is aligned with the Horizon Europe Programme (2021–2027), aiming to develop advanced technological solutions for intelligent and sustainable infrastructures, with industrial applicability and strategic relevance at the European level.

1.2. Aim and Objectives of the Thesis

In this complex context, the present doctoral thesis aims to contribute to the optimization of performance in urban drinking water supply systems through advanced monitoring and control of performance indicators, with a particular focus on energy efficiency and the critical interdependence between water and energy resources.

The general objective of this work is to improve the performance of urban drinking water supply systems during the energy transition period, in order to support integrated efforts toward achieving the goals of sustainable development.

This objective is pursued through a rigorous scientific approach, grounded in systemic analysis, operational modeling, and the integration of digital solutions for the control and optimization of critical water infrastructure.

To achieve this general objective, the research has been structured around four major specific objectives:

Specific Objective 1: To determine the technical, functional, and operational characteristics of the urban water supply system as part of critical infrastructure and to analyze the dynamic relationship between water and energy.

Specific Objective 2: To develop and implement a monitoring system for performance and operational safety indicators, through the integration of SCADA technology.

Specific Objective 3: To formulate strategies for increasing the energy efficiency of the main energy consumers within the urban water system, especially pumping stations.

Specific Objective 4: To improve the integrated management of the water supply system by strengthening its interconnection with other critical infrastructures, particularly in relation to emergency response (e.g., firefighting).

1.3. Research Methodology

The research integrated both theoretical and experimental components within a scientific approach based on systemic analysis and operational modeling, aiming to evaluate the energy performance of urban drinking water supply systems, with a particular focus on pumping subsystems.

This approach enabled the validation of hypotheses using experimental data obtained under real operating conditions, within two systems managed by local operators in the municipality of Brașov.

The theoretical component included an extensive review of national and international literature on the water–energy nexus, the efficiency of pumping processes, methodologies for evaluating hydraulic performance, and the relevance of water infrastructure in the urban context. Various computational models, standards, and regulations related to energy efficiency were analyzed.

The experimental part was carried out in collaboration with technical teams of the operators, involving direct measurements and the adaptation of the methodology to the operational realities of the systems. Data validation was supported by ongoing interaction with the advisory committee and key decision-makers, contributing to methodological optimization and enhancing the practical relevance of the research.

The study was conducted within an interdisciplinary doctoral program and provided a solid foundation for the development of a standardized methodology for energy evaluation, aimed at identifying effective strategies for optimizing consumption in pumping subsystems, in line with current objectives for sustainability and resilience of critical infrastructure.

1.4. Thesis Structure

The doctoral thesis is organized into five chapters and includes 81 figures, 25 tables, and 123 bibliographic references.

Chapter 1: “Introduction” presents the scientific motivation, the overall aim, and the specific objectives of the research, all framed by the energy transition, climate change, and rising urban demand. It details the mixed methodology—both theoretical (analysis of the water–energy nexus and emerging technologies) and experimental (field monitoring and validation).

Chapter 2, “Analysis of urban water supply systems,” describes water infrastructure from a historical, technological, and environmental perspective. Functional components and requirements for efficiency, quality, and safety are described. The water-energy nexus is highlighted through analytical models such as the Mega-System Model. The chapter also includes an analysis of strategic directions in environmental policy and energy transition.

Chapter 3, “Contributions to monitoring and control in urban water supply systems,” proposes a theoretical and practical framework for integrating modern automation technologies and assessing system performance. Eleven energy indicators (EI1–EI11) are defined and SCADA functionalities are described, including architectural evolution and cybersecurity requirements. Three case studies in the municipality of Brașov validate the proposed framework.

Chapter 4, “Contributions to increasing energy efficiency in water pumping stations,” details the technical and economic analysis of the Măgurele pumping station. It substantiates the need for a predictive model for optimizing energy consumption. Pump performance curves, electrical component efficiencies, and energy losses are examined. A practical application using 2024 SCADA data identifies intervals of low efficiency and proposes technological optimization measures.

By integrating the theoretical, experimental, and applied contributions, this thesis synthesizes the findings and offers concrete solutions for enhancing energy efficiency and the resilience of urban drinking water infrastructures.

1.5. Research Significance and Future Directions

Urban drinking water distribution networks represent critical infrastructures, whose energy efficiency directly impacts public health, emergency response capacity, and ecological footprint reduction. The simultaneous reduction of hydraulic losses and energy consumption in pumping stations is essential for achieving sustainable development goals.

The integration of SCADA systems with advanced monitoring, predictive modeling, and performance indicators enables real-time operational optimization by reducing specific energy consumption and water losses.

Future research directions include the application of artificial intelligence in SCADA platforms for anomaly detection, demand forecasting, and automatic pump operation control. Additionally, there is a growing

need to standardize methodologies for the continuous evaluation of energy efficiency across all system levels.

Cybersecurity and operational resilience call for redundant edge–cloud architectures, encrypted communications, and distributed data systems integrated with blockchain technology to ensure traceability and auditability. Explainable models are becoming indispensable for transparency and the validation of automated decisions.

2. Analysis of urban water supply systems

2.1. Preliminary considerations

Urban water supply systems are critical infrastructures that ensure the provision of potable water and support public safety functions, including fire suppression. Although these systems have undergone significant technological and structural advancements, they currently encounter multiple challenges, such

as the escalation of water demand, degradation of source water quality, distribution network losses, and high energy consumption. The concept of the Water-Energy Nexus highlights the interdependence between water and energy systems, promoting an integrated and holistic approach to operational optimization. This study explores modernization strategies that incorporate digital technologies—including Supervisory Control and Data Acquisition (SCADA) systems, sensor arrays, and predictive analytics—as well as the adoption of renewable energy sources. The objective is to improve system efficiency, minimize environmental impacts, and enhance the resilience and sustainability of urban water infrastructure.

2.2. Study of Water Supply Infrastructure in Human Habitations

Since antiquity, human settlements have developed in close proximity to water sources, reflecting a direct correlation between the evolution of civilizations and access to freshwater resources. The earliest centralized water supply systems in Europe date back to the Bronze Age, while the Greek and Roman civilizations constructed advanced distribution networks based on aqueducts and reservoirs, which proved to be remarkably efficient, as evidenced by recent studies, including the one dedicated to the city of Perge.

In the modern era, water supply systems transitioned toward centralized infrastructures supported by pumps, metal pipelines, and treatment plants, with development significantly accelerated by the Industrial Revolution. In Romania, hydraulic infrastructure has Dacian origins, later expanded during the Roman period. By the 19th century, cities such as Bucharest and Brașov had implemented modern water networks, which have continued to expand over time. Currently, the city of Bucharest is served by three main water treatment plants equipped with advanced treatment technologies.

Contemporary systems, automated through SCADA platforms and Internet of Things (IoT) technologies, offer enhanced operational efficiency. However, they are increasingly exposed to energy-related and cybernetic vulnerabilities, which necessitate sustainable management practices and continuous investment to ensure reliable and safe access to drinking water.

2.3. Analysis of the Specific Characteristics of Modern Urban Water Supply Systems

Modern water supply systems are functionally integrated networks designed to ensure the continuous provision of potable water intended for human consumption and food-related uses. These systems support public health, urban hygiene, industrial processes, and fire safety by maintaining the necessary pressure and flow rates within firefighting networks. Due to their essential role in urban infrastructure, they contribute significantly to community resilience and the reliable operation of vital public services.

Moreover, such networks foster social cohesion and urban security, thereby justifying the need for strategic planning, preventive maintenance, and sustained investment, in alignment with the principles of sustainable development and risk management. Urban drinking water supply systems encompass all interconnected components responsible for the production, treatment, conveyance, and distribution of water to consumers within a defined urban area [12].

The fundamental requirements for the design and operation of an urban water supply system are systematically presented in Table 2.1.

Table 2.1. Fundamental Requirements for Urban Water Supply Systems

No.	Requirement	Description
1	Provision of an adequate source	A reliable, sustainable, and sufficient water source capable of meeting the consumption needs of the urban population.
2	Compliance with water quality	Elimination of physical, chemical, and biological contaminants to meet public health standards.
3	Continuity of water supply	Continuous availability of water, including during peak demand periods and emergency situations.
4	Efficiency	Minimization of water and energy losses through modern infrastructure, active monitoring, and preventive maintenance.

No.	Requirement	Description
5	Sustainability of resource use	Responsible exploitation of water resources without compromising natural reserves or aquatic ecosystems.
6	Resilience to external factors	System's capacity to operate under extreme conditions such as earthquakes, floods, droughts, technical failures, or cyberattacks.
7	Integration of modern technologies	Deployment of intelligent systems (e.g., SCADA, IoT) for real-time monitoring, efficient control, and operational adaptability.
8	Equitable access for all users	Guaranteeing access to potable water regardless of geographic location or socio-economic status, promoting equity and social inclusion.

A sustainable water supply system must balance the increasing demand of the urban population with the availability of water resources, in accordance with the Dublin Principles and the Brundtland Report. Emphasizing the importance of equitable and efficient access to resources, the United Nations Sustainable Development Goals (SDGs) support this endeavor. The integration of sustainability entails reducing energy consumption and adopting technical, economic, and environmental solutions tailored to local conditions. Water supply systems thereby function as critical infrastructures, managing the processes of abstraction, treatment, conveyance, and distribution in an efficient manner (Fig. 2.3).

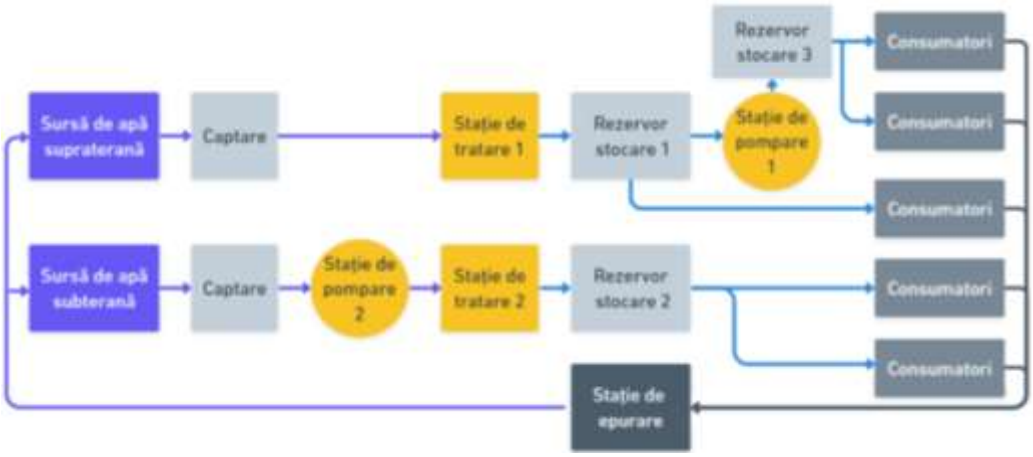

Fig. 2.3. Block Diagram of an Urban Water Supply System

The urban water supply system comprises integrated processes that ensure the continuous and safe abstraction, treatment, storage, and distribution of potable water. Water is abstracted from either surface or groundwater sources, followed by sequential treatment of the raw water—typically including coagulation, filtration, and disinfection—in order to comply with drinking water quality standards. Distribution is carried out through automated networks, with intermediate storage in balancing reservoirs to ensure pressure stability and supply continuity. In addition to its primary function, the system supports public safety by supplying hydrants for firefighting purposes.

2.4. Current Challenges in the Field of Water Supply

Urban water supply systems are essential to the sustainability of cities, yet they face significant challenges such as aging infrastructure, unevenly increasing demand, and low energy efficiency. These issues are further exacerbated by climate change and demographic pressure [17], [19]. More than 2.2 billion people still lack access to safe drinking water [18], while rapid urbanization contributes to increased water losses within distribution networks and the degradation of water quality [20]. Additionally, over-abstraction and agricultural pollution are leading to declining groundwater levels and contamination of freshwater resources [21], [23].

Aquatic ecosystems are experiencing significant biodiversity losses due to hydrological imbalances and pollution [24], [25], with extreme climatic events intensifying these effects [22]. Moreover, social

inequalities and underdeveloped infrastructure in rural areas necessitate the adoption of sustainable and resilient water resource management models [26], [27].

Water losses and theft in urban networks, which can reach up to 30% of the total volume conveyed, result in a substantial increase in energy consumption—by as much as 30% [28]. Sustainable water resource management requires an integrated approach that incorporates innovative technologies such as desalination, wastewater treatment, and the application of artificial intelligence for real-time monitoring and network optimization [29]. The success of these interventions depends on coherent public policies, sustained investment, and population education [27].

In the context of climate pressures and accelerated urbanization, complex interventions are needed to ensure equitable water access, proper wastewater management, and the prevention of waterborne diseases [30], [31]. Therefore, effective and resilient solutions, coupled with responsible governance, are critical to safeguarding water as a strategic resource and ensuring long-term sustainability.

2.5. Energy Analysis of Urban Water Supply Systems

Urban water supply systems are intrinsically linked to the energy sector, as the processes of water abstraction, treatment, and distribution require substantial energy inputs. This interdependence, defined by the concept of the Water-Energy Nexus (WEN), has a direct impact on the sustainability of urban infrastructure. The present section examines the evolution of water and energy consumption, introduces relevant conceptual models, and identifies the key determinants of this relationship, emphasizing the importance of sustainable solutions and emerging technologies in enhancing the efficiency of these systems.

2.5.1. Evolution of Water and Energy Demand and Consumption

Global water and energy consumption have increased significantly as a result of urbanization, economic development, and industrial expansion, thereby intensifying the pressure on natural resources and infrastructure systems. The analysis of the water–energy interdependence provides insights into the sustainable use of these resources [32]. Between 1901 and 2014, global water consumption rose from under 1 trillion cubic meters to approximately 4 trillion cubic meters, accompanied by a marked increase in energy use, particularly in Asia, where fossil fuels remain the dominant energy sources.

The water–energy interdependence is bidirectional: water is essential for energy production (e.g., cooling in thermal power plants, hydropower generation), while energy is required for water abstraction, treatment, and distribution. This relationship reflects a structural dependency between the two sectors, with significant implications for long-term sustainability. In 2023, global energy consumption surpassed 15,000 million tonnes of oil equivalent, still dominated by conventional sources such as oil, coal, and biomass.

Urbanization, through high population densities and increased service demands, accounts for approximately 45–55% of global energy consumption [33]. Climate change exacerbates the imbalances between resource demand and availability, posing additional challenges to existing infrastructure systems. By 2050, global energy demand is projected to increase by 50%, along with intensified water abstraction, particularly in developing countries [35].

To effectively manage the water–energy nexus, the adoption of advanced technologies is essential. These include renewable energy integration, high-efficiency pumping systems, smart water networks, and energy recovery solutions [36]. Such approaches contribute to reducing resource consumption, limiting system losses, and protecting environmental integrity, thereby supporting the implementation of a sustainable resource management model.

2.5.2. Integrated Models for Describing the Dependency Between Water and Energy Consumption

he water–energy interaction is influenced by factors such as population growth, urbanization, economic development, and climate change, all of which affect resource availability and energy production—particularly under drought conditions [37]. To better understand and optimize this relationship, analytical models have been developed, such as the Mega-System Model, which conceptualizes water and energy

infrastructures as globally integrated and interdependent systems. This model incorporates socio-economic, climatic, and technological variables to simulate systemic interactions [38]. The outputs derived from such simulations allow for the anticipation of vulnerabilities and the formulation of sustainable strategies, particularly in the context of diminishing water resources.

Complementary to these models, intelligent systems equipped with sensors and artificial intelligence enable real-time monitoring and optimization of resource consumption. Additionally, water–energy microgrids facilitate the integration of renewable energy sources and enhance the operational efficiency of urban infrastructure [39]–[41].

The water–energy relationship necessitates the implementation of integrated management solutions focused on sustainability and resilience. The use of advanced cooling technologies in thermoelectric power plants significantly reduces water withdrawal, while the transition toward renewable energy sources mitigates pressure on hydrological systems by eliminating the water requirements inherent to conventional energy generation processes. As such, the adoption of renewable energy becomes a critical strategy for reducing water consumption and fossil fuel dependency [37].

In this context, advanced modeling approaches for managing the water–energy nexus provide an essential analytical framework for supporting decision-making processes concerning critical infrastructure systems (Fig. 2.10).

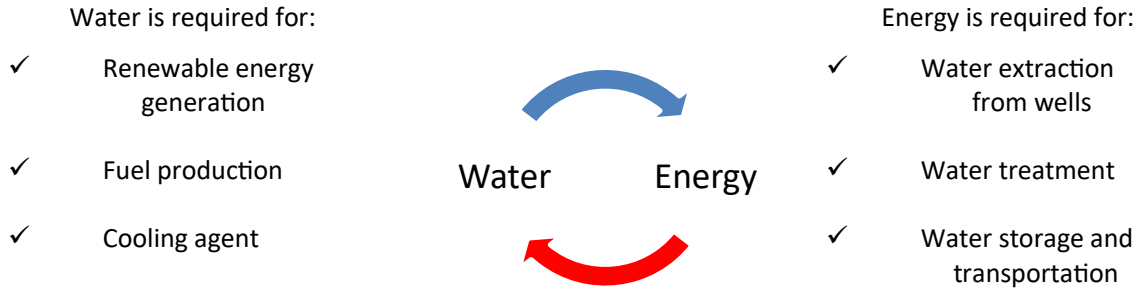

Fig. 2.10. The Bidirectional Relationship Between Water and Energy

A multidimensional approach to the water–energy connection enables the development of innovative technological solutions aimed at reducing water losses and optimizing resource consumption. The integration of energy microgrids with water distribution systems provides the means to balance supply and demand in a sustainable and adaptive manner.

A relevant applied example is the use of virtual energy storage units within water distribution networks, where pumps and reservoirs are intelligently managed to balance consumption fluctuations and alleviate stress on the electrical grid [42].

In conclusion, the water–energy nexus constitutes a fundamental pillar of sustainable development. The models analyzed offer complementary perspectives: the Mega-System Model enables integrated assessment of interrelations among water, energy, and land use; smart systems optimize consumption through digital technologies; and integrative models support sustainable management in both urban and industrial contexts. The implementation of advanced technologies and strategies derived from these models is essential for minimizing ecological impact and enhancing energy resilience.

2.5.3. Analysis of the Factors Influencing the Water–Energy Nexus

Rapid urbanization and city expansion intensify the demand for water and energy, thereby increasing pressure on urban infrastructure systems. In this context, efficient resource management, reduction of losses, and optimization of energy consumption become essential.

The expansion of built-up areas and increased population density result in elevated water consumption for domestic, industrial, and municipal purposes, which is closely associated with a heightened energy demand for powering households and urban infrastructure. These combined pressures contribute to the rise in greenhouse gas emissions and the degradation of water quality through the discharge of untreated

wastewater, contamination of sources with chemical pollutants, and the diminished self-purification capacity of aquatic ecosystems due to reduced flow rates.

Moreover, the intensification of anthropogenic activities increases reliance on non-renewable resources, further exacerbating the vulnerability of urban water and energy systems [39]. The key driving factors of this interaction are synthesized in Fig. 2.12 [39].

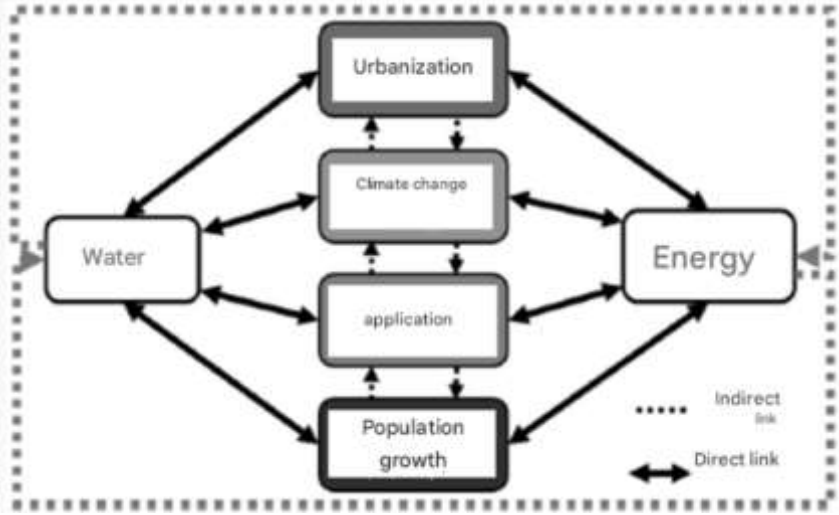

Fig. 2.12. Factors Affecting the Water–Energy Nexus

Climate change exacerbates imbalances within the water–energy nexus by inducing variability in precipitation patterns, increasing the frequency of extreme temperature events, and intensifying severe weather phenomena. These impacts directly affect the availability of water resources, thereby influencing hydropower production and the performance of cooling processes in thermoelectric power plants [43].

Rapid urbanization and demographic growth further increase pressure on existing infrastructure, necessitating the adoption of efficient technological solutions. The use of Pumps as Turbines (PATs) and District Metered Areas (DMAs) enables energy recovery and reduction of water losses within distribution networks [44], while microgrids based on renewable energy sources help reduce dependence on fossil fuels [45].

Smart technologies, including Artificial Intelligence (AI) and the Internet of Things (IoT), allow for real-time monitoring and autonomous control of resource flows, thereby improving operational efficiency [46]. Leak detection and adaptive consumption management are critical for minimizing waste and enhancing system performance [39].

Urban governance plays a key role in supporting a circular and sustainable model through energy efficiency policies, water reuse strategies, and public–private partnerships [47].

In this context, an integrated approach to the water–energy nexus—centered on sustainability, efficiency, and resilience—is essential. Solutions such as Life Cycle Assessment (LCA), WEN-based microgrids, and infrastructure modernization through DMAs and IoT sensor networks [38], [42], [44] are instrumental in fostering adaptive and balanced urban development aligned with the principles of sustainable development [44], [47].

2.6. Analysis of Environmental Policies and the Energy Transition

Urban water supply systems are increasingly subject to pressures arising from climate change, accelerated urbanization, aging infrastructure, and growing sustainability requirements. Efficient management of these systems necessitates an integrated approach that combines environmental policies, advanced technologies, and energy transition strategies, including the use of renewable energy sources, digitalization (IoT, artificial intelligence), and wastewater recycling [46], [49], [50].

Decentralized and hybrid models—such as the case study from Funchal—demonstrate the viability of energy self-sufficiency through the exploitation of local resources (e.g., photovoltaic, micro-hydropower, biogas) [63]. In order to reduce water losses, energy consumption, and greenhouse gas emissions, solutions such as intelligent pressure control, district metering, green infrastructure, and smart networks are required. These systems must be supported by predictive models and advanced climate scenarios [39], [62], [64].

In this context, the integration of renewable energy into hydrotechnical infrastructure, the promotion of circular economy principles, and the application of multi-objective optimization technologies contribute directly to the achievement of the Sustainable Development Goals (SDGs 6 and 7) [60], [65].

Intersectoral governance, cross-border collaboration, and public–private partnerships are essential for protecting resources, ensuring equitable access, and building a sustainable and resilient urban model [61], [66]. The energy transition of water systems thus emerges as a strategic priority in the face of global urbanization and climate crises.

2.7. Conclusions

(1) Urban water supply systems are facing increasingly complex challenges, driven by accelerated urbanization, climate change, and growing pressure on natural resources. In this context, the modernization of critical infrastructure and the adoption of sustainable management strategies have become imperative.

(2) The interdependence between water and energy, analyzed through the Water–Energy Nexus framework, underscores the need for integrated management. Energy is indispensable for the processes of water abstraction, treatment, and distribution, while water plays a fundamental role in energy production processes. Conceptual models such as the Mega-System and WEN Smart Systems, complemented by Life Cycle Assessment (LCA) evaluations, support resource optimization and reduction of ecological impact.

(3) Imbalances between supply and demand, exacerbated by climate change, increase operational risk and call for investment in digitalization, energy efficiency, and the integration of renewable energy sources. Emerging technologies—including smart grids, microgrids, advanced metering systems, and Pumps as Turbines (PATs)—enhance the efficiency and resilience of water supply systems.

(4) Environmental policies and the energy transition are essential to supporting urban sustainability, in alignment with the Sustainable Development Goals (SDGs). Collaboration among public authorities, industry, academia, and civil society is critical for implementing an adaptive and responsible urban development model.

(5) Decentralized solutions—such as local water recycling stations and autonomous energy generation systems—can alleviate pressure on centralized networks. The integration of artificial intelligence into decision-making processes facilitates risk anticipation and resource optimization, accelerating the transition toward smart and sustainable cities.

(6) The efficient management of water systems requires an integrated approach focused on optimizing the water–energy interaction. In the face of systemic vulnerabilities, the development of advanced monitoring and control mechanisms becomes essential. Modern SCADA systems and specific performance indicators can support efficient system operation, consumption reduction, and risk anticipation. The following chapter presents methodological and applied contributions dedicated to these directions, aiming to strengthen the response capacity and adaptability of urban water supply systems.

3. Contributions to Monitoring and Control in Urban Water Supply Systems

3.1. Preliminary considerations

Urban water systems are vital components of city infrastructure, responsible for the safe distribution of potable water and the management of wastewater. These systems require advanced monitoring and control solutions to ensure water quality, optimize operations, and maintain operational safety.

A strategic role of urban water networks is to support emergency interventions, particularly firefighting. By providing the required flow rates and pressure levels, the water distribution network directly contributes to public safety. System design incorporates elements such as redundancy, buffer storage tanks, and alternative sources, thereby enhancing infrastructure resilience.

This chapter is structured into three main sections. The first section outlines key performance indicators (KPIs) used to assess operational efficiency, detect malfunctions, and support optimization decisions. The second section analyzes the role of SCADA technologies in real-time monitoring and control of water networks, highlighting their contribution to safety and efficiency improvements. The final section explores modern management practices, focusing on loss reduction, improved energy efficiency, and the promotion of sustainability in water infrastructure administration.

3.2. Performance Monitoring Indicators

Performance monitoring, conducted through specific indicators, is crucial for assessing hydraulic efficiency, water losses, and operational reliability in urban water supply systems. These indicators provide utility operators and regulatory bodies with a rigorous tool for both qualitative and quantitative network analysis, supporting informed technical and managerial decision-making.

At the international level, the International Water Association (IWA) framework proposes a structured set of performance indicators covering technical, operational, financial, and service quality dimensions. Meanwhile, at the European level, WAREG (the Association of European Water Regulators) focuses on harmonizing methodologies and integrating energy-related indicators to optimize resource consumption and enhance system resilience.

As such, performance indicators have become fundamental instruments in economic regulation processes, ensuring the alignment of performance outcomes with tariff policies and promoting the long-term sustainability of public water services.

3.2.1. Integrated Performance Analysis of the System

The performance evaluation of urban water supply systems requires an integrated approach, encompassing technical, economic, environmental, and social dimensions. This approach enables the diagnosis of network functionality, identification of vulnerabilities, and support for strategic decision-making.

Energy consumption affects both operational costs and the carbon footprint. Key indicators include: Total specific energy consumption (kWh/m³), Energy consumption for pumping, CO_2 emissions associated with electricity use.

Water quality is assessed through: Microbiological parameters (e.g., E. coli), Chemical composition (nitrates, heavy metals), Physical characteristics (taste, odor, turbidity).

Operational performance is defined by: Continuity of water supply, Pressure management, Volume of non-revenue water, resulting from technical and commercial losses.

Financial sustainability involves: Cost recovery through tariffs, Efficiency of billing and collection processes, Level of infrastructure investment.

Environmental impact is determined by: Greenhouse gas emissions, Volume of abstracted water, Quality of discharged wastewater

Key indicators include: Total specific energy consumption, expressed as the energy used per unit of treated and distributed water (kWh/m³), Energy consumption related to pumping processes (kWh/m³), Carbon

dioxide (CO_2) emissions associated with electricity use (kg CO_2/kWh), Water quality is evaluated based on microbiological parameters, such as the presence of Escherichia coli (CFU/100 mL), chemical composition—including nitrate concentrations (mg/L) and heavy metals (mg/L)—as well as physical characteristics of water such as taste, odor, and turbidity (NTU).

Operational performance is assessed by continuity of supply (h/day), efficiency of pressure management (bar) within the distribution network, and volume of non-revenue water resulting from technical and commercial losses (m^3 or % of total distributed volume).

Financial sustainability includes cost recovery through applied tariffs (currency/m^3), efficiency of billing and collection (as a percentage of total monthly billings), and the level of infrastructure investment (currency/year).

Environmental impact is determined by greenhouse gas emissions (kg CO_2/year), the volume of water abstracted from natural sources (m^3/year), and the quality of discharged wastewater, evaluated based on parameters such as suspended solids concentration (mg/L) and biochemical oxygen demand (mg/L).

Social sustainability is reflected by: Population access to the water supply network, Quality of services provided to users, Degree of community involvement in decision-making processes.

The integration of these components, using multicriteria methods such as AHP (Analytic Hierarchy Process), enables a synthetic performance evaluation and supports evidence-based decision-making for improving the urban water system in the direction of sustainability.

3.2.2. Definition and Characterization of Indicator Classes

The classes of performance indicators for urban water systems provide a systematic structure for the parameters required to assess the functionality, efficiency, and impact of these systems, thereby facilitating decision-making processes in resource management.

Water quality indicators include: Microbiological quality – highlights the presence of pathogenic agents such as Escherichia coli, signaling contamination risks [70], Chemical quality – monitors contaminants such as lead, nitrates, or chlorine, originating from industrial or agricultural sources [71], Physical quality – parameters such as turbidity, color, and taste, which influence water acceptability.

Service quality indicators focus on: Continuity of supply – measures the frequency and duration of service interruptions [72], Pressure management – ensures adequate flow rates and reduces the risk of system failures [73], Response time – reflects the promptness with which user requests and incidents are resolved [79].

Operational efficiency indicators include: Volumetric losses – the proportion of produced water that is not billed, caused by physical losses or metering inaccuracies [74], Energy efficiency – quantifies energy consumption in operational processes [67], Maintenance – frequency of failures and effectiveness of corrective interventions [80].

Financial performance indicators refer to: Cost recovery – the utility's capacity to cover current expenditures and invest in infrastructure [75].

These indicators provide a coherent basis for monitoring and optimizing the performance of urban water systems, contributing to operational efficiency, sustainability, and service reliability.

Efficiency indicators for emergency response and firefighting operations

For the management of emergency situations such as fires, the urban water supply system incorporates external fire hydrants into the distribution network, designed to supply intervention equipment with pressurized water.

From the perspective of a system dedicated to firefighting, the primary objective is to ensure a flow rate and pressure level that enable rapid and effective suppression of fire outbreaks.

However, considering the increasingly frequent constraints related to the condition of urban water infrastructure—namely network losses, pressure fluctuations, and the energy consumption associated with water conveyance—there is a need for an approach that includes specific performance indicators:

- Monthly Water Consumption for Firefighting – Represents the total volume of water consumed within a one-month period for firefighting operations in the designated study area:

$$Cl_{HE} = \sum_{i=1}^{N} Vi_{zilnic} \quad (3.1)$$

where $\mathrm{Vi_{zilnic}}$ represents the daily volume of water consumed;

- Annual Water Consumption for Firefighting – Refers to the total volume of water consumed over the course of one year for firefighting purposes within the analyzed area:

$$Ca_{HE} = \sum_{i=1}^{N} Vi_{lunar} \quad (3.2)$$

where $\mathrm{Vi_{lunar}}$ represents the volume of water consumed on a monthly basis;

- Specific Consumption – Represents the monthly volume of water consumed for firefighting, normalized per 1,000 inhabitants within the studied area:

$$Cs_{HE} = \frac{Cl_{HE}}{1000} \quad (3.3)$$

where $\mathrm{Cl_{HE}}$ represents the monthly specific water consumption for firefighting;

- Maximum operating time of external fire hydrants – This is an operational indicator that expresses the theoretical duration of continuous operation for a single external fire hydrant. It is calculated based on the total monthly volume of water distributed through the external hydrant network, divided by the minimum discharge rate of a hydrant. The indicator reflects, by analogy, the number of continuous operating minutes required for a single hydrant to consume the total volume of water actually used in a given month, regardless of the actual number of hydrants simultaneously activated:

$$TMU_{HE} = \frac{\sum_{i=1}^{N} Vi_{zilnic}}{Q_{min}} \quad (3.4)$$

where $\mathrm{Q_{min}}$ represents the minimum flow rate that must be ensured.

Depending on the value of the indicator, it may be necessary to increase the number of hydrants or to implement technical measures (such as repositioning, network extension, or alternative water supply solutions) in order to ensure the required flow rate for firefighting operations, in compliance with fundamental fire safety requirements.

The implementation of such a monitoring and control system can support both the maximization of the hydraulic efficiency of the installations and the maintenance of intervention capacity under critical fire scenarios.

IWA Indicators

IWA (International Water Association) and WAREG (European Water Regulators) have developed a comprehensive methodology for evaluating urban water systems, employing performance indicators classified into six main categories and thematic sub-classes. This detailed classification, comprising 170 quantitative and qualitative indicators, facilitates performance assessment, efficient resource allocation, and evidence-based decision-making.

By covering key areas such as water resources, human resources, technical infrastructure, operational processes, user-perceived service quality, and economic and financial aspects, this methodology supports the effective, transparent, and sustainable management of water services.

The total number of indicators included in this framework is 170 (Table 3.1).

Table 3.1. Classification of Indicators According to the International Water Association (IWA)

Main Class	Subclass	Number of Indicators
1. Water Resources Indicators (WR)	-	4
2. Personnel Indicators (Pe)	Total personnel	2
	Personnel by core functions	7
	Technical personnel by activity	6
	Personnel qualifications	3
	Staff training	3
	Occupational health and safety	1
3. Physical Indicators (Ph)	Overtime	1
	Water treatment	2
	Storage	4
	Pumping	2
	Transport and distribution	4
	Metering	2
4. Operational Indicators (Op)	Automation and control	6
	Inspection and maintenance of physical assets	5
	Calibration of measurement equipment	3
	Inspection of electrical and signal transmission equipment	1
	Vehicle availability	5
	Rehabilitation of pipes, valves, and service connections	2
	Rehabilitation of pumps	7
	Operational water losses	6
	Failures	4
	Water metering	5
5. Service Quality Indicators (QS)	Water quality monitoring	5
	Service coverage	4
	Public taps and fountains	8
	Pressure and continuity of supply	5
	Quality of supplied water	3
	Connection and installation/repair of meters	9
6. Economic and Financial Indicators (Fi)	Customer complaints	3
	Revenues	3
	Costs	5
	Structure of operating costs by type	5
	Structure of operating costs by main functions	6
	Structure of costs by technical activities	2
	Structure of capital expenditures	3
	Investments	2
	Average water tariffs	9
	Efficiency	2
	Debt	1
	Liquidity	5
	Profitability	2

The IWA methodology proposes 170 indicators for the evaluation of water services; however, only a small subset of these indicators directly addresses energy consumption and efficiency, being included under the categories of Physical Indicators (Ph) and Financial Indicators (Fi). Although valuable for standardization purposes, the IWA framework may present limitations if applied rigidly, without adaptation to local specificities, potentially resulting in overregulation and inefficiencies in performance assessment.

For a more accurate analysis of energy performance, complementary indicators are frequently employed to fill the gaps left by the IWA framework and to provide a more representative view of the efficiency of water supply systems. These will be presented in the following section.

3.2.3. Energy Efficiency and Specific Indicators

In urban water systems, energy is required for the following key processes:

- Water Extraction – Pumping of groundwater or surface water to treatment facilities.
- Water Treatment – Energy-intensive processes such as filtration, chemical treatment, and desalination.
- Water Distribution – Pumping treated water to residential, commercial, and industrial consumers.
- Wastewater Collection and Treatment – Transport and treatment of wastewater prior to discharge or reuse.

Each of these stages involves specific energy demands that must be carefully managed to optimize operational efficiency, reduce greenhouse gas emissions, and support the sustainable functioning of the water supply and sanitation infrastructure.

Energy consumption constitutes a major determinant of operational costs in the management of urban water distribution systems (UWD), and the energetic optimization of pumping and distribution equipment is essential for enhancing both efficiency and sustainability [55], [67]. The integration of modern technologies, such as high-efficiency pumps, variable frequency drives (VFDs), and advanced monitoring systems, enables the reduction of energy losses and the improvement of overall system performance [67].

Lowering energy consumption directly contributes to the reduction of greenhouse gas (GHG) emissions, aligning with global climate objectives and supporting the mitigation of air pollution [71], [77]. These measures are instrumental in achieving the Sustainable Development Goals (SDGs), particularly SDG 6 – Clean Water and Sanitation, and SDG 7 – Affordable and Clean Energy [78]. They also align with the European Union's regulatory targets, which mandate at least a 55% reduction in GHG emissions by 2030 compared to 1990 levels, and a minimum 32.5% increase in energy efficiency [53].

In Eastern Europe, including Romania, infrastructure modernization projects for water systems are currently being implemented with the support of European funds. Notable examples include initiatives in Poland and Hungary [81]. To support these efforts, a set of energy performance indicators has been developed and applied in the analysis of the urban water supply system of Brașov Municipality. These indicators, presented in Table 3.2, provide a methodological framework for the continuous optimization of energy performance within the urban water sector.

Table 3.2. Specific Energy Performance Indicators

No.	Symbol	Indicator name and definition	Calculation formula
1	EI1	**Energy Intensity –** defined as the ratio between the total active energy consumed and the volume of water delivered during the analysis period; [kWh/m³]	$\mathrm{EI1} = \sum_{i=1}^{n} \frac{E_{a_i}}{V_i}$ (3.10)
2	EI2	**Standardized Energy Intensity –** represents the energy consumed per cubic meter of pumped water, normalized to a reference head of 100 meters; [kWh/m³/100 m]	$\mathrm{EI2} = \frac{E_{a_i}}{V_i \cdot \frac{H}{100}}$ (3.11)
3	EI3	**Average Active Power –** represents the mean quantity of active power utilized during the analyzed time interval Δt; [kW]	$\mathrm{EI3} = \frac{\sum_{i=1}^{n} P_{a_i}}{N}$ (3.12)

No.	Symbol	Indicator name and definition	Calculation formula
4	EI4	**Maximum Active Power** – represents the peak value of active power consumed during the analyzed period; [kW]	$\mathrm{EI4} = \max(P_{a_1}, \ldots, P_{a_i})$ (3.13)
5	EI5	**CO_2 Emissions –** represent the total quantity of CO_2 released as a result of energy consumption, calculated using the standard emission factor ef, which for Romania is currently estimated at approximately 0.232 [$kgCO_{2e}$/kWh]*	$\mathrm{EI5} = E_{a_t} \cdot ef$ (3.14)
6	EI6	**Reactive Energy Intensity** – defined as the ratio between the reactive energy consumed and the volume of water delivered during the analyzed period; [kVAr/m³]	$\mathrm{EI6} = \frac{E_{r_i}}{V_i}$ (3.15)
7	EI7	**Standardized Reactive Energy Intensity** represents the reactive energy consumed per cubic meter of pumped water, normalized to a reference head of 100 meters; [kVArh/m³/100 m]	$\mathrm{EI7} = \frac{E_{r_i}}{V_i \cdot \frac{H}{100}}$ (3.16)
8	EI8	**Average Reactive Power** represents the mean quantity of reactive power utilized during the analyzed time interval Δt; [kVAr]	$\mathrm{EI8} = \frac{\sum_{i=1}^{n} P_{r_i}}{N}$ (3.17)
9	EI9	**Maximum Reactive Power** represents the peak value of reactive power consumed during the analyzed period; [kVAr]	$\mathrm{EI9} = \max(P_{r_1}, \ldots, P_{r_i})$ (3.18)
10	EI10	**Energy Reactivity Index** indicates the percentage ratio between reactive energy and active energy consumed in the system and is inversely proportional to the power factor; [%]	$\mathrm{EI10} = \frac{E_{r_i}}{E_{a_i}} \cdot 100$ (3.19)
10	EI11	**Pump Utilization Rate** indicates the extent to which the maximum available capacity of pumping equipment is effectively used during an evaluated period. It is calculated as the ratio between the energy consumed by all pumps during the peak consumption period and the energy that would have been consumed if the pumps had operated at full capacity; [%]	$\mathrm{EI11} = \left(\frac{E_{a_{max}}}{P_{a_n} \cdot t_i}\right) \cdot 100$ (3.20)

* According to [82]

These indicators provide a comprehensive framework for analyzing and improving the energy performance of water pumping and distribution systems.

They allow for systematic benchmarking and facilitate targeted interventions to increase operational efficiency and sustainability. An application of these indicators is presented in section 3.4.2.

3.3. Proposals regarding the monitoring of urban water supply systems

SCADA systems are advanced monitoring and control platforms used in critical infrastructures, including water and energy distribution. They allow for the collection and analysis of data in real time, facilitating the optimization of resource consumption and the integration of renewable energy sources. By supporting predictive maintenance and reducing operational losses, SCADA contributes to increasing energy efficiency and achieving sustainable development goals. Thus, these systems become essential tools in the modernization and sustainability of urban infrastructures.

3.3.1. SCADA capabilities

SCADA systems, initially developed in the 1950s for industrial control, have evolved into complex digital platforms that are essential for the intelligent management of urban water supply infrastructure. The

integration of advanced Industry 4.0 technologies—such as Cloud Computing, Artificial Intelligence, and the Internet of Things (IoT)—has enabled extensive automation, operational optimization, and real-time monitoring of quality parameters, while also amplifying cybersecurity risks.

The architectural evolution of these systems, from monolithic structures to networks based on smart sensors, has increased efficiency and scalability but simultaneously imposed heightened security requirements. In this context, SCADA stands as a cornerstone of hydro-technical digitalization, playing a critical role in operational sustainability and resilience.

3.3.2. SCADA structure for water supply systems in Brașov

The design of a SCADA system involves collaboration among process engineers, IT specialists, and experts in automation and networking. In the municipality of Brașov, the Water Company employs a distributed SCADA architecture to monitor and control the infrastructure for potable water treatment, pumping, storage, and distribution. The system collects data through sensors and actuators connected to Remote Terminal Units (RTUs) and Programmable Logic Controllers (PLCs), which transmit information to central servers where it is analyzed and visualized in real time via Human-Machine Interfaces (HMIs).

The modernization efforts focus on migrating towards a networked SCADA architecture with open protocols (e.g., TCP/IP) and integrating the firefighting network, including hydrants equipped with flow and pressure sensors for automatic detection and real-time alerts. Communication is achieved through a hybrid infrastructure comprising optical fiber, radio, and GSM/4G technologies, depending on topology and security requirements.

The hardware components include sensors, actuators, RTUs, and communication modules, while the software integrates HMIs, alarm modules, historical databases, and standardized protocols such as Modbus and DNP3. The system enables loss detection, calibration of hydraulic models, and optimization of interventions, providing a scalable and resilient platform for the intelligent management of the urban water network.

3.3.3. Challenges in Implementing SCADA

SCADA systems are essential components of critical infrastructures, providing automated control, real-time monitoring, and operational analysis through historical data logging [100], [101]. The use of standardized protocols and remote access capabilities facilitates interoperability and efficient management of distributed networks.

However, the integration of IoT and Cloud platforms, while expanding functionality, increases vulnerability to cyberattacks, especially in the absence of stringent security policies [89], [100]. Technological and organizational limitations—such as high costs, the need for specialized personnel, and architectural complexity—can impact operational resilience.

To protect critical infrastructure, an integrated security approach is necessary, based on advanced encryption, network segmentation, continuous monitoring, and periodic audits.

3.4. Applications and Case Studies

3.4.1. Analysis of variations in drinking water quality indicators

Between January 2019 and May 2021, a case study was conducted to monitor the physical quality of water at a specific point in the Brașov distribution network. The parameters analyzed were turbidity and conductivity, both essential for assessing drinking water quality. Turbidity was measured in NTU and FNU units, in accordance with ISO 7027 standards, with the collected data compiled in Appendix 1.

Figure 3.10 presents the evolution of water turbidity in the Brașov system over the period from January 2019 to May 2021.

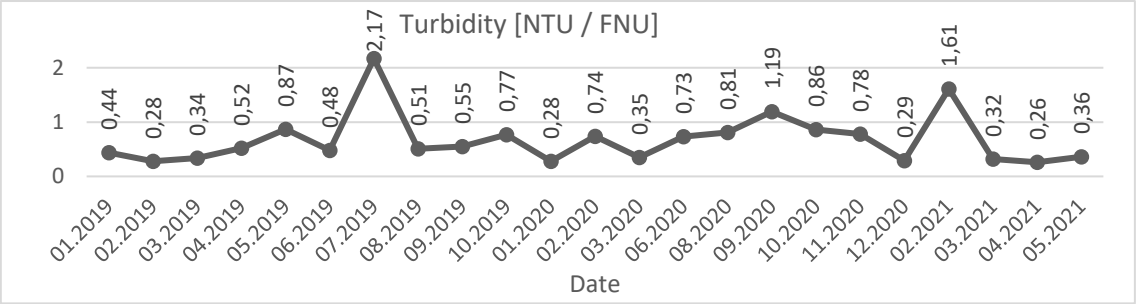

Fig. 3.10. Variation of Drinking Water Turbidity During the Period January 2019 – May 2021

Turbidity values generally remained below the threshold of 1 NTU/FNU, indicating appropriate water quality. However, two significant increases were recorded: in June 2019 (exceeding 2 NTU) and December 2020 (approximately 1.6 NTU), which may suggest contamination events or treatment malfunctions. The rapid return to normal values indicates effective corrective interventions. Overall, quality control in the Brașov Urban Water System (UWS) network was adequate, with only occasional fluctuations [102].

Figure 3.11 illustrates the evolution of the electrical conductivity of water in the Brașov urban water system during the period from January 2019 to May 2021.

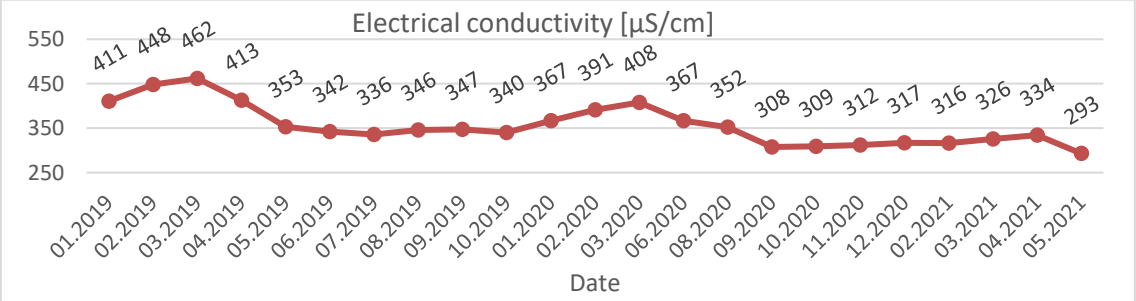

Fig. 3.11. Variation of electrical conductivity of drinking water between January 2019 and May 2021

Water conductivity varied between 293 and 462 µS/cm, reaching a peak in March 2019, followed by an overall decreasing trend. A local spike was observed in March 2020, which was subsequently followed by a reduction below 310 µS/cm during the second half of that year. Towards the end of the monitoring period, values stabilized between 310 and 330 µS/cm, with a final decrease to 293 µS/cm in May 2021, indicating a reduction in dissolved salts and stabilization of water quality.

Figure 3.12 illustrates the evolution of free chlorine concentration in the drinking water of the system during the period from January 2019 to May 2021.

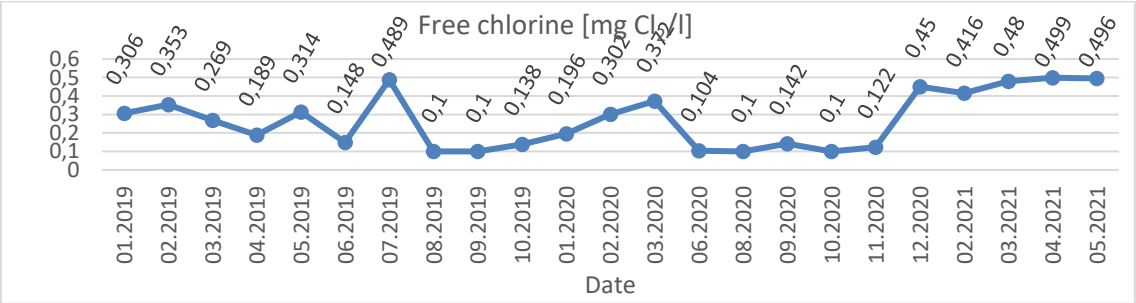

Fig. 3.12. Variation in the amount of free chlorine in drinking water between January 2019 and May 2021

Between January 2019 and May 2021, the concentration of free chlorine in the UWS Brașov network ranged between 0.1 and 0.496 mg/l, within legal limits [102]. The peaks in July 2019 and April–May 2021 reflect adjustments in disinfection to maintain microbiological quality. Analysis of turbidity, conductivity and free chlorine indicate good overall water quality, with occasional fluctuations effectively managed through interventions in the treatment processes.

3.4.2. Case Study – Water Consumption for Supplying External Fire Hydrants

The study analyzes water consumption used for firefighting and emergency interventions in urban areas serving approximately 74,000 inhabitants in the central region [103]. Data collected between 2022 and 2024 (see Appendix 2) focus on evaluating the efficiency of the external fire hydrant network. Four indicators were monitored: monthly and annual water consumption, specific consumption, and hydrant usage time. The analysis covers the period from January 2022 to November 2024.

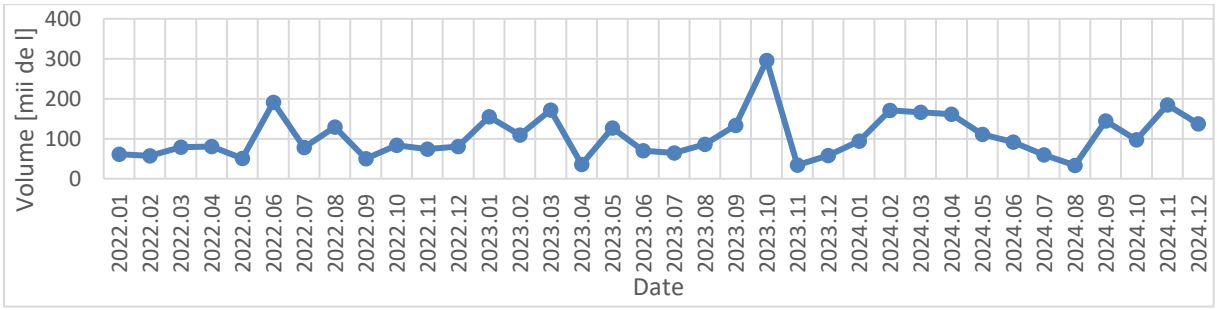

Fig. 3.13. Monthly Water Consumption for Supplying External Fire Hydrants During the Period 2022–2024

The graph highlights significant variations in the volume of water consumed during the period 2022–2024, with isolated peaks, the most pronounced occurring in October 2023, suggesting sporadic usage linked to emergency situations. A possible seasonality is observed, with a tendency for increased consumption during the spring and autumn months.

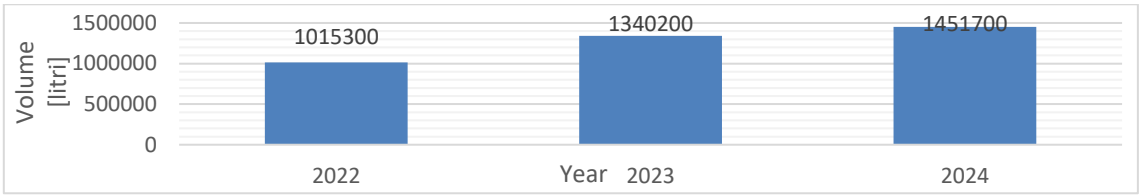

Fig. 3.14. Annual water consumption for supplying external hydrants in 2022-2024

Fig. 3.14 presents the annual evolution of the total volume of water consumed by external hydrants in the period 2022-2024, highlighting a constant increase from 1,015,300 liters in 2022 to 1,451,700 liters in 2024. This increase is directly associated with the intensification of the use of the hydrant network for firefighting interventions or other operational uses.

Fig. 3.15 illustrates the specific water consumption determined using relation 3.3.

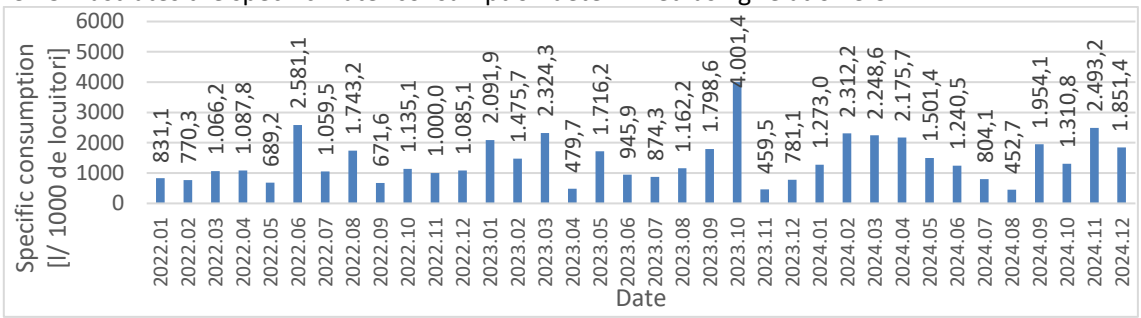

Fig. 3.15. Specific water consumption – external hydrants

The specific water consumption from external fire hydrants during the period 2022–2024 ranged from a minimum of 479.1 liters per 1,000 inhabitants in May 2023 to a maximum of 4,001.4 liters per 1,000 inhabitants recorded in October 2023. The annual averages were approximately 1,270 liters per 1,000 inhabitants in 2022, 1,680 liters per 1,000 inhabitants in 2023, and 1,700 liters per 1,000 inhabitants in 2024. The overall average for the entire analyzed period was about 1,550 liters per 1,000 inhabitants, with isolated variations due to exceptional usage events.

Figure 3.16 illustrates the maximum operating time of external fire hydrants, calculated according to equation 3.4.

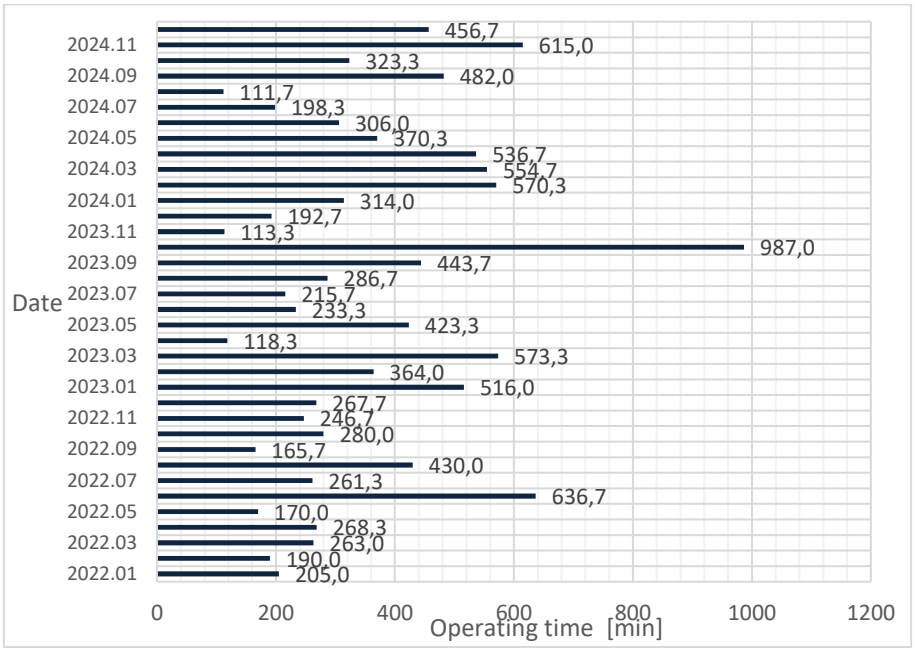

Fig. 3.16. Maximum operating time of external fire hydrants

Between 2022 and 2024, the operating time of external fire hydrants varied monthly from 111.7 minutes (August 2024) to 987 minutes (October 2023), reflecting varying intervention intensities according to operational needs. High values indicate extended periods of water system usage for firefighting.

These results underscore the importance of continuous monitoring of water consumption and hydrant usage to optimize interventions and reduce losses. Establishing a dedicated database and implementing a system for analyzing these parameters are essential for operational efficiency and energy sustainability of the urban water network.

3.4.3. Comparative Study of Energy Indicators for Two Water Pumping Stations

The study compares the energy indicators of two pumping stations with different technical configurations, based on local measurements conducted on October 20, 2024 (Appendix 3). Pumping Station I (PS I), dedicated to the distribution of potable water, is equipped with pumps featuring variable frequency drives (VFDs), allowing adjustment of rotational speed according to flow and pressure requirements, thereby contributing to the optimization of electric energy consumption; the configuration of this station is illustrated in Figure 3.17. Pumping Station II (PS II), used for water lifting, operates with pumps driven by fixed-speed motors, which limits adaptability to consumption variations and may result in higher specific energy consumption.

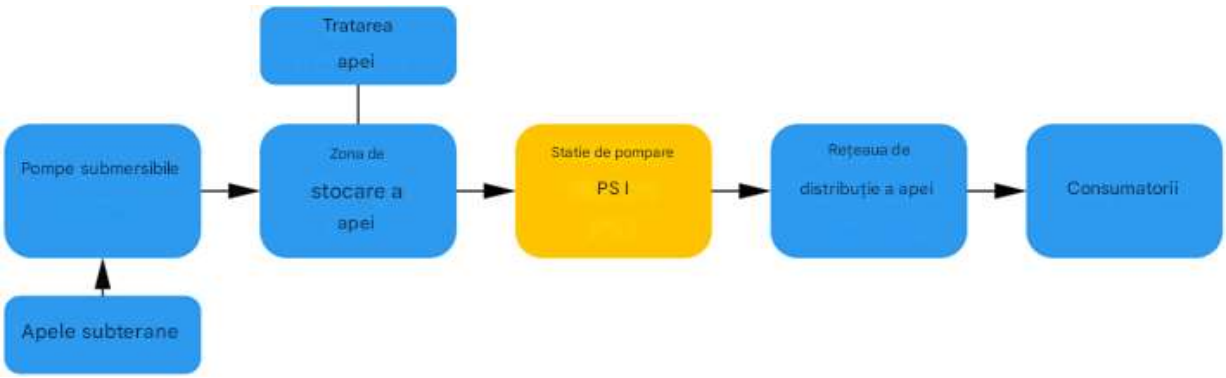

Fig.3.17. Pumping Station PS I for Water Distribution

Pumping Station PS I consists of five vertical multistage centrifugal pumps of the CR 64-3-2 A-F-A-E-HQQE type. The technical specifications of a single pump are presented in Table 3.3.

Table 3.1. Technical specifications of a pumping unit within PS I

Technical Characteristic	Value
Hydraulic Specifications	
Nominal Flow Rate	64 m^3/h
Nominal Pumping Head	52,8 m
Maximum Pumping Head	70,1 m
Maximum Operating Pressure	16 bar
Nominal Speed	2923 rpm
Electrical Specifications	
Motor Type	160MD2
Nominal Power P2	15 kW
Network Frequency	50 Hz
Nominal Voltage	Δ 380-415 V / Y 660-690 V
Nominal Current	Δ 26-28 A / Y 15,6-16,2 A
Maximum Current	Δ 28,5-31 A / Y 17,2-17,8 A
Nominal Speed	2930-2950 rpm
Power Factor (cos ϕ)	0,89-0,87
Efficiency Class IE	IE3 – 91,9%
Frequency Converter Type	FC 202
Supported Power	15 kW
Output Current	30 A
Output Voltage	0-480 V
Output Frequency	0-590 Hz

Each pumping unit within Pumping Station I (PS I) is controlled by an FC 202 frequency converter configured in a master-slave arrangement, where the master converter (C1) regulates the pressure within the urban distribution network. Converter C1 operates in a closed-loop mode based on feedback from a pressure sensor, while the secondary converters (C2–C5) function in open-loop mode, receiving speed control commands from the master controller.

This system enables sequential pump control, alternation between pumps, and balancing of operating times to reduce wear. Additionally, the mechanical torque disable function ensures safe equipment shutdown without interrupting power supply.

Figure 3.20 illustrates the configuration of the water supply system associated with Pumping Station II (PS II), designed to manage altitude variations predominantly through gravitational transport.

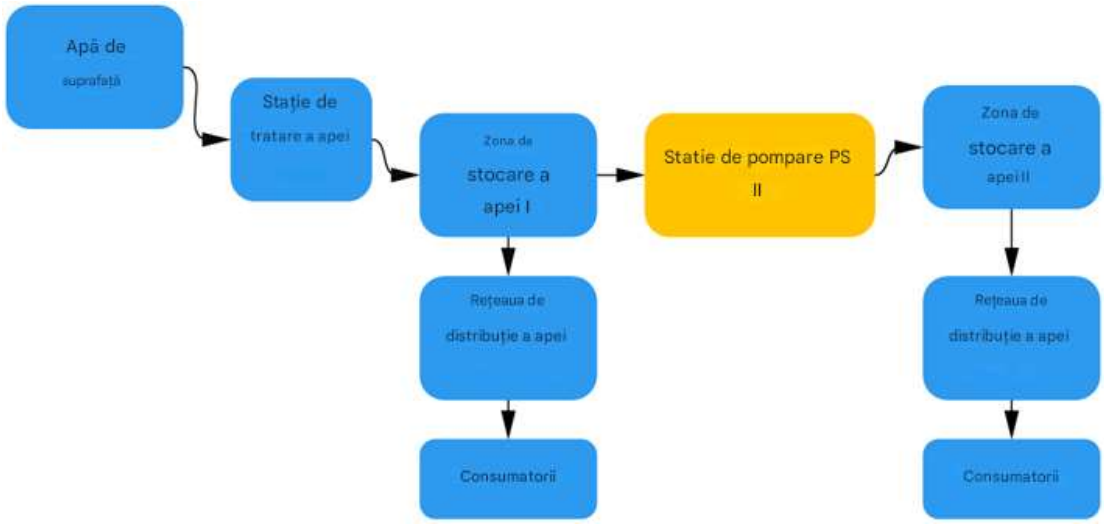

Fig. 3.20. PS II pumping station for water lifting

Surface water is captured from a reservoir lake and transported by gravity to a treatment plant. Subsequently, it is stored in Storage Zone I (19,000 m³). From this zone, part of the water is supplied directly to consumers, while the remainder is pumped by Pumping Station II (PS II) to Storage Zone II (18,000 m³), located at a higher elevation. PS II is equipped with three constant-speed centrifugal pumps, model 10LR18. The technical specifications are presented in Table 3.4.

Table 3.2. Technical Specifications of a Pumping Unit within PS II

Technical Characteristic	Value
Hydraulic Specifications	
Nominal Flow Rate	1,170 m³/h
Nominal Pumping Head	38.5 m
Maximum Operating Pressure	24 bar
Electrical Specifications	
Motor Type	315S/M-4
Efficiency Class IE	IE2 – 90%
Nominal Power P2	150 kW
Network Frequency	50 Hz
Nominal Voltage	380V / 400V / 415V / 660V / 690V
Nominal Current	276 A (380V/50 Hz), 265 A (400V/50 Hz), 258 A (415V/50 Hz), 159 A (660V/50 Hz), 154 A (690V/50 Hz)
Power Factor (cos ϕ)	0.86
Nominal Speed	1,480 rpm

The drive motor is an asynchronous squirrel-cage type with air cooling, featuring a nominal efficiency of 90% and classified under the IE2 energy efficiency category according to the manufacturer's specifications. The pump casing is constructed from ductile iron and bronze to provide resistance against mechanical wear and corrosion.

For the evaluation of energy indicators, both systems were analyzed from technical and operational perspectives, aiming to determine their actual efficiency under representative operating conditions**.**

Energy Performance Monitoring at Pumping Station PS I

The results of the conducted monitoring are summarized in Figure 3.22, which enables a comparative analysis of the electrical and hydraulic parameters of the pumping units within Pumping Station PS I. The functional relationship between the temporal evolution of electric power and water flow rate is highlighted. Measurements were taken for the entire pumping group, covering both electrical parameters and flow rates.

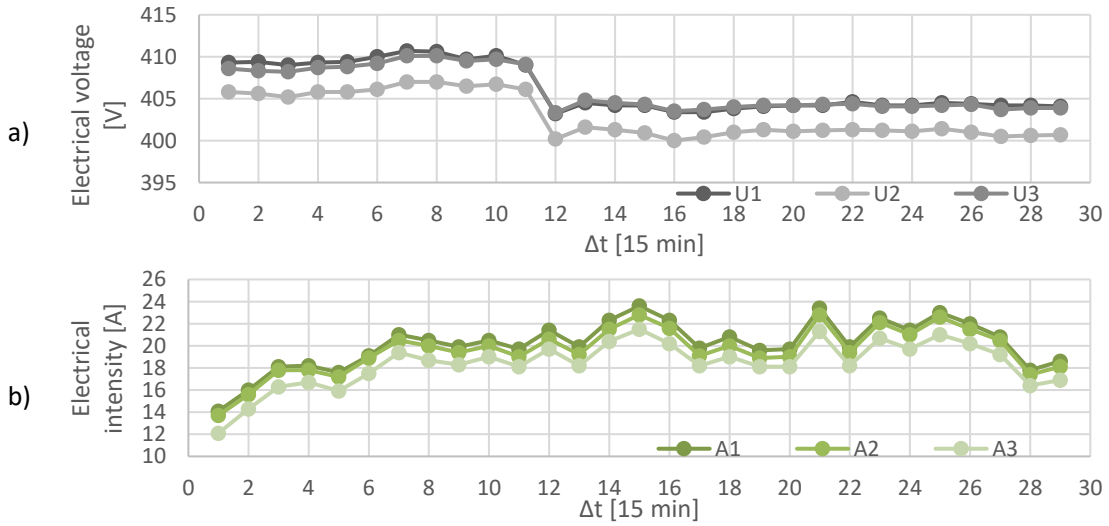

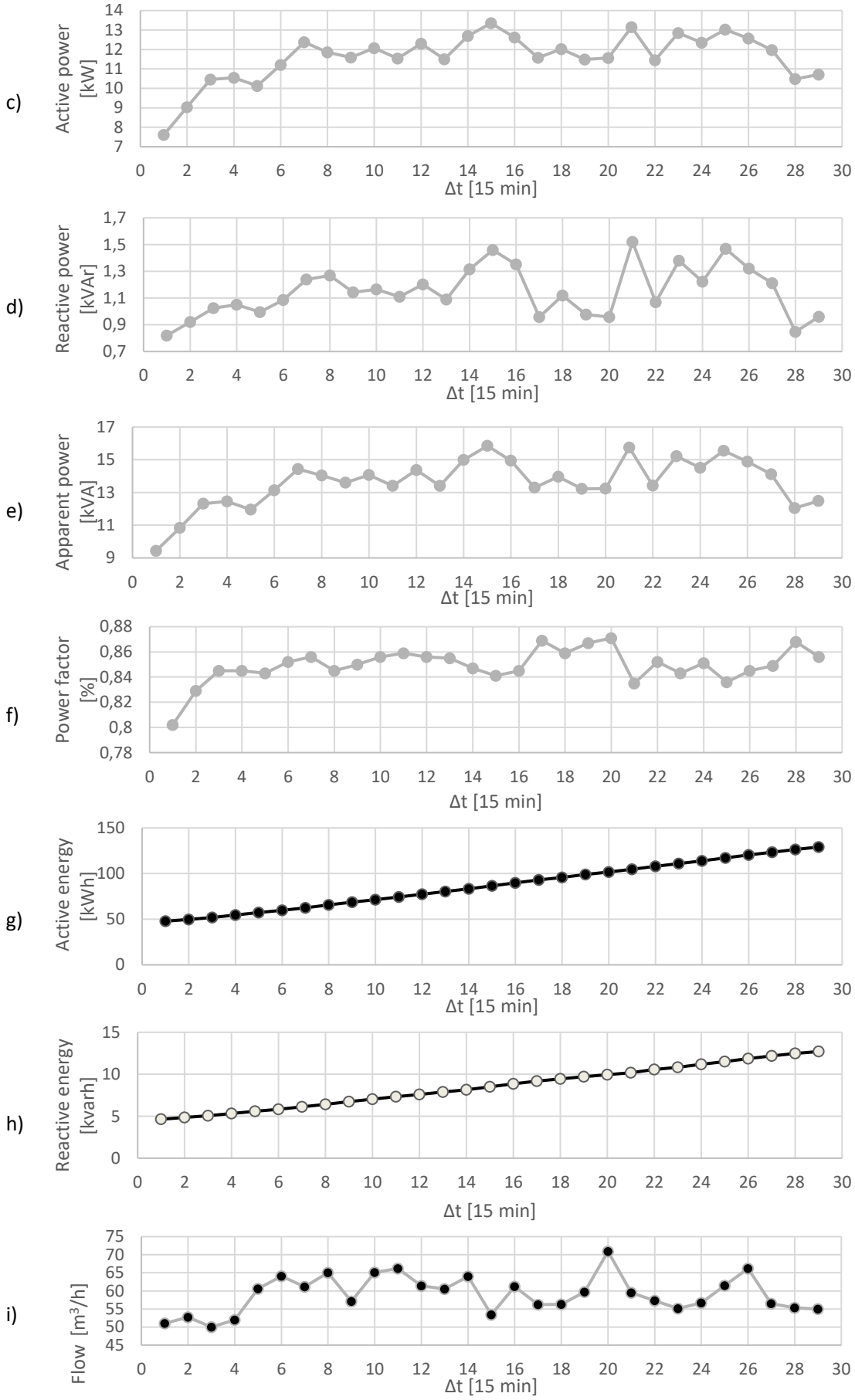

Fig. 3.22. Monitoring of Electrical and Hydraulic Parameters at Pumping Station PS I (29 Measurements)

Monitoring of 29 measurements at Pumping Station PS I enabled the analysis of the system's electrical and hydraulic behavior under variable operating conditions. The three-phase voltage exhibited a sharp drop between points 10 and 12, suggesting load changes, while the electric current progressively increased up to the same interval, subsequently maintaining moderate fluctuations with good phase balance.

Active power showed significant variations, peaking between points 20 and 26, while reactive power followed a correlated trend, reflecting the presence of inductive or capacitive loads. Apparent power provided an integrated view of the energy demand, and the power factor remained between 78% and 88%, indicating good but improvable efficiency.

Active energy increased linearly, reflecting a stable operating regime, with reactive energy following a similar trend but at a lower slope. Water flow rate experienced significant variations, with a pronounced peak around point 20, directly influencing energy consumption. The results highlight the correlation between electrical demand and the hydraulic dynamics of the pumping station.

II. Energy Performance Monitoring at Pumping Station PS II

The second study, conducted for PS II, provides a detailed analysis of electrical and hydraulic performance through a series of graphs presented in Figure 3.23.

a)

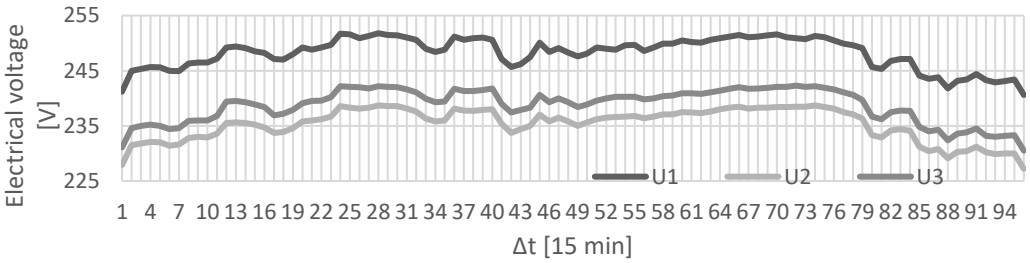

b)

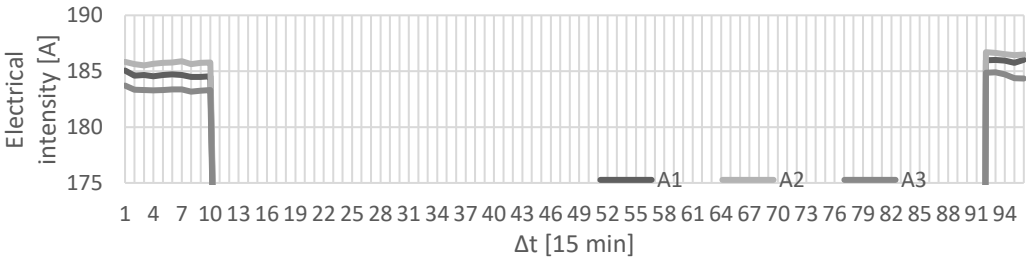

c)

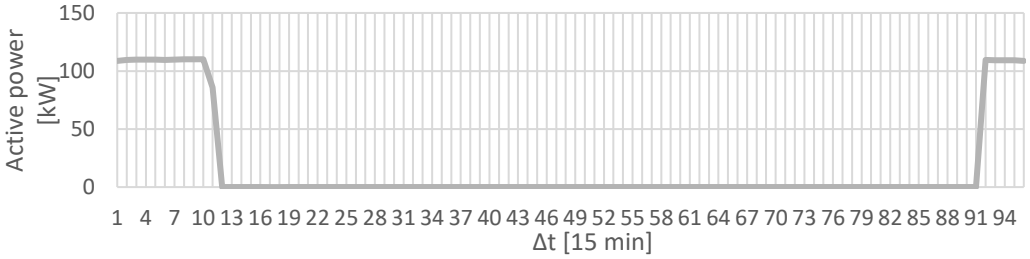

d)

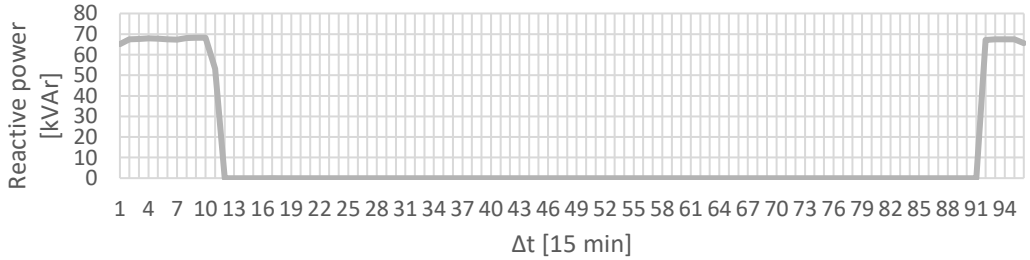

e)

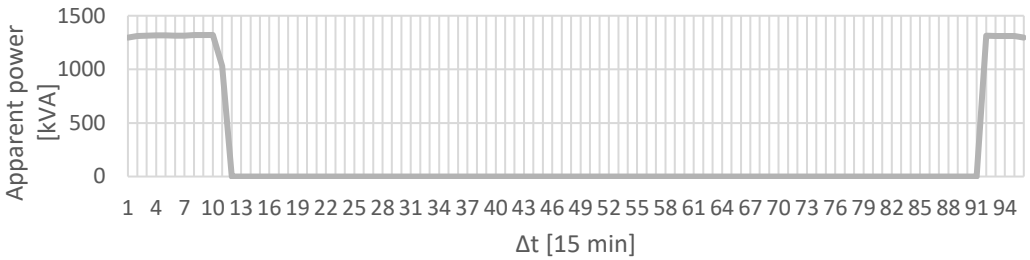

f)

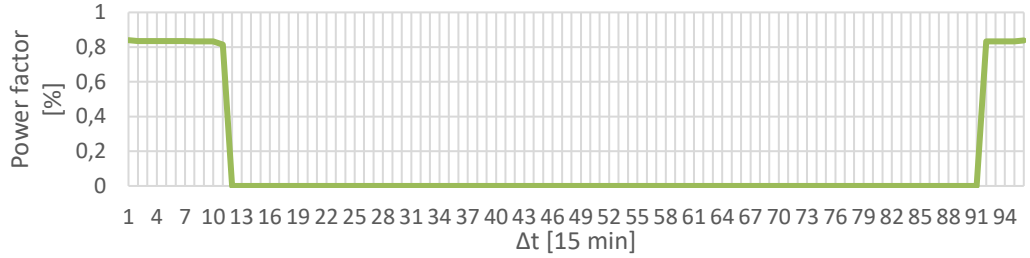

g)

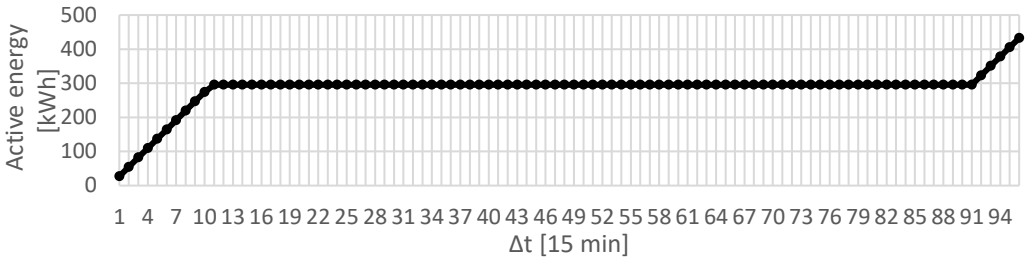

h)

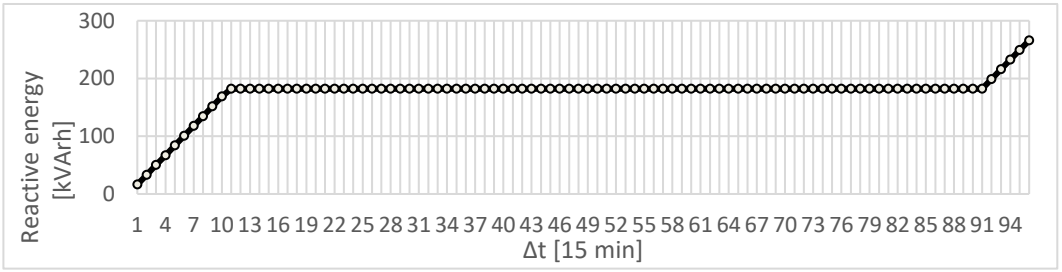

i)

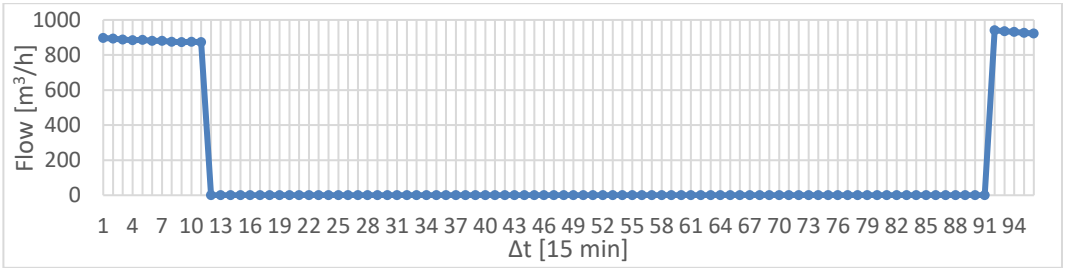

Fig. 3.231. Monitoring of electrical and hydraulic parameters at PS II (96 measurements)

The analysis of PS II reveals a discontinuous behavior of the electrical and hydraulic parameters, with voltage variations and sudden current drops at shutdown. The powers and flows follow the same cycle of constant operation, shutdown and restart, the power factor remaining at approximately 0.85 in active mode. Although the energy indicators for PS II (constant speed - CSD) and PS I (variable speed - VSD) are centralized, a direct comparison of their performances requires a detailed context, given the fundamental difference between VSD and CSD systems.

Table 3.3. Energy performance indicators for PS I and PS II

Symbol	Indicator name and definition	PS I	PS II
EI1	Energy Intensity [kWh/m³]	0,1956	0,1308
EI2	Standardized Energy Intensity [kWh/m³/100 m]	0,3705	0,3396
EI3	Average Active Power [kW]	10,6130	108,0840

Symbol	Indicator name and definition	PS I	PS II
EI4	Maximum Active [kW]	15,3820	110,1190
EI5	CO_2 [$kgCO_{2e}$/kWh]*	61,3083	100,2936
EI6	Reactive Energy Intensity [kVAr/m³]	0,0203	0,0804
EI7	Standardized Reactive Energy Intensity [kVArh/m³/100 m]	0,0384	0,2088
EI8	Average Reactive Power [kVAr]	1,1040	66,4560
EI9	Maximum Reactive Power [kVAr]	2,0780	68,2190
EI10	Energy Reactivity Index [%]	0,1036	0,6149
EI11	Pump Utilization Rate [%]	14,6811	12,0083

Findings:

PS II demonstrated superior energy efficiency concerning active energy consumption (0.1308 kWh/m³) compared to PS I (0.1956 kWh/m³), with both values below the IWA performance threshold. However, PS II exhibited significantly higher reactive energy consumption, indicating inefficient management and the need for reactive power compensation. While PS I consumes more active energy, it manages reactive energy more effectively. Both stations operate with a low pump utilization rate (below 15%), adversely affecting overall efficiency. Optimization of active energy consumption at PS I, reactive power compensation at PS II, and more efficient equipment utilization at both stations are necessary.

3.5. Conclusions

The use of performance indicators in accordance with IWA and WAREG standards enables a comparable and objective evaluation of water supply system operations, providing a foundation for strategic and operational decision-making (1). In the municipality of Brașov, the application of a multidimensional analysis—covering technical, energetic, financial, ecological, and social aspects—has identified vulnerabilities and guided the optimization of energy consumption, reduction of losses, and enhancement of service reliability (2).

For the hydrant network, indicators such as water consumption for firefighting and maximum usage time allow for appropriate sizing of emergency interventions (3). The introduction of an energy indicator set (EI1–EI11) for pumping stations facilitated the assessment of energy efficiency and monitoring of CO_2 emissions impact (4).

SCADA modernization, through the transition to open network architectures and the integration of IoT technologies, has expanded monitoring capabilities, including for the hydrant network, enabling real-time response, predictive maintenance, and operational optimization. Concurrently, this requires strengthening cybersecurity measures and data protection (5).

The integration of sustainability criteria, aligned with EU policies on energy efficiency and emission reduction, has enabled the alignment of Brașov's water infrastructure with sustainable development goals (7). The case study confirms the effectiveness of an integrated approach, based on indicators and advanced technologies (SCADA, IoT), in enhancing resilience, sustainability, and efficiency of urban water systems (8).

The implementation of a rigorous monitoring methodology, supported by specific indicators and digital tools, decisively contributes to public safety, environmental protection, and the sustainability of public water services

4. Contributions to Improving Energy Efficiency in Water Pumping Stations

4.1. Introductory Elements

The operation of urban water supply systems involves high electrical energy consumption, particularly in pumping stations, which is influenced by factors such as equipment type, network configuration, and user behavior. The efficiency of these stations depends on their operational mode, level of automation, and balance of reserves; excessive consumption or energy losses indicate the need for optimization.

In this context, the research proposes the development of a dynamic predictive model for estimating the energy consumption of pumping stations in the Brașov area. The model integrates technical, hydraulic, and operational data, aiming to assess power quality, perform energy balance analyses, and evaluate operating condition variability.

This study supports Objective 3 of the doctoral research by developing strategies to increase energy efficiency, including: performance modeling of equipment, energy quality analysis, SCADA-based monitoring, identification of energy losses, and the proposal of techno-economic solutions. The results provide a concrete foundation for reducing consumption, improving operational stability, and enhancing the overall efficiency of the system.

4.2. Performance Characteristics and Efficiency Analysis of Pumping Units

4.2.1. Energy Flow Analysis in Water Pumping Units

The analysis of the energy performance of a pumping unit primarily involves the evaluation of the efficiency of its two main components: the pump and the electrical supply and drive system.
Figure 4.1 illustrates the structure of a potable water pumping system comprising pump P, which transports water from reservoir R1 to a higher elevation reservoir R2, located at height H.
The drive system consists of the drive motor M and the variable frequency drive (VFD) CFV. Electrical power is supplied to the system from the utility grid via a transformer TR.

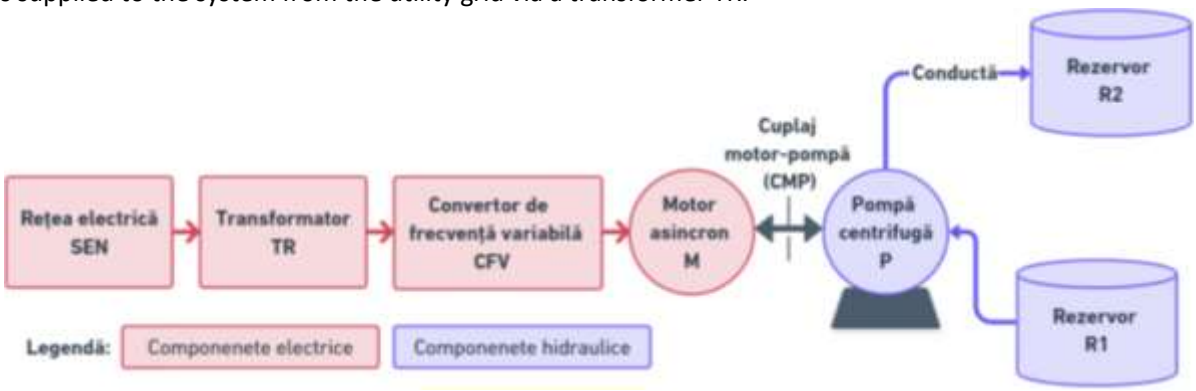

Fig. 4.1. Energy flow and structure of a water pumping unit

In this case, the energy flow consists of supplying electrical energy to the asynchronous motor M, with parameters defined by the CFV converter, transforming electrical energy into mechanical energy at the electric motor shaft, via the motor-pump coupling CMP, converting mechanical energy at the pump rotor, into hydraulic energy – in the form of kinetic and potential energy of the fluid being pumped, characterized by specific hydraulic parameters: flow rate and pressure. The energy conversion process involves energy losses at all components of the pumping unit, starting with electrical losses in the TR transformer and ending with hydraulic losses in the piping system [106], [107], [108].

4.2.2. Performance and loss analysis in the centrifugal pump and motor–pump coupling

A. Losses in the centrifugal pump

The functional behavior of the centrifugal pump within a hydraulic system and the evaluation of its performance requires the analysis of characteristic curves (Fig. 4.2), namely:

- The energy performance curve: $H = H(Q)$
- The characteristic curve of the installation: $H_{inst} = H_{inst}(Q)$;
- The hydraulic efficiency curve: $\eta = \eta(Q)$

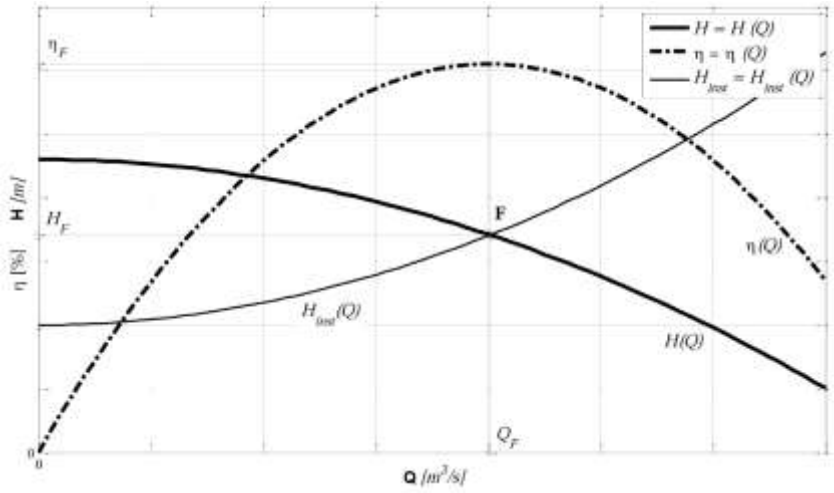

Fig. 4.2. Characteristic curves for pumps, according to [106]

The energy performance curve is the energetyc characteristic of the pump $H = H(Q)$, representing the specific hydraulic energy per unit of weight that the pump can deliver for a given flow rate Q.

The characteristic curve of the installation reflects the variation of the hydraulic load H_{inst} as a function of the flow rate $H_{inst} = H_{inst}(Q)$, and represents the variation of the specific energy per unit of weight required by the installation to ensure the water flow in the hydraulic system.

The pump efficiency curve $\eta = \eta(Q)$ depends on the energy performance of the pump and the load characteristic.

The hydraulic efficiency of a centrifugal pump, as an overall efficiency, expresses the total efficiency of the conversion of the energy taken from the pump shaft into useful hydraulic energy required to transport the water, integrating all categories of internal losses that affect the performance of the pump: hydraulic losses ΔP_h, volume losses ΔP_v, and mechanical losses ΔP_m.

The efficiency is expressed by the relationship:

$$\eta_p = \frac{P_h}{P_h + \Delta P_h + \Delta P_v + \Delta P_m} = \eta_h \cdot \eta_v \cdot \eta_m \quad (4.1)$$

where: : η_h is the hydraulic efficiency, which reflects energy losses caused by internal friction, turbulence, and shocks in the fluid; η_v is the volumetric efficiency, which reflects flow losses due to internal leaks and recirculation; η_m represents the mechanical efficiency, which reflects energy losses due to friction in bearings, seals, and the rotor's side plates.

The useful hydraulic power transmitted to the fluid is:

$$P_h = \rho \cdot g \cdot Q \cdot H \quad (4.2)$$

where: ρ is the density of water, g is the gravitational acceleration, Q is the water flow rate conveyed by the pump, H is the pumping height.

A pump operates optimally when the energy supplied corresponds exactly to the requirements of the installation, this balance defining the point of maximum energy efficiency. The flow rate can be adjusted quantitatively, using valves or bypasses (with energy losses), or qualitatively, by changing the speed with a frequency converter, which is a more energy-efficient method.

Reducing the speed significantly lowers energy consumption, avoiding additional losses associated with quantitative control. Thus, qualitative control is recommended for increasing the efficiency of the pumping system.

In the case of operation with a motor powered by a variable frequency converter, Fig. 4.4 illustrates the process of determining the operating point when the pump speed is reduced to $n' < n$.

The operating point moves from F, corresponding to the flow rate Q_F, to the point corresponding to the flow rate $Q_{F'}$. Depending on the shape of the efficiency curve, the shift from point F to point F' is equivalent to a corresponding change in efficiency.

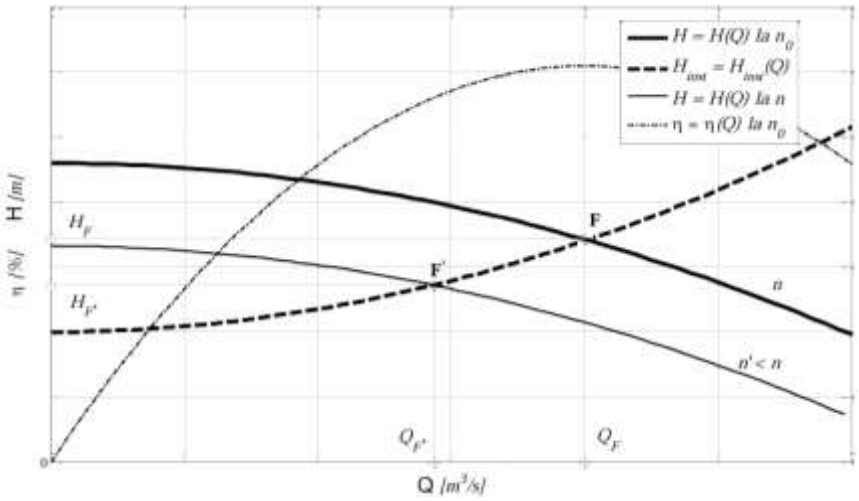

Fig. 4.4. Determining the operating point of the pump for $< Q_n$, adapted from [106]

In a system where the load varies, the implementation of a pump driven by a variable speed motor is a solution that contributes to reducing energy consumption.

B. Losses in the motor-pump coupling

The electric motor is coupled to the centrifugal pump by rigid or elastic couplings, and accordingly, the efficiency of the motor-pump coupling can be written as:

$$\eta_{cpm} = \frac{P_p}{P_{M1}} \tag{4.3}$$

where: P_p represents the power of the pump, and P_{M2} represents the power of the pump motor
In terms of efficiency, rigid and elastic couplings have low mechanical losses, with power transmission of over 99%.

4.2.3. Analysis of losses in the pump's electrical power supply and drive system

In the energy analysis of the centrifugal pump drive system, total losses are the result of the cumulative contribution of several sources, namely: internal losses in the asynchronous electric motor (M), mechanical losses in the motor-pump coupling, and losses in the frequency converter (CFV), all of which directly influence the overall efficiency of the pumping system.

A. Losses in the drive motor

Asynchronous motors are frequently used to drive pumps due to their simple construction, high reliability, good efficiency, low cost, and direct supply from the three-phase mains. However, their rigid mechanical characteristics require the use of control systems to regulate speed and optimize energy consumption.

Speed control is achieved by changing the supply frequency and voltage, keeping the U/f ratio constant to maintain maximum torque. The frequency converter allows efficient speed adjustment with low losses. Motor performance is analyzed by the torque-slip (M=f(s)) and speed-torque (n_2=f(M)) characteristics, which are essential for evaluating behavior during start-up and under load.

The efficiency of an asynchronous motor depends on the mechanical power transferred to the pump:

$$\eta_M = \frac{P_{M2}}{P_{M1}} = \frac{P_{M2}}{P_{M2} + \Delta P_{Cu_1} + \Delta P_{Fe_1} + \Delta P_{Cu_2} + \Delta P_{\mathrm{m}}} \tag{4.4}$$

where: P_{M2} is the useful mechanical power, , P_{M1} is the electrical power absorbed by the motor.

The active power absorbed by the motor P_{M1} includes the useful power and losses in the motor:

$$P_{M1} = P_{M2} + \Delta P_{Cu_1} + \Delta P_{Fe_1} + \Delta P_{Cu_2} + \Delta P_{\mathrm{m}} \quad (4.5)$$

where: ΔP_{Cu_1} are the losses due to the Joule effect in the stator winding:

$$\Delta P_{Cu_1} = m_1 \cdot R_1 \cdot I_1^2 \quad (4.6)$$

where: m_1 represents the number of phases of the stator winding, R_1 represents the electrical resistance of a phase of the stator winding, and I_1 is the phase current intensity.

ΔP_{Fe_1} represents losses in the stator magnetic circuit, which occur due to magnetic hysteresis losses ΔP_{H} and eddy currents ΔP_{T}:

$$\Delta P_{Fe_1} = \Delta P_{\mathrm{H}} + \Delta P_{\mathrm{T}} \quad (4.7)$$

ΔP_{Cu_2} Joule losses in the rotor are generated by the resistance of the rotor windings:

$$\Delta P_{Cu_2} = m_2 \cdot R_2' \cdot I_2'^2 \quad (4.8)$$

where: m_2 represents the number of rotor phases, R_2' represents the equivalent electrical resistance of the rotor winding, I_2' and is the rotor current intensity.

ΔP_{m} represents mechanical losses caused by friction in bearings, rotor, and fan.

The efficiency of an asynchronous motor (4.4) is determined by the quality of the active materials (copper, electrical steel), the design dimensions, the rated power, and the technological solutions adopted, such as the reduction of mechanical friction and the optimization of ventilation. Current trends are towards the use of high-efficiency asynchronous motors in line with energy performance and sustainability requirements.

B. Losses in the frequency converter

A frequency converter dynamically adjusts the speed of a motor to optimize pumping, reducing energy consumption and wear. It operates in either scalar or vector control, maintaining a constant U/f ratio for magnetic flux stability, although it generates various losses that require management.

The sum of all losses in the converter can be expressed as follows:

$$\Delta P_{\mathrm{CFV}} = \Delta P_{\mathrm{cond}} + \Delta P_{\mathrm{com}} + \Delta P_{mag} + \Delta P_{cap} + \Delta P_{aux} + \Delta P_{mec} + \Delta P_{par} + \Delta P_{emi} \quad (4.9)$$

The converter efficiency is defined by the relationship:

$$\eta_{CVF} = \frac{P_{M1}}{P_{M1} + \Delta P_{CFV}} \quad (4.10)$$

where: P_{M1} is the input power to the electric motor and ΔP_{CFV} are the losses in the frequency converter. Losses in the variable frequency converter cause a decrease in the power delivered to the motor, and its efficiency reflects the ratio between the useful energy transmitted and the total energy absorbed from the network.

C. Transformer losses

In order to adapt the electric drive system of the water pumping unit to the power supply network, in many cases it is necessary to connect it to the power supply network via an electric transformer. Thus, in the electric power flow (Fig. 4.1), it is also necessary to consider the losses in the transformer ΔP_{Tr}.

The active electrical power at the transformer terminals P_{Tr1} is given by the relationship:

$$P_{Tr1} = P_{Tr2} + \Delta P_{Tr} = P_{Tr2} + \Delta P_o + \beta^2 \cdot \Delta P_{sc} \quad (4.11)$$

where:

P_{Tr2} is the active electrical power at the secondary winding terminals of the transformer;

ΔP_o are the losses in the transformer during no-load operation; P_{sc} are the losses in the transformer during short-circuit operation; β – transformer load factor, which can be calculated using the following equation

$$\beta = \sqrt{\frac{P_{cons}}{P_n}} \quad (4.12)$$

The transformer efficiency is defined by the relationship:

$$\eta_{Tr} = \frac{P_{Tr2}}{P_{Tr1}} = \frac{P_{Tr2}}{P_{Tr2} + \Delta P_o + \beta^2 \cdot \Delta P_{sc}} \quad (4.13)$$

The overall efficiency of the system is affected by transformer losses, which significantly influence the total efficiency, especially in partial load conditions.

4.2.4. Pumping unit efficiency – Discussion and outlook

The total efficiency of the pumping unit is defined by the following equation:

$$\eta_{UP} = \frac{P_{hu}}{P_a} = \eta_P \cdot \eta_M \cdot \eta_{CMP} \cdot \eta_{CVF} \cdot \eta_{Tr} \quad (4.14)$$

where: η_{tot} represents the total efficiency of the system; η_P is the pump efficiency; η_M is the efficiency of the electric motor; η_{CMP} is the mechanical coupling efficiency; η_{CVF} is the efficiency of the variable frequency converter; η_{Tr} is the efficiency of the electrical transformer.

In a pumping system, each component contributes in a specific way to the overall efficiency of the installation, and the table below summarizes the typical efficiency and loss values for the main components.

Table 4.1 shows the efficiency values for components of pumping unit supply and control systems [108]; [112]; [113].

Table 4.1. Losses in pumping units

No.	Components in the pumping system	Efficiency (%)	Losses (%)
1	Pumps	85–90	10–15
2	Couplings	~99	~1
3	Motors	>90	<10
4	Cables	~98	~2
5	Variable frequency converter	95–98	2–5
6	Transformer	~99	~1

The use of high-performance equipment and constant evaluation of operating parameters are important elements in the sustainable development of pumping systems.

Discussions and perspectives

To reduce costs and consumption in pumping systems, it is crucial to improve the hydraulic efficiency of pumps and energy efficiency throughout the conversion chain. This is achieved by using high-efficiency asynchronous motors, which offer superior efficiency. Frequency converters are also essential for dynamically adapting the motor speed to the process requirements, thereby reducing consumption and mechanical wear.

4.3. Determination of energy consumption and energy intensity at the Măgurele pumping station

4.3.1. Description of the water pumping station

The Măgurele pumping station is an integral part of the drinking water supply system of the municipality of Brașov, located in the western part of the city, at an altitude of 585 meters. It plays an essential role in supplying water to the Poiana Brașov resort, ensuring water transport to high areas to maintain the pressure and flow required by consumers.

The main water source is the Măgurele catchment area, consisting of three boreholes equipped with submersible pumps, with a total flow rate of 172 m³/h. The second source comes from the urban network, with a supply of 115 m³/h. The water from the two sources is collected in the R_1 and R_2 suction tanks (total capacity 1200 m³), from where it is pumped to the R_3 tank (2000 m³), intended for distribution to consumers.

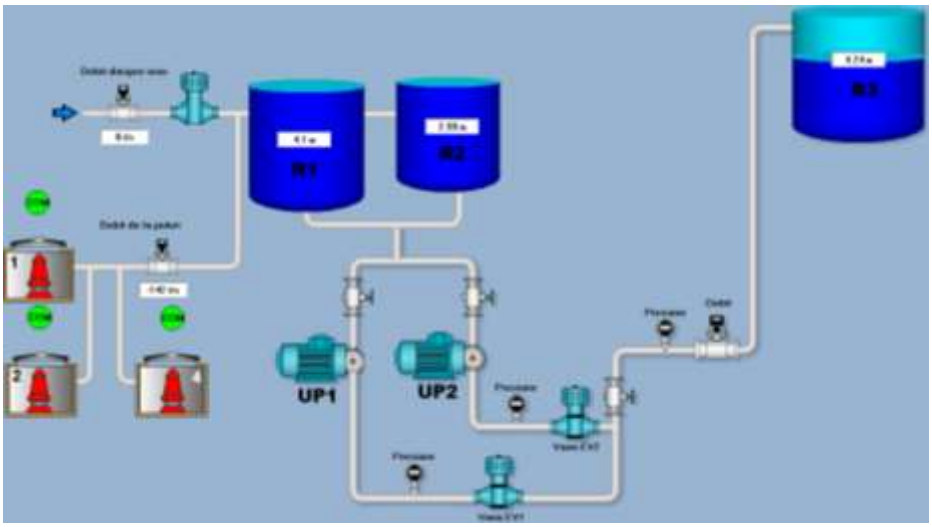

Fig. 4.4. Hydraulic diagram of the Măgurele pumping station

Between 2009 and 2010, pumping units UP1 and UP2 were modernized and equipped with two multistage centrifugal pumps type MTC A (Q_n = 299.99 m³/h, H_n = 450 m), driven by 500 kW three-phase asynchronous motors, powered at 0.4 kV. To protect the network and reduce the starting current, MCD3500 soft starters were installed, which ensure smooth motor start-up and reduce mechanical wear.

Fig. 4.10.a shows the two pump-motor units, with the discharge pipes of the two pumps mounted in parallel and the fittings certified at a nominal pressure of 64 bar, the body of the two four-stage centrifugal pumps and the electric valves on the discharge pipe. Fig. 4.10.b shows the characteristics of the pumps when operating in parallel.

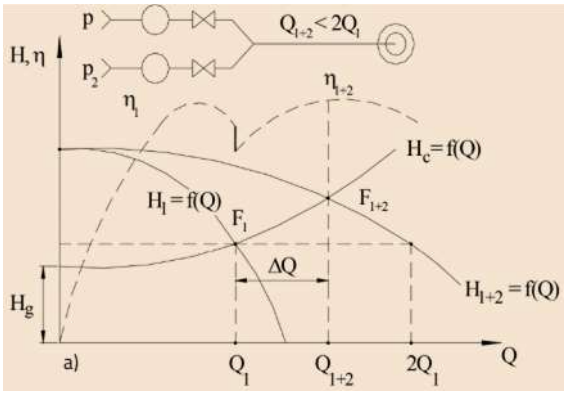

a) b)

Fig. 4.10. Group of pumps type MTC A 125/1LA8 357-2AC60 – 500 kW: a) general view; b) performance characteristics when pumps are operating in parallel

The pump station operates in alternating mode, so that only one pump is used at a time. This strategy ensures a balance between energy efficiency, equipment protection, and continuity of the pumping process.

Before modernization, the station operated with four TA 150-100-400/418 CX39 centrifugal pumps manufactured by Aversa Bucharest, each with a flow rate of Q_n= 230 m³/h and a pumping height H = 225m, at a synchronous speed of n_s =3000 rpm. These pumps were driven by three-phase asynchronous electric motors, type JB560M1, manufactured by Jiamusi Electric Motor Works, with a rated power of P_n= 250 kW, supplied at a voltage of 6 kV.

Table 4.2 shows the hydraulic and electrical characteristics of the pumping units.

Table 4.2. Technical characteristics of the pumping units at the Măgurele pumping station

Technical characteristics	Pumping units in operation	Backup pumping units
Hydraulic specifications		
Pump manufacturer	KSB	Aversa
Pump model	MTC A 125/04-101-22.67	TA 150-100-400/4180X39
Flow rate (Q_n)	299.99 m³/h	230 m³/h
Pumping height (H_n)	450 m	225 m
Rotational speed (n_n)	2982 rpm	3000 rpm
Pump year of manufacture	2008	1985
Electrical specifications		
Motor manufacturer	Siemens	Jiamusi Electric Motor Works
Motor model	1LA8 357-2AC60	JB 560 M
Rated power (P_n)	500 kW	250 kW
Rated voltage (U_n)	0,4 kV (Δ), 0,69 kV (Y)	6 kV (Y)
Rated frequency (f_n)	50 Hz	50 Hz
Rated current (I_n)	820 A(Δ), 475 A (Y)	30,7 A (Y)
Service (IEC 60034-1)	Continuous service usage S1	Continuous service usage S1
Rated speed (n_n)	2982 rpm	2976 rpm
Motor weight	2200 kg	2700 kg
Motor year of manufacture	2008	1983

Monitoring system

Monitoring of electrical and hydraulic parameters, including active electrical energy E_a, reactive energy E_r, flow rate Q, and pressure p, is performed by a SCADA system dedicated to monitoring these quantities. Electrical parameters are monitored at the measuring point located on the 20 kV busbars and partly on the 6 kV busbar (Fig. 4.12). The collected data is used both for system performance analysis and for billing the energy consumption of the pumping station.

Hydraulic parameters, water volume, flow, and pressure are monitored at the pump station and in the control room. The collected data is monitored at the control room and used to make decisions regarding the start/stop of pump groups, the adjustment/closure of certain routes, or the identification of various problems. The pump groups are started and stopped at the station by the shift on duty.

Analysis of this data highlights critical points associated with energy losses and inefficiencies in the operational process. Based on the information obtained, the performance of the system will be evaluated in order to inform decisions aimed at reducing energy consumption and optimizing sustainability in the interaction between water and energy resources.

4.3.2. Energy quality analysis with local measurements

Electrical energy quality refers to the behavior of electrical quantities over time and their maintenance within the limits specified by standards, so as to ensure the correct operation of electrical equipment [119].

The analysis proposed in this study aimed to identify any voltage variations, load imbalances, or current fluctuations that could influence the operating mode of the asynchronous motor driving the pump in the UP1 pumping unit.

Description of the data set

In order to analyze the quality of the electrical energy supplied to the UP1 pumping unit, the set of electrical measurements taken at the PM2 measuring point on the 0.4 kV busbars was considered. A Qualistar three-phase electrical network analyzer was used for the measurements.

The data was provided by the water supplier and is presented in Annex 4. Fig. 4.13 shows the two measuring points.

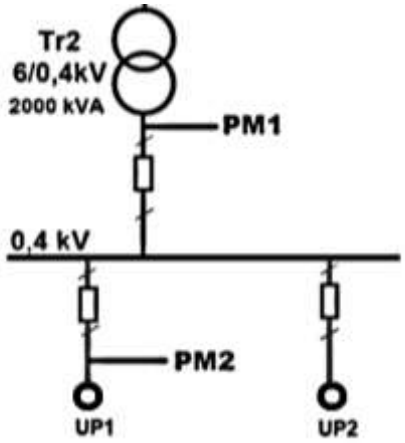

Fig.4.13. Measurement points for electrical quantities for unit UP1 within the Măgurele pumping station

The measurements were taken on January 21, 2020, during continuous operation of the motor-pump assembly, over a period of 639 seconds, for two measurement intervals:

- Data set 1: January 21, 2020, interval 10:18:00-10:21:44, total measurements 361;
- Data set 2: January 21, 2020, interval 10:28:00-10:32:43, total measurements 278.

The duration of the measurements was determined taking into account local technical and organizational conditions, including the availability of measuring equipment, access to the station's electrical infrastructure, and the presence of operating personnel.

The electrical quantities monitored were: line voltage U_l, electric current intensity I, active power P_a, and reactive power P_r. These variables are used to evaluate the electrical performance of the equipment and allow the analysis of the power supply regime from the perspective of electrical energy quality.

Using the monitored data presented in Annex 4, the line voltage curves $U_l(t)$ were plotted for the considered interval at the two measurement points (Fig. 4.14).

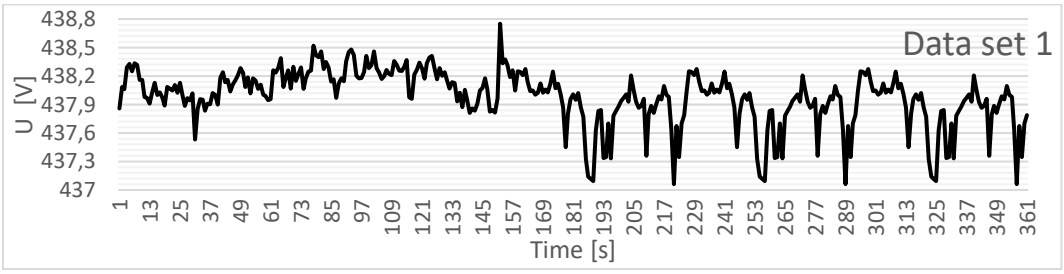

a)

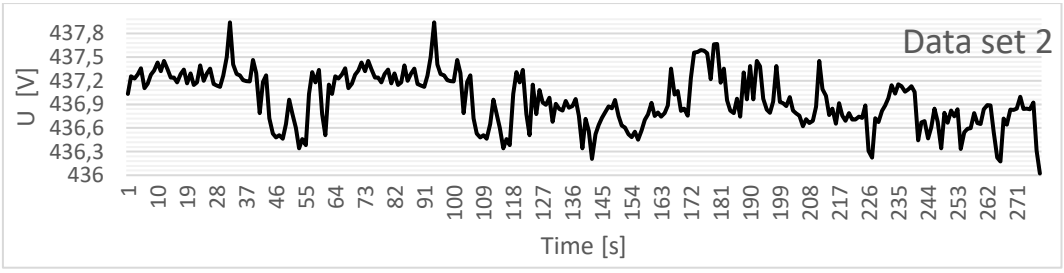

b)

Fig. 4.14. Line voltage curve $U_l = f(t)$ for pump unit UP1 with: a) Data set 1, b) Data set 2

Using the monitored data (Annex 4), the load current intensity curve *I*(*t*) was plotted for the considered interval at the two measurement points (Fig. 4.15).

a)

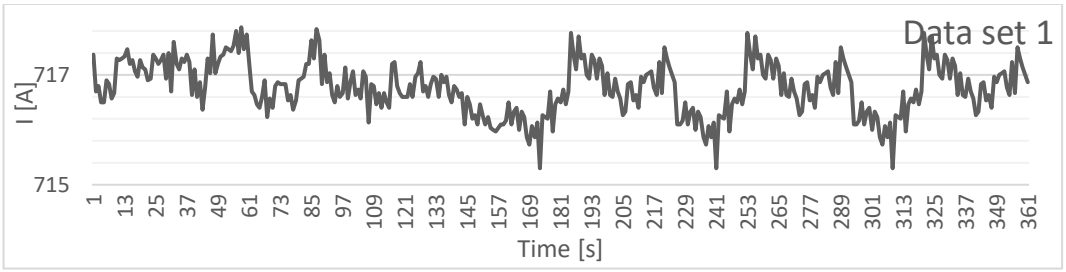

b)

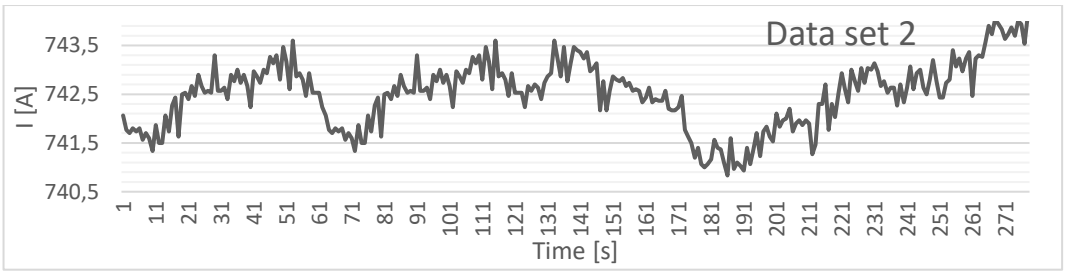

Fig. 4.15. Load current intensity curve $I = f(t)$ for pump unit UP1
with: a) Data set 1, b) Data set 2

Using the monitored data (Annex 4), the active power consumption curve $P_a = f(t)$ was plotted for the time interval considered, at the two measurement points (Fig. 4.16).

a)

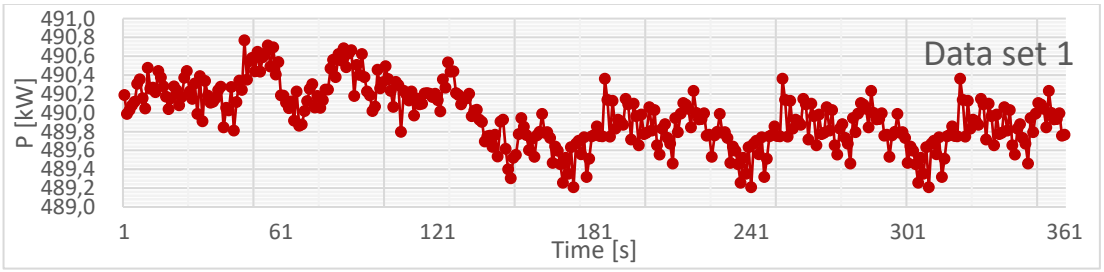

b)

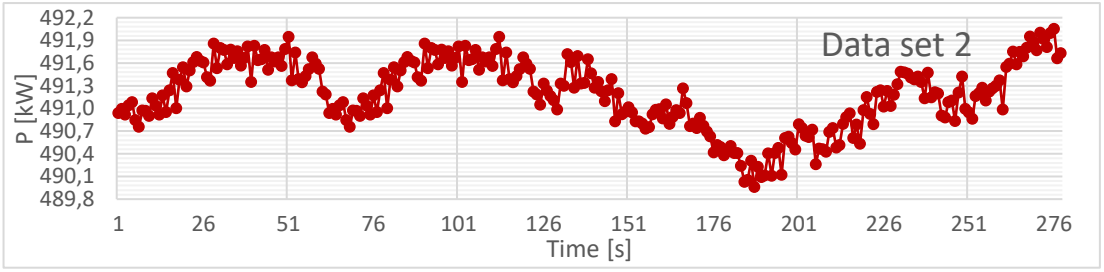

Fig. 4.16. Active power curve $P_a = f(t)$consumed by the UP1 pumping unit with:

a) Data set 1; b) Data set 2

With the monitored data (Annex 4), Fig. 4.17 shows the curves for the power factor in the considered time interval at the two measurement points.

a)

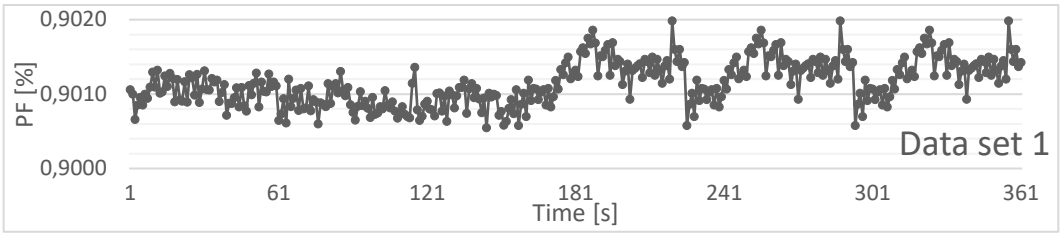

b)

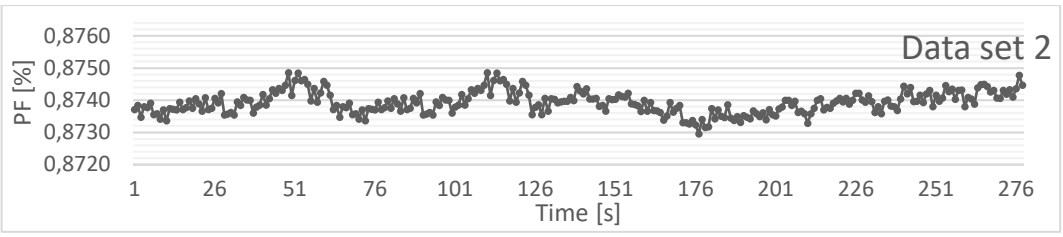

Fig. 4.17. Curve $\cos\varphi = f(t)$ for the power supply of UP1 with: a) Data set 1; b) Data set 2

The results obtained allow the conformity between the characteristics of the power supply and the operating requirements of the motor-pump system to be assessed, providing a basis for the formulation of measures to adjust or improve the operating regime, with a view to more efficient use of energy and reduction of unwanted demands on the pumping unit and internal service consumers.

Statistical processing

Given the large volume of data, processing it in a short time requires the establishment of appropriate procedures for statistical data processing. Descriptive statistics provide simple and easy-to-implement concepts and procedures [120]; [121].

Specific measures that can characterize the data series {x_1, x_2, ..., x_N} are:

The arithmetic mean is calculated using the following formula:

$$X_{med} = \frac{1}{N} \cdot \sum_{i=1}^{N} x_i \tag{4.15}$$

where N is the total number of elements in the sequence, x_i is the value of the i element of the sequence, and X_{med} is the arithmetic mean of the data sequence.

The mean square deviation is obtained as the square root of the dispersion D_s using the following formula:

$$s = \sqrt{D_s} = \sqrt{\frac{1}{N-1}\sum_{i=1}^{N}(x_i - X_{med})^2} \tag{4.16}$$

where: s is the mean square deviation, and X_{med} represents the arithmetic mean value of the data series.

The coefficient of variation of the data series is obtained as the percentage ratio between the mean square deviation and the arithmetic mean of the values in the data series:

$$CV = \frac{s}{X_{med}} \cdot 100\ [\%] \tag{4.17}$$

The coefficient of variation can be used to compare the dispersion of different distributions according to variables expressed in different units of measurement. The coefficient of variation provides information on whether or not the data series is homogeneous.

The coefficient of variation can take values between $0 < CV < 100\ \%$. When CV tends towards zero, the variability is low, so the population is homogeneous and the mean has a high degree of representativeness. The closer the coefficient of variation is to 100%, the greater the variability, the more heterogeneous the population, and the lower the representativeness of the mean.

As a result, the coefficient of variation can be used as a test of the representativeness of the mean, considering the following significance thresholds:

$0 < CV \leq 17\ \%$ - the mean is strictly representative;

$17 < CV \leq 35\ \%$ - the mean is moderately representative;

$35 < CV \leq 50\ \%$ - the mean is representative in a broad sense;

$CV > 50\ \%$ - the mean is unrepresentative.

The shape coefficient depends on the coefficient of variation CV and is calculated using the following formula:

$$k_f = \sqrt{1 + (CV)^2} \tag{4.18}$$

The standard error depends on the mean square error s and is calculated using the following formula:

$$SE = \frac{s}{\sqrt{N}} = \frac{\sqrt{\frac{1}{N-1}\sum_{i=1}^{N}(x_i - X_{med})^2}}{\sqrt{N}} \tag{4.19}$$

Standard error is used to determine the confidence interval of the mean. The mean and standard error are the main descriptors for a series of data resulting from measurements. If the standard error is large, the mean is not representative of the data series.

(1) Data analysis for electrical voltage

Electrical voltage is the fundamental quantity that determines the potential for transferring electrical energy between two points in a circuit. The stability and nominal value of the voltage ensures the quality of the electrical energy, directly influencing the operation of the equipment and the efficiency of the pumping unit. Voltage variation analysis allows the identification of fluctuations, imbalances, and possible deviations from normal operating conditions, factors that can affect equipment performance and reliability.

According to SR EN 50160:2011, in low-voltage networks (400 V), the permissible voltage variation is ±10%. For a nominal voltage of 400 V, the permissible range is: $(400 \pm 40)\ V$.

Using relations (4.1) – (4.5), statistical indicators were calculated for the series of line voltage values {U_i}, measured at measurement point PM1 (N=361) and measurement point PM2 (N=271).

The data was processed in Excel to obtain the statistical parameters. The values obtained are summarized in Table 4.3.

Table 4.1. Statistical parameters for the supply voltage of the UP1 pumping unit

for data sets 1 and 2

Measurement point	U_{med} [V]	U_{min} [V]	U_{max} [V]	s [V]	SE [V]	CV [V]
Data set 1	437,9774	437,0613	438,7509	0,0154	0,0154	0,0006
Data set 2	436,9618	436,0228	437,9409	0,3378	0,0202	0,0007

Findings:

The average electric current intensity in Data Set 1 (716.76 A) and Data Set 2 (742.50 A) indicates that the motor is operating under partial load, below the rated intensity of 820 A. The difference between the two data sets is due to the distinct positioning of the measurement points: Set 2 reflects the direct consumption of the motor, while Set 1 records an aggregate current, influenced by other consumers or losses. Current fluctuations are lower in Data Set 1 due to the compensating effect of several consumers, while Set 2 directly captures variations in the motor load.

(2) Data analysis for load current intensity

The electric current intensity is a key parameter in the analysis of the operating regime of equipment, playing a direct role in assessing the quality of the supplied electrical energy. Variations in current intensity reflect consumption fluctuations, phase imbalances, or transient states within the pump–motor system, thereby influencing both energy efficiency and operational stability.

Using equations (4.1) through (4.5), statistical indicators were calculated for the current load {I_i}, series measured in Dataset 1 (N = 361) and Dataset 2 (N = 271).

Data processing for the determination of statistical parameters was performed using Microsoft Excel. The resulting values are summarized in Table 4.4.

Table 4.2. Statistical Parameters for Electric Load Current Intensity – Dataset 1 and Dataset 2

Measurement point	I_{med} [A]	I_{min} [A]	I_{max} [A]	s [V]	*SE*	CV
Data set 1	716,76	715,30	717,86	0,4724	0,0248	0,0006
Data set 2	742,50	740,83	744,13	0,6785	0,0406	0,0009

Constatări:

The mean electric current intensity recorded in Dataset 1 (716.76 A) and Dataset 2 (742.50 A) indicates that the motor operates under a partial load regime, below its nominal current rating of 820 A. The difference between the two datasets is attributed to the distinct placement of the measurement points: Dataset 2 reflects the direct current consumption of the motor, while Dataset 1 captures an aggregated current value, influenced by additional consumers or distribution losses.

Current fluctuations are lower in Dataset 1 due to the compensatory effect of multiple consumers within the measurement scope, which leads to an averaging behavior. In contrast, Dataset 2 directly captures the dynamic variations of the motor load, thus presenting higher variability. This distinction is critical for the correct interpretation of the electrical behavior of the system and for identifying specific operational characteristics of the pump–motor assembly.

(3) Data analysis for active power

The load curve for the pump unit describes the variation in active power P_a consumption over a period t of operation: $P_a = f(t)$. The measured data was statistically processed using Excel. Using equations (4.1) to (4.5), statistical indicators were calculated for the series of active power values {P_{ai}}, measured at measurement point PM1 (N=361) and measurement point PM2 (N=271). Table 4.5 shows the values obtained for: mean, standard deviation, and asymmetry.

Table 4.5. Statistical parameters for the active power input into the UP1 pumping unit, measured at measurement points Data set 1 and Data set 2

Table 4.3. . Statistical parameters for the active power input into the UP1 pumping unit, measured at measurement points Data set 1 and Data set 2

Measurement point	P_{med} [kW]	P_{min} [kW]	P_{max} [kW]	S[kW]	*SE*	CV
Data set 1	489,9599	489,2080	490,7670	0,3148	0,0165	0,0006
Data set 2	491,1921	489,9590	492,0530	0,4524	0,0271	0,0009

Findings:

- The average values for the active power input into the UP1 pump unit are P_{med_1}= 489.95 kW (in the case of data set 1) andP_{med_2} = 491.19 kW (in the case of data set 2), which are values below the electrical power corresponding to operation in nominal mode: $P_{a_n} = P_n/\eta_n = 549{,}45$ kW.
- Operation of the electric motor driving the pump below the nominal point involves a shift of the hydraulic operating point to areas characterized by lower hydraulic and energy efficiencies, according to the information in section 4.2.2.A.
- The standard deviation of the active power is lower in Data Set 1 (0.314867 kW) compared to Data Set 2 (0.452410 kW), which indicates a lower dispersion of values and, implicitly, a higher stability of consumption in the first case.
- The minimum active power value is higher in Dataset 2 (489.959 kW) than in Dataset 1 (489.208 kW), suggesting that in Dataset 2, power consumption did not reach such low minimum levels.

- The maximum active power value is also higher in Data Set 2 (492.053 kW) than in Data Set 1 (490.767 kW), indicating the presence of more pronounced consumption peaks in the second case.

The utilization factor is the ratio between the average value of a quantity and the nominal value of the same quantity, and is used to express the degree of utilization of the nominal capacity of an electrical system or equipment.

The utilization factor for the active power measurement set is calculated using the following equation:

$$k_{u_P} = \frac{P_{a_{med}}}{P_{a_n}} \tag{4.20}$$

where$P_{a_{med}}$ is the average active power, andP_n is the nominal power.

This dimensionless quantity provides additional information about the efficiency of available resources and the effective load on the system:

- A utilization factor close to 1 suggests that the average active power is close to the rated power, indicating efficient and almost complete utilization of the system's capacity.

- Values significantly lower than 1 indicate underutilization of available resources, suggesting that the system is operating well below its rated capacity.

The average value of the active power calculated for the measurement interval considered, as well as the value of the utilization factor, are presented in Table 4.6.

Table 4.4 Calculated values of average active power and utilization factor for measurements at Pumping Unit 1

No.	Measured physical quantity	Symbol	Data set 1	Data set 2
1	Average active power absorbed [kW]	$P_{a_{med}}$	489,95	491,19
2	Nominal active power at shaft [kW]	P_{a_n}	500	500
3	Load factor [%]	k_{u_P}	0,97	0,98

The rated power of the motor is the shaft power, i.e. the mechanical power.

Findings:

The values very close to 1 determined for the load factor indicate that the system is operating close to its rated capacity at both measurement points, suggesting efficient use of available resources.

The percentages of 97.99% in the first case and 98.24% in the second case show that there is no overload and that the system is operating in an optimal mode.

(4) Data analysis for the power factor

The power factor, defined as the ratio between active power and apparent power, is an essential indicator of energy efficiency and electricity quality. For an optimal energy regime, technical standards require that it be maintained above 0.92. Data set 1 complies with this requirement, indicating an efficient regime, while data set 2 shows a drop below the regulated threshold, suggesting energy losses and the need for intervention. Therefore, corrective measures such as reactive energy compensation and load balancing are required to restore the efficiency and quality of the power supply.

4.3.3. Analysis of electricity consumption for 2024

The energy efficiency of the pumping station is directly related to the efficiency of the pumping units and the way the equipment is operated and used.

In order to determine ways to increase the efficiency of the Măgurele pumping station, data provided by the SCADA system on active and reactive electricity consumption for 2024 was taken into account.

Description of the data set

The data set reflects the values recorded at the PMC measuring point located on the 20 kV busbar, allowing the consumption of the entire assembly supplied from the medium voltage network to be monitored via the ELSTER A1800 ALPHA meter. The measurement circuit includes transformers Tr1, Tr2, and Tr3, as well as the main consumers (UP1 and UP2) and auxiliary consumers (heating – 24 kW, lighting – 3 kW, various equipment – 3.5 kW).

The data monitored by the SCADA system includes active and reactive energy measurements taken at the PMC measuring point throughout the year 2024, with a recording frequency of one hour for active energy (N= 8,784) and 15 minutes for reactive energy and power factor (N=35,136).

The recorded data, together with the relevant statistical processing and related graphical representations, are presented in Annex 5.

Fig. 4.19 shows the curves of active energy consumption, reactive energy consumption, and the evolution of the power factor for 2024. To represent this graph, the data for daily consumption was processed and the values obtained are represented graphically.

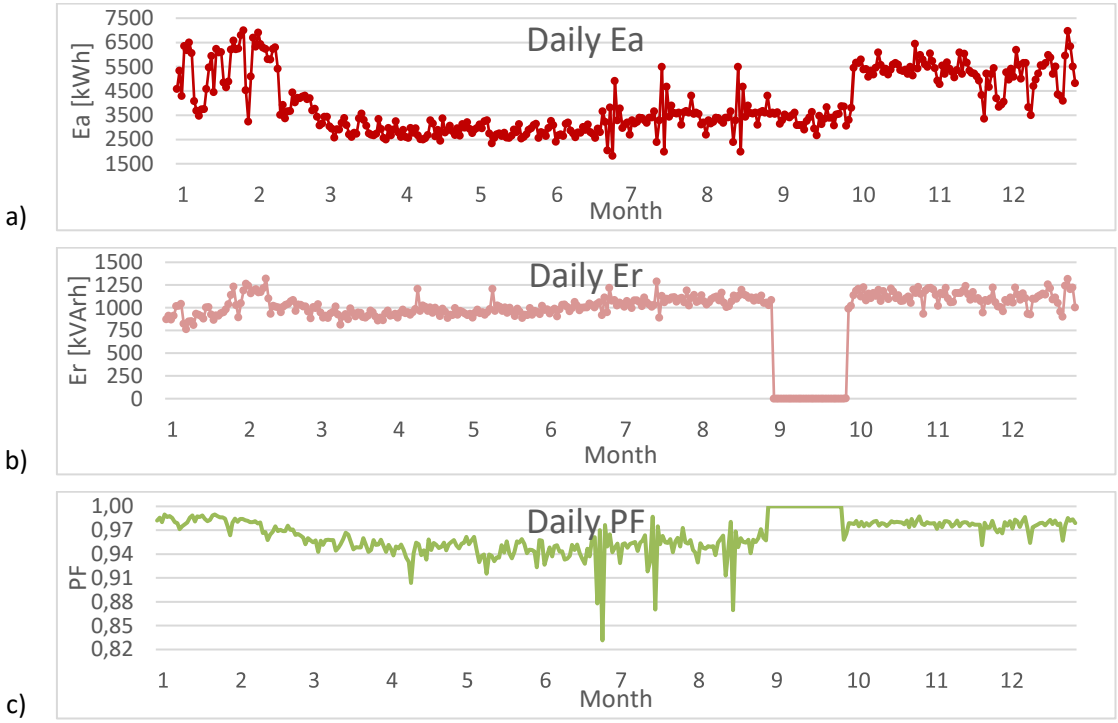

Fig. 4.19. Graph of data monitored with SCADA at the Măgurele Pumping Station in 2024 for: a) Active electrical energy, b) Reactive electrical energy, c) Power factor

The three graphs in Fig. 4.19 show the evolution of daily active energy consumption (Ea), reactive energy (Er), and power factor (PF) throughout 2024, indicating significant seasonal variability in active energy, zero reactive energy consumption in September (due to exemption from payment), and a power factor that generally remains above 0.94, with occasional decreases in April, June, and July, suggesting temporary episodes of energy inefficiency.

(1) Analysis of monthly electricity consumption for 2024

Given that consumption is reported on a monthly basis, the uniformity of electricity consumption in 2024 at the Măgurele pumping station was first analyzed. The data was processed in Excel.

The monthly active and reactive energy consumption for 2024, expressed in MWh, is shown in Fig. 4.20 and Table 4.7.

a)

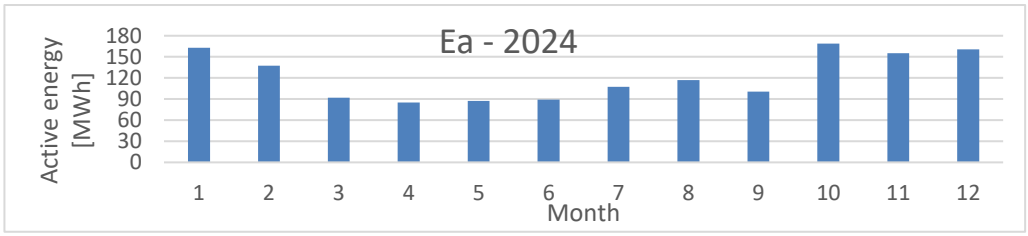

b)

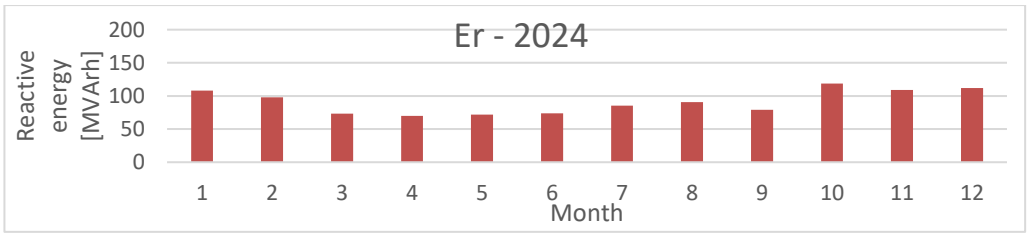

Fig. 4.2. Graph showing monthly consumption of active energy (a) and reactive energy (b) at the Măgurele pumping station in 2024

Fig. 4.20 shows a seasonal variation in active and reactive energy consumption in 2024, with minimum values in the spring months (March–May), corresponding to a reduced operating regime, and maximum values in the autumn and winter months (October–December), when an increase in energy load is observed, possibly associated with specific operating conditions or increased technological requirements.

Findings:

The station's energy consumption varies seasonally, with maximums in October (169 MWh active, 118.87 MVArh reactive) and minimums in April, indicating fluctuating demand. The annual average is 121.89 MWh active energy and 90.79 MVArh reactive energy, with moderate fluctuations. There is an average discrepancy of 61.56 MVArh between the measured and billed reactive energy, which requires attention in order to optimize consumption and adapt the operating regime.

(2) Analysis of daily electricity consumption for 2024

For a detailed assessment of the operating regime of the Măgurele Pumping Station in 2024, the daily values of active electricity Ea, reactive electricity Er, and power factor $\cos \varphi$ were centralized and analyzed based on measurements taken in the PMC, retrieved by SCADA, and presented in Annex 5. This analysis aimed to identify consumption trends, evaluate daily energy performance, and support decisions on optimizing energy use, including through measures to reduce reactive energy and improve the power factor.

Hourly data was processed in Excel to obtain daily values and determine statistical parameters. For the Ea, Er, and PF values, a total of N=1098 values were obtained, which are summarized in Table 4.8.

Table 4.5. Statistical processing for daily active energy consumption, reactive energy, and power factor for the year 2024.

Statistical processing	E_{az} [kWh]	E_{rz} [kVArh]	PF_z [%]
Average value	3970,32	953,12	0,9643
Standard error	64,16	15,79	0,0011
Standard deviation	1227,563	302,17	0,0221
Minimum value	1826	6,03	0,8314
Maximum value	6997	1320,33	1
Number of readings	366	366	366

Findings:

Variations in the station's daily energy consumption are manifested by maximums of 6997 kWh active energy (Ea) and 1320.33 kVArh reactive energy (Er), influenced by the inductive load. The daily average is

3970.32 kWh for Ea and 953.12 kVArh for Er. There is an average daily discrepancy of 61.56 kVArh between the measured reactive energy and the billed reactive energy, which may be justified by the contract.

(3) Determination of the actual operating time of the pumping units

The analysis of the ratio between the operating time of the pumping units and the downtime was performed by processing the set of data for active energy $\mathrm{Ea(t)}$,, monitored with the SCADA system and presented in Annex 5.

From the series $\{t_i\}$ corresponding to the monitored time intervals (N=8784), the series of data with operating times $\{t_{fi}\}$ and the series with non-operating/shutdown times $\{t_{oi}\}$, were separated and constructed, with the following condition: $t_{oi} \neq 0$ pentru $E_{\mathrm{a}} \leq 0{,}350$ kWh.

The operating times T_{fi} and shutdown times T_{oi} were calculated for each month of 2024 by summing the terms of the strings corresponding to the operating/shutdown hours.

$T_{fi} = \sum_i t_{fi}$, cu *i*= 1, ... , 12 (4.21)

$T_{\mathrm{oi}} = \sum_i t_{oi}$, cu *i*= 1, ... , 12 (4.22)

Fig. 4.21 shows the graph of operating times and downtimes for all months of 2024 for the pumping units at the Măgurele pumping station.

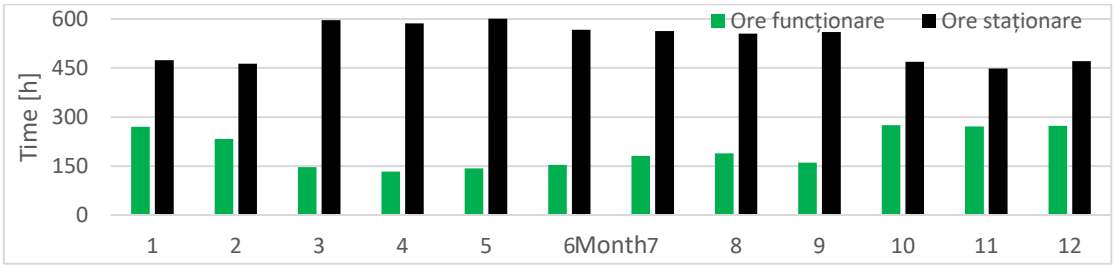

Fig. 4.21. Graph showing operating times and corresponding shutdown times for pumping units for the months of 2025

Table 4.9 summarizes the operating and shutdown times, in hours and %, in 2024 for the pumping units within the SPM.

Table 4.9. Operating and shutdown times for each month of 2024 for the pumping units at the Măgurele Pumping Station

Month	T_{f1}		T_{o1} [h]		Total per month
	[h]	[%]	[h]	[%]	[h]
January	270	36.3	474	63.7	744
February	233	33.5	463	66.5	696
March	147	19.8	597	80.2	744
April	133	18.5	587	81.5	720
May	143	19.2	601	80.8	744
June	153	21.3	567	78.7	720
July	181	24.3	563	75.7	744
August	189	25.4	555	74.6	744
September	160	22.2	560	77.8	720

Month	T_{f1}		T_{o1} [h]		Total per month
	[h]	[%]	[h]	[%]	[h]
October	275	37.0	469	63.0	744
November	271	37.6	449	62.4	720
December	273	36.7	471	63.3	744
TOTAL	*2428*		*6356*		*8784*

Table 4.10 presents a detailed statistical analysis of the operational behavior of the pumping units, by calculating specific descriptive indicators (monthly average, standard deviation, etc.) for operating and shutdown hours.

Table 4.10. Statistical indicators of the operating and shutdown time of the pumping units in 2024

Statistical processing	Operating hours	Non-operating hours
Monthly average	202,33	529,66
Standard error	16,68	17,00
Standard deviation	57,80	58,89
Minimum monthly value [h]	133	449
Maximum monthly value	275	601
Total	*2428*	*6356*

Findings:

Pumping units record the longest operating times in October, November, and December, signaling high seasonal demands, while March and April show reduced operating times. Statistically, the units operate an average of 202.33 hours per month and are shut down for 529.66 hours, indicating a regime dominated by inactivity. The energy efficiency of the system depends on the use of high-efficiency equipment and the optimization of the operating mode by adapting to demand and advanced control strategies.

4.3.4 Determination of Energy Intensity

For the Măgurele Pumping Station, the energy intensity was determined based on SCADA data from the year 2024, calculated as the ratio between the active electrical energy consumed (Annex III) and the volume of water pumped (Annex IV), in accordance with Table 3.2.

The analysis was conducted for representative days in August, September, and October, selected according to the annual consumption variability, differentiating between working days and non-working days to assess the impact of operational regime on energy consumption.

(1) Flow measurement system

The dataset extracted from the SCADA system includes time series for the water flow rate in the discharge pipe of the pumping units UP1/UP2, covering the period from August 25, 2024, at 15:42 to October 22, 2024, at 20:11. Fig 4.22 presents the hydraulic scheme of the Măgurele Pumping Station.

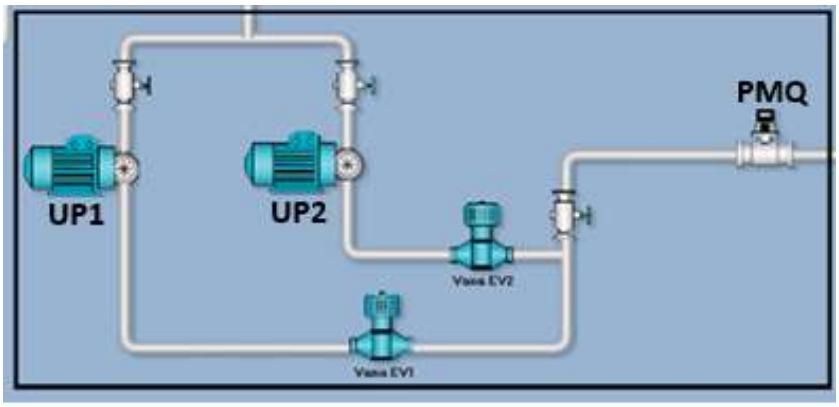

Fig. 4.22. Hydraulic Scheme of the Măgurele Pumping Station

The UP1 and UP2 units transport water from reservoirs R1 and R2 to reservoir R3. The hydraulic parameters were monitored at the measurement point PMQ using a remote-reading electromagnetic flowmeter. The recordings were made with a sampling frequency of 1 minute, totaling N = 83,778 values, as presented in Annex 6. Data processing was performed using Microsoft Excel.

(2) Determination of the daily characteristic curve for the analyzed period and statistical processing

The daily flow curve highlights the overall variation of the discharge over time and allows for the observation of increasing trends or fluctuations in the volume of water processed on a daily basis, providing a synthetic and relevant overview of the system's operating regime over the short and medium term.

Figure 4.23 presents the variation curves of active electric energy consumption and flow rate corresponding to the analyzed period, which spans from August 26, 2024, to October 22, 2024.

a)

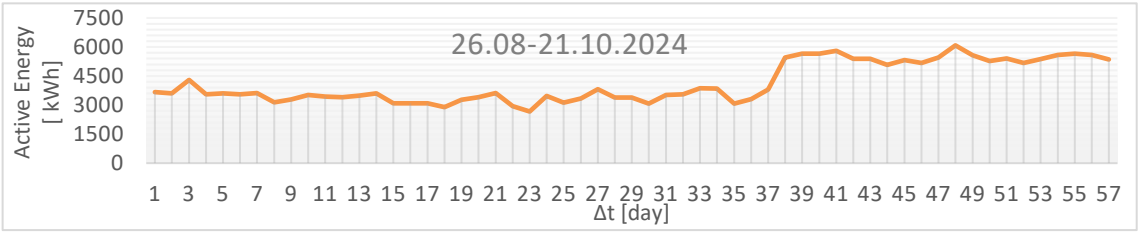

b)

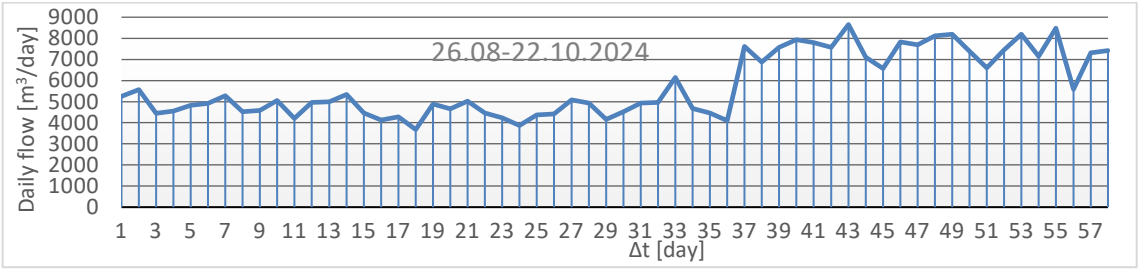

Fig. 4.23. Consumption curve during the period 26.08-22.10.2024: a) electricity, b) water flow

This graphical representation highlights the overall variation of the flow rate over time and serves as the basis for the associated statistical processing, which is employed to analyze the behavior of the hydraulic system during the corresponding period.

Table 4.11 presents the values obtained for the total daily flow during the period 26.08-22.10.2024, for N=59.

Table 4.11 Daily flow values during the period 26.08-22.10.2024

Parameter	Measured Value	Mean Value	Minimum Value	Maximum Value
Daily active energy [kWh]	4167,7	2669	6085	1040,02

Daily water flow volume [m³/zi]	138447,9	88239,3	207695	36045,2

The station's daily flow exhibits significant fluctuations, with an average of 138,447.9 m³/day and considerable deviations, ranging between 88,239.3 m³/day and 207,695 m³/day. The daily active energy consumption is correlated with these variations, presenting an average value of 4,167.7 kWh and oscillating between 2,669 kWh and 6,085 kWh. This behavior indicates an operating regime characterized by variable load conditions.

(3) Obtaining uptime and downtime

The operating time was determined by summing the minutes during which the system was in an operational state, while the downtime was calculated by aggregating the intervals of inactivity throughout the entire monitoring period. This approach allowed the durations to be expressed in both minutes and percentages for defined time intervals. Figure 4.24 illustrates, for the period between August 25, 2024, and October 22, 2024, a total monitored time of 1,396.3 hours, of which 463.72 hours (33%) correspond to system operation and 932.58 hours (67%) to system stoppage. The bar chart indicates an increase in the percentage of operational time in October (43%) compared to August (30%) and September (28%).

Findings:

During the August–October 2024 interval, a total of 83,778 minutes (1,396.3 hours) were monitored, out of which 27,823 minutes (463.7 hours) corresponded to operational periods (33.2%), while 55,955 minutes (932.6 hours) represented system downtime (66.8%). In August, the operating time amounted to 2,700 minutes (29.6%), and in September to 11,880 minutes (27.5%), indicating a reduced operational availability. A significant increase in functionality was observed in October, with 13,620 minutes (43.2%), reflecting an improvement of approximately 15% relative to the average of the previous two months.

The temporal distribution indicates a fluctuating usage regime, with minimum availability recorded in August and September, followed by a recovery trend in October. These variations suggest possible changes in operational requirements or interventions on the equipment, which require correlation with additional technical data to determine the underlying causes.

(4) Determining the energy intensity for the typical consumption day

Establishing characteristic days

The analysis of the water and active energy dataset, presented in Annex IV, revealed a daily cyclicity in the flow rate curves, as well as significant seasonal variability. Based on this evaluation, two representative days were selected to interpret the system's behavior according to the operational regime: Wednesday, representative of working days, with flow rate values corresponding to August 28, 2024, September 18, 2024, and October 16, 2024; and Saturday, characteristic of non-working days, with data extracted from August 31, 2024, September 21, 2024, and October 19, 2024

Fig. 4.25 illustrates the dynamics of the operating regime for working days.

a)

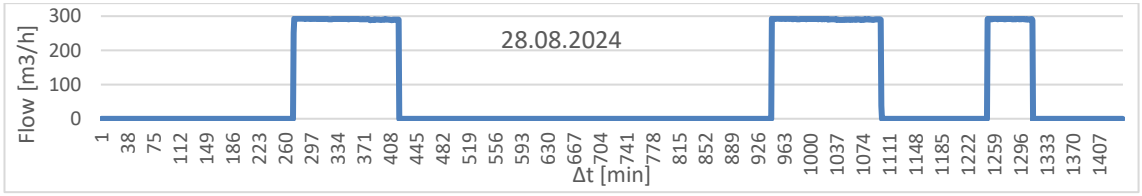

b)

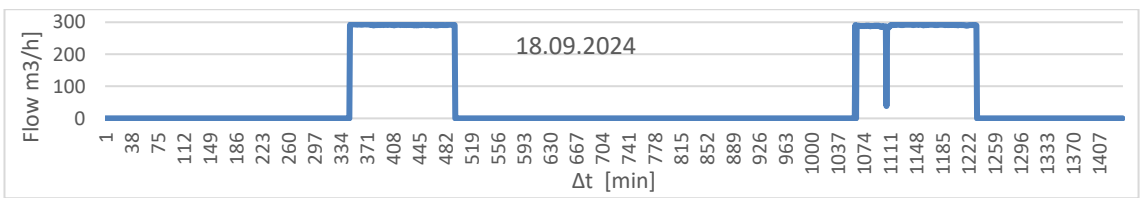

c)

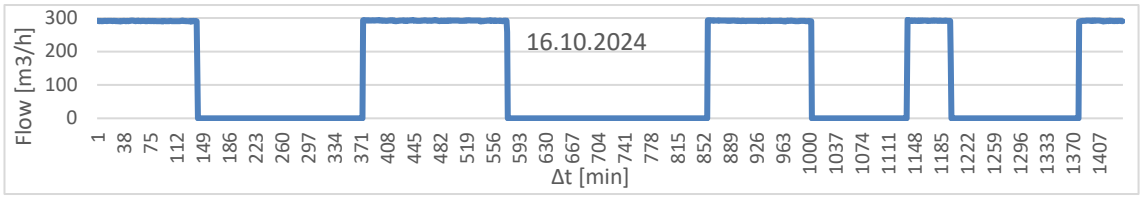

Fig. 4.25. Flow curves for characteristic days of Wednesday: a) ZL1 (28.08.2024); b) ZL2 (18.09.2024); c) ZL3 (16.10.2024)

Table 4.12 summarizes data on flow rates and operating/stop times for typical working days.

Table 4.12. Parameters determined for typical working days in the analyzed period

No.	Charact. Day	Operating Interval	Operation time [min]	Operation time [ore]	Operation [%]	Qmed [m3/h]	Qmin [m3/h]	Qmax [m3/h]	V med [m3]
1	ZL1	I	149	2,48	10,35	290,97	250,00	293,71	722,576
2		II	155	2,58	10,76	291,03	288,63	293,30	751,838
3		III	65	1,08	4,51	291,40	287,62	292,76	315,687
		Total ZL1	**369,00**	**6,15**	**25,63**				**1790,10**

No.	Charact. Day	Operating Interval	Operation time [min]	Operation time [ore]	Operation [%]	Qmed [m3/h]	Qmin [m3/h]	Qmax [m3/h]	V med [m3]
1	ZL2	I	149	2,48	10,35	291,82	290,24	293,79	724,681
2		II	171	2,85	11,88	289,07	283,00	292,73	823,835
		Total ZL2	**320,00**	**5,33**	**22,22**				**1548,52**

No.	Charact. Day	Operating Interval	Operation time [min]	Operation time [ore]	Operation [%]	Qmed [m3/h]	Qmin [m3/h]	Qmax [m3/h]	V med [m3]
1	ZL3	I	141	2,35	9,79	289,93	289,85	292,35	681,343
2		II	203	3,38	14,10	292,02	257,62	293,47	988,001
3		III	146	2,43	10,14	291,64	290,05	293,29	709,657
4		IV	62	1,03	4,31	292,00	291,04	295,11	301,735
5		V	62	1,03	4,31	291,51	289,56	292,83	301,227
		Total ZL3	**614,00**	**10,23**	**42,64**				**2981,96**

Findings:

In October (Working Day 3 – WD3), the operating duration increased significantly to 10.23 hours (42.64% of the day), compared to 6.15 hours in August (WD1) and 5.33 hours in September (WD2), suggesting an increased water demand or intensified activity dependent on water supply. The total volume pumped on WD3 (2,981.96 m³) is nearly double that of WD1 and twice as much as on WD2, indicating a sustained operational regime.

The average flow rate (Q_{avg}) remains consistent, between 290 and 292 m³/h, reflecting the system's operational stability and efficiency. Flow variability is low; however, in WD3, Interval II recorded a minimum of 257.62 m³/h, suggesting a possible transient fluctuation or a functional adjustment.

The daily operation percentage is proportional to the pumped volume, highlighting, in WD3, the system's capacity to flexibly respond to hydraulic demands. WD2 stands out by having the lowest operating time and the smallest processed volume, which may be associated with either reduced demand or improved efficiency in operation.

Fig. 4.26 illustrates three characteristic Saturday days: 31.08, 21.09 and 19.10.2024

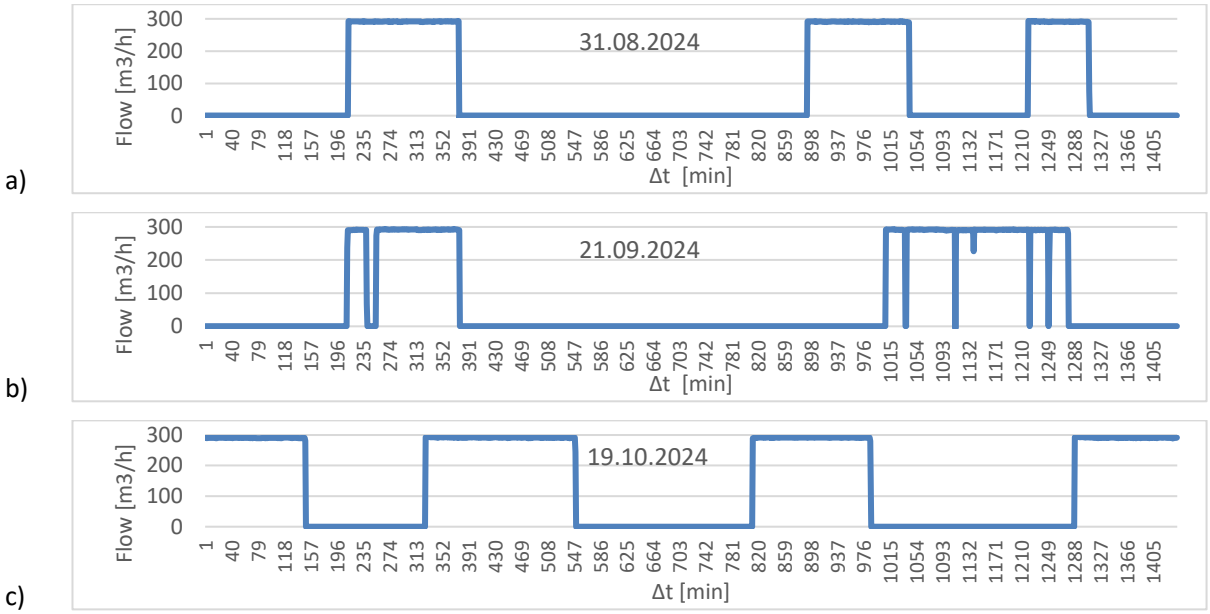

Fig. 4.26. Flow curves for characteristic days on Saturday: a) ZN 1 (31.08.2024); b) ZN 2 (21.09.2024) and c) ZN 3 (19.10.2024)

Table 4.13 summarizes the data for operating and non-operating time for typical working days.

Table 4.13. Parameters determined for characteristic non-working days in the analyzed period

No.	Charact. Day	Operating Interval	Operation time [min]	Operation time [ore]	Operation [%]	Qmed [m3/h]	Qmin [m3/h]	Qmax [m3/h]	V med [m3]
1	ZN1	I	165	2,75	11,46	291,7	289,8	293,1	802,126
2		II	151	2,52	10,49	291,2	289,2	295,6	732,921
3		III	91	1,52	6,32	291,3	289,9	293,6	441,831
		Total ZN1	**407,00**	**6,78**	**28,26**				**1976,88**

No.	Charact. Day	Operating Interval	Operation time [min]	Operation time [ore]	Operation [%]	Qmed [m3/h]	Qmin [m3/h]	Qmax [m3/h]	V med [m3]
1	ZN2	I	154	2,57	10,69	291,2	289,2	295,6	747,483
2		II	267	4,45	18,54	290,9	226,8	293	1294,54
		Total ZN2	**421,00**	**7,02**	**29,24**				**2042,02**

No.	Charact. Day	Operating Interval	Operation time [min]	Operation time [ore]	Operation [%]	Qmed [m3/h]	Qmin [m3/h]	Qmax [m3/h]	V med [m3]
1	ZN3	I	149	2,48	10,35	290,4	281,7	292	721,252
2		II	223	3,72	15,49	291,6	244,7	294,1	1083,77
3		III	175	2,92	12,15	291,4	279,9	293,6	850,051
4		IV	152	2,53	10,56	291,2	288,7	293,8	737,636
		Total ZN3	**552,00**	**9,20**	**38,33**				**2680,74**

Findings:

The operating duration of the water supply system increased significantly from 6.78 hours in zone ZN1 (28.26%) to 9.20 hours in zone ZN3 (38.33%), indicating higher demand during October, including on non-working days. The average hourly flow rate (Q_{avg}), ranging between 290.44 and 291.68 m³/h, reflects a stable operational regime. The closely aligned maximum flow rates (Q_{max})—ranging from 291.97 to 295.55 m³/h—confirm the system's ability to efficiently manage load variations.

In zone ZN2, the minimum recorded flow rate (Q_{min}) of 226.84 m³/h may suggest either a temporary decrease in demand or a short-term optimization of operations. The total volume pumped in ZN3 (2,680.74 m³) highlights a high level of operational activity, including during the weekend regime.

The stability of flow parameters and the similarity in consumption patterns between working and non-working days support the characterization of a constant operational regime. The energy intensity indicator, expressed in kWh/m³, serves as a critical metric in evaluating the energy efficiency of the system. It facilitates comparative assessments across zones and time periods and supports the development of sustainable resource management strategies. The energy intensity values were determined and are illustrated in the graph presented in Figure 4.27.

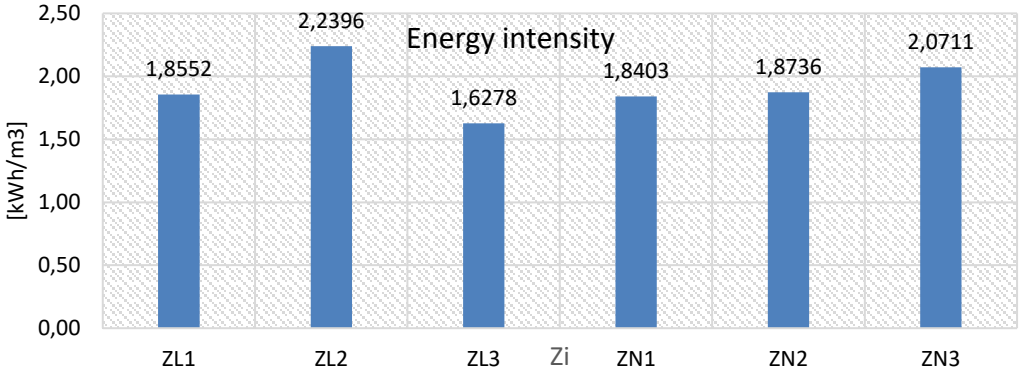

Fig. 4.27. Energy intensity at the Măgurele Pumping Station for typical working days (ZL1-3) and non-working days (ZN1-3)

The analyzed chart presents the energy intensity values recorded during the August–October 2024 period, highlighting significant variations between the analyzed days. The highest value was observed on September 18, 2024 (a working day), with a specific energy consumption of 2.2396 kWh/m³, while the lowest value, 1.6278 kWh/m³, was recorded on October 16, 2024, also a working day.

The values corresponding to non-working days ranged between 1.8403 and 2.0711 kWh/m³, indicating variable energy efficiency even under reduced operating regimes.

The average value calculated for the entire period is 1.9179 kWh/m³, reflecting a moderate energy performance. These data confirm the importance of continuous monitoring of this indicator—emphasized in Chapter 3 of the thesis—to detect deviations from the optimal operational regime and to support the development of operational optimization measures.

The energy intensity values obtained during the analyzed period can be considered relatively high when compared to technical benchmarks reported in the specialized literature. According to the International Water Association (IWA), for well-optimized water supply systems, energy intensity typically ranges between 0.4 and 1.2 kWh/m³, which is considered standard for modern networks with high operational efficiency [67].

In the comparative study conducted under the European AquaRatio project, most water utility operators in Europe reported values between 0.6 and 1.6 kWh/m³, depending on the network configuration, the level of automation, and water loss rates [122].

Values exceeding the threshold of 2.0 kWh/m³ are characteristic of systems operating under unfavorable topographic conditions, using low-efficiency pumping equipment, or functioning under excessive pressure conditions [75]. Therefore, the values obtained in this analysis reflect a specific energy consumption above the European average, suggesting a significant potential for energy efficiency improvement.

Recommended interventions include the modernization of pumping equipment, implementation of high-efficiency technologies, and reduction of water losses through advanced pressure control strategies, in accordance with best practices promoted by the IWA and the European Union directives on energy efficiency [123].

4.4. Hourly Energy Balance for Pumping Unit UP1

Based on the recognition that the energy balance is an essential tool for evaluating energy performance and supporting decision-making regarding the efficiency of electrical supply systems to consumers, this case study aims to establish the hourly energy balance for pumping unit UP1 within the Măgurele pumping station.

According to methodology [PE 902/86], the energy balance enables detailed assessment of energy flows within a defined technical boundary. For the pumping unit UP1, the balance boundary includes the 20 kV busbar, the 20/6 kV electrical transformer Tr1, the 6/0.4 kV electrical transformer Tr2, the 0.4 kV busbar, and the pumping unit UP1 itself.

The energy balance is established based on the equation:

$$E_i = E_u + \Delta E_P + \Delta E_{cmp} + \Delta E_M + \Delta E_{L0,4} + \Delta E_{Tr2} + \Delta E_{L0,6} + \Delta E_{Tr1} \quad (4.23)$$

where: $\mathrm{E_i}$- electrical energy input into the system boundary, $\mathrm{E_u}$- useful energy delivered by the pump to the transported fluid și $\Delta\mathrm{E}$- losses in the components of the power supply system of pumping unit UP1.

The preparation of the hourly energy balance is based on the dataset measured with the Qualistar analyzer, described in Appendix 4, on January 21, 2020, during the interval 10:28:00–10:32:43. These data were processed and analyzed in Section 4.3.1. The hourly active power consumption for pumping unit UP1 was considered as the average of the measured and analyzed values (Table 4.19), assuming that the pumping unit operates under the same conditions for one hour.

Table 4.19. Hourly Active Power Consumption for Pumping Unit UP1

Active Power Consumption	P_{med} [kW]	P_{min} [kW]	P_{max} [kW]
	490,57	489,20	492,05

Hourly Water Flow Rate Pumped by Pumping Unit UP1

Hourly Flow Rate	Q_{med} [m³/h]	Q_{min} [m³/h]	Q_{max} [m³/h]
	291,5	289,7	293

Electric Current Intensity Supplying Pumping Unit UP1

Electric Current Intensity	I_{med} [A]	I_{min} [A]	I_{max} [A]
	729,63	715,30	744,13

The energy balance is conducted in an ascending manner (bottom-up), starting from the pumping unit and tracing the energy flows toward the 20 kV supply busbar.

A. Loss calculation of pumping unit UP1

The power required to drive the motor is $P_{M1} = 490{,}57$ kW (Table 4.19); Considering the motor efficiency $\eta_M = 0{,}91$ the motor's useful power output is $P_{M2} = 446{,}42$ kW, with motor losses of $\Delta P_M = 44{,}15$ kW.

The power at the input to the motor-pump coupling is $P_{cpm1} = 446{,}42$ kW; Given the coupling efficiency $\eta_{cpm} = 0{,}99$ the useful power transmitted through the coupling is $P_{cpm2} = 441{,}95$ kW, with losses in the coupling of $\Delta P_{cpm} = 4{,}46$ kW.

The power required to drive the pump is $P_{P1} = 441{,}95$ kW; For a pump efficiency $\eta_P = 0{,}73$ the useful power transmitted to the fluid is $P_u = 322{,}62$ kW, while the pump losses amount to $\Delta P_P = 119{,}32$ kW.

The pump's useful power, is the hydraulic power $P_u = P_{P2} = \rho \cdot q \cdot H \cdot Q$, s determined based on the hydraulic system operating parameters. For an hourly flow rate Q=291,5 m^3/h and pumping head H=410 m the useful power results in $P_u = 325{,}34$ kW.

The discrepancy $\Delta P_u = 2{,}72$ kW between the two approaches for determining the pump's useful power arises from the variability of the hydraulic parameters within the considered time interval.

This energy balance approach for pumping unit UP1 highlights all losses occurring along the supply chain of the Pump-Motor-Transformers system.

B. Calculation of Losses on the Power Supply Line of Pumping Unit UP1

In the case of supplying Pumping Unit UP1 from the Măgurele Pumping Station, it is necessary to determine the losses in the transformers and associated power supply lines.

The parameters of the power supply network are presented in Table 4.21.

Table 4.216. Technical Data for Transformers and Power Cables Associated with the Supply of Pumping Unit UP1

Technical Characteristics	Primary Voltage	Secondary Voltage	Rated Power	No-load Losses	Short-circuit Losses	U_0	Ik	Cable Type	Specific Resistance	Cable Cross-section	Cable Length
-	kV	kV	kVA	kW	kW	%	%	-	Ω/km	mm²	m
Tr1	20	6	1600	4,35	20,2	6	1,7	ACYABY	0,153	3x240 +120	10
Tr2	6	0,4	2000	2,9	16,5	6,5	0,54	CYABY	0,0754	2×3×240 +2×120	25

Pierderile de energie în transformator se determină cu relația:

$$\Delta E_T = (\Delta P_o + \beta^2 \cdot \Delta P_{sc}) \cdot \tau \quad (4.24)$$

Where: ΔP_0 – no-load losses in the transformer, ΔP_{sc} – short-circuit losses in the transformer, τ- time, β – transformer load factor, calculated using the relation:

$$\beta = k_f \cdot \frac{I_{med}}{I_n} \approx \frac{S}{S_n} \quad (4.25)$$

Where: I_{med} - the average value of the current intensity through the transformer, over the time interval corresponding to the reference duration of the energy balance, I_n - the rated current of the transformer and k_f - the form factor of the current variation

$$k_{f\_I} = \frac{I_{mp}}{I_{med}} = \sqrt{N} \cdot \frac{\sqrt{\sum_{i=1}^{N} I_i^2}}{\sum_{i=1}^{N} I_i} \quad (4.26)$$

Where: I_{mp} – the root mean square value of the current measured at the load end of the line;

I_{med} – the average value of the current measured at the supply end of the line; N – the number of equal time intervals at which current readings are recorded;

The electrical losses in the power supply cables are determined using the following relation:

$$\Delta E_L = 3 \cdot k_{fI}^2 \cdot I_{med}^2 \cdot R_L \cdot \tau \quad (4.27)$$

Where: τ - epresents the reference duration associated with the energy balance (in this case, one hour), R_L- the specific resistance of the line, calculated using the following relation:

$$R_L = r * L \quad (4.28)$$

Where: r- specific resistance [Ω/km], L- length [km];

The determination of hourly losses for each component within the energy balance boundary is presented below:

Power loss calculations for the 0.4 kv line

Considering the values: form factor $k_f = 1$, verage current intensity according to Table 4.21, $\tau = 1$ h and line resistance $R_L = 0{,}001885\ \Omega$, the resulting energy loss is: $\Delta E_{L0,4} = 3{,}01$ kWh.

Power loss calculations in transformer tr2

Considering the measured secondary current of the transformer $I_{TR2} = 729{,}6$ A and the load factor $\beta = 0{,}25$, the resulting energy loss in transformer TR2 is $\Delta E_{TR2} = 3{,}95$ kWh

Power loss calculations for the 6 kv line

Considering the values: $k_f = 1$, the primary current of transformer TR2 calculated as $I_{1\,tr2} = \frac{I_{2\,tr2} \cdot U_{2\,tr2}}{U_{1\,tr2}}$ =48,64 A, $\tau = 1$ h and $R_L = 0{,}00153$ the resulting energy loss is: $\Delta E_{L0,4} = 0{,}01$kWh.

Power Loss Calculations in Transformer TR1

Considering the measured secondary current $I_{TR2} = 48{,}64$ A and the load factor $\beta = 0{,}31$, r loss in transformer TR1 is $\Delta E_{tr1} = 6{,}36$ kWh

C. Preparation of the Hourly Energy Balance for Pumping Unit UP1

Table 4.23 presents the hourly energy balance for Pumping Unit UP1 from the Măgurele Pumping Station, based on the measurements taken on January 21, 2020.

Table 4.23. Hourly energy balance for the UP1 pumping unit

Symbol	Balance Component	Energy and Losses [kWh]	Energy [%]	Losses [%]
Ei	Energy input at 20 kV in transformer Tr1	503,90	100	-
ΔE_{Tr1}	Loss in transformer Tr1 (U=6/20 kV, S=1600 kVA)	6,36	-	1,2622
$\Delta E_{l\,6}$	Loss in 6 kV line (ACYABY 3x240 + 120 mm², l=10m)	0,01	-	0,0020
Ei_{Tr2}	Energy input at 6 kV in transformer Tr2	497,53	98,7359	-
ΔE_{Tr2}	Loss in transformer Tr2 (U=0.4/6 kV, S=2000 kVA)	3,95	-	0,7839
$\Delta E_{l\,0,4}$	Loss in 0.4 kV line (2 x CYABY 3x240 + 120 mm²)	3,01	-	0,5973
Ei_M	Energy input into drive motor	490,57	97,3546	-
ΔE_M	Loss in motor	44,15	-	8,7617
Ei_{cmp}	Energy input into motor-pump coupling	446,42	88,5930	-
ΔE_{cmp}	Loss in motor-pump coupling	4,46	-	0,8851
Ei_p	Energy input at pump shaft	441,96	87,7079	-
ΔE_p	Loss in pump	119,32	-	23,6793
Eu	Useful energy	322,64	64,0286	-

In Fig. 4.29 the graph with the hourly energy balance for the pumping unit UP1 is represented

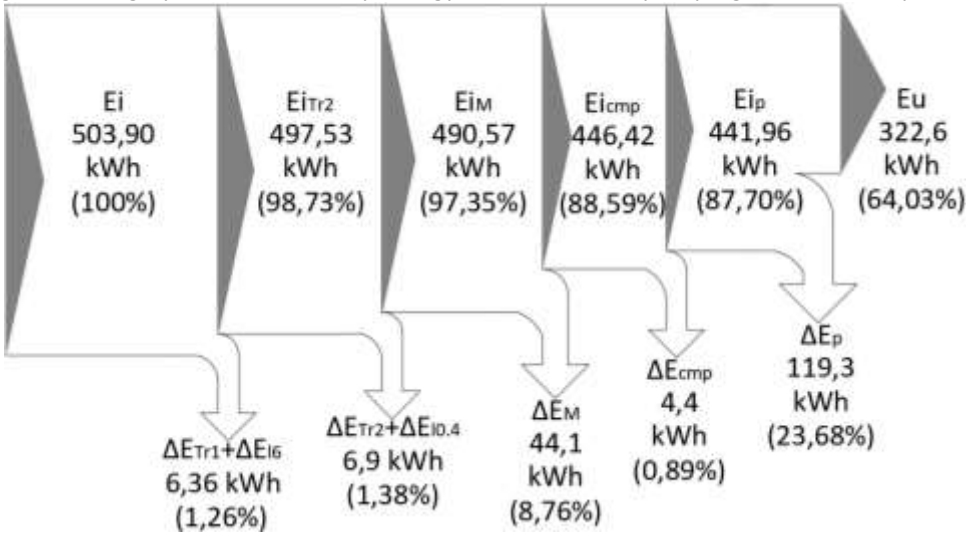

Fig. 4.293. Hourly energy balance graph for pumping unit UP1

D. Findings and Discussions:

The analysis of the results indicates that the useful energy output represents 64.03% of the total energy consumption of pumping unit UP1, while the associated energy losses are substantial: 23.68% occur within the pump (primarily due to hydraulic inefficiencies), 8.76% are attributed to the electric motor (electromagnetic and thermal losses), and 2.64% arise from the power supply network, including transmission lines and transformers. In order to mitigate these losses at the Măgurele Pumping Station, the following technical measures are recommended: optimization of the pump's operating regime to ensure operation near its Best Efficiency Point (BEP), thereby improving hydraulic performance; revision and enhancement of maintenance procedures, aimed at minimizing mechanical wear and reducing internal leakage losses; technical assessment for potential replacement of the motor with a high-efficiency class unit (e.g., IE4 or superior), to improve electrical-to-mechanical conversion efficiency; optimization of the electrical supply topology, through reconfiguration or upgrading of power transformers and conductors, to reduce resistive losses and enhance power quality delivered to the pumping unit..

4.5. Proposals regarding the use of numerical simulation for the evaluation of energy efficiency in water pumping stations

4.5.1. Strategies for loss analysis using NEPLAN software

Numerical simulation tools are essential for the analysis, optimization, and design of power systems, offering both technical and economic support for the safe and efficient operation of transmission, distribution, and industrial supply networks. In this study, the NEPLAN platform was employed, which integrates advanced modules for simulating the operation and protection of complex power supply systems. NEPLAN enables power flow analysis under both balanced and unbalanced three-phase operating conditions, with capabilities for optimizing network topology and energy distribution in order to reduce technical losses.

The case study conducted at the Măgurele Pumping Station focuses on optimizing the electrical power supply to pumping units UP1 and UP2, with the objective of minimizing energy losses.

On Line I, following the Tr1 transformer (20/6 kV, rated power Sn = 1600 kVA, manufactured by Electroputere Craiova), the Tr2 transformer (6/0.4 kV) was integrated to supply both pumping units (UP1 and UP2) at a voltage level of 0.4 kV. On Line II, the Tr3 transformer (20/0.4 kV) provides electricity for auxiliary systems: central heating (24 kW), lighting (4 kW), and computing systems (2 kW).

The technical specifications for transformers Tr1 and Tr2 are provided in Table 4.21, while the characteristic technical data for transformer Tr3 and the associated supply cables for Line II are presented in Table 4.22.

Table 4.22. Technical Data for Transformer Tr3 and the Associated Power Cables of Line II

Technical Characteristics	Primary Voltage	Secondary Voltage	Rated Power	No-load Losses	Short-circuit Losses	U_0	Ik	Cable Type	Specific Resistance	Cable Cross-section
-	kV	kV	kVA	kW	kW	%	%	-	mm²	m
Tr3	20	0,4	1600	4,35	20,2	6,0	1,7	CYABY	3×240+120	20

The proposed configurations for the analysis of the electrical power supply system of the Măgurele Pumping Station are as follows:

- Configuration 1: Current situation – pumping units UP1 and UP2 are powered via Line I, while the auxiliary services are supplied through Line II (as illustrated in Fig. 4.31);
- Configuration 2: Pumping units UP1 and UP2, together with the auxiliary services, are supplied entirely from Line I, by implementing a longitudinal coupling at the 0.4 kV level;
- Configuration 3: Pumping units UP1 and UP2, along with the auxiliary services, are fully supplied from Line II, using the longitudinal coupling at the 0.4 kV level;
- Configuration 4: Pumping units UP1 and UP2 and the auxiliary services are powered entirely from Line II (via longitudinal coupling at 0.4 kV), with an additional integration of a renewable energy source on the 0.4 kV busbar to provide supplemental power to the electrical loads.

4.5.2. Determining Power Flow and Losses Using NEPLAN Software

Configuration 1

In Figure 4.31, the configuration illustrates that the power supply to pumping unit UP1 is achieved from the 20 kV busbar via transformer Tr1 (20/6 kV), followed by transformer Tr2 (6/0.4 kV). The 0.4 kV bus-tie (longitudinal coupling) is kept open, ensuring galvanic separation between the two power supply sources. The auxiliary services (internal loads) are independently supplied through Line II, from the 20 kV busbar via transformer Tr3 (20/0.4 kV).

The simulation was carried out under an operational regime in which the asynchronous motor of pumping unit UP1 is supplied with a power of 500 kW. In the same scenario, the auxiliary services were modeled with a constant power demand of 30 kW, corresponding to the estimated energy requirements for lighting, control systems, automation, and other internal processes of the station.

Figure 4.32 presents the simulation results obtained using NEPLAN software, showing the power flow distribution and technical losses in the system, under the conditions defined for Configuration 1

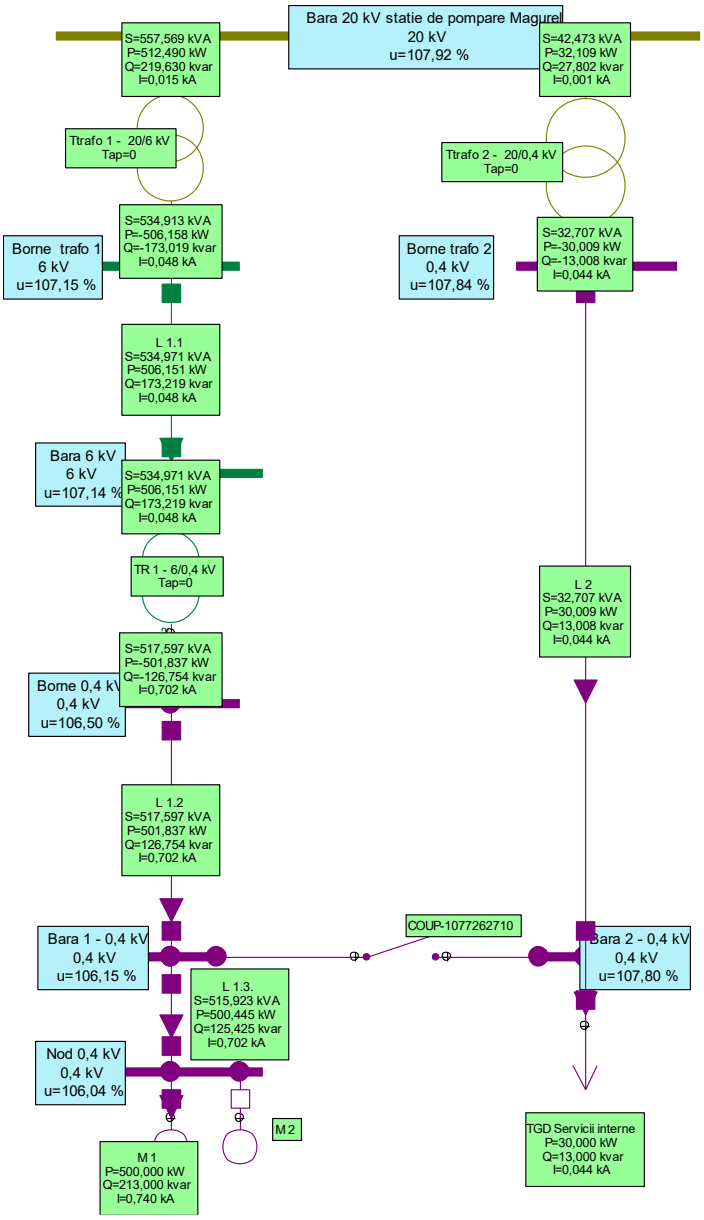

Fig. 4.32. Configuration 1 – Results in NEPLAN for Power Flow and Losses

Configuration 2

Fig. 4.34 illustrates the results obtained using the NEPLAN software for power flow and losses in each individual component of the power supply chain for the pumping unit UP1 and for the Auxiliary Services.

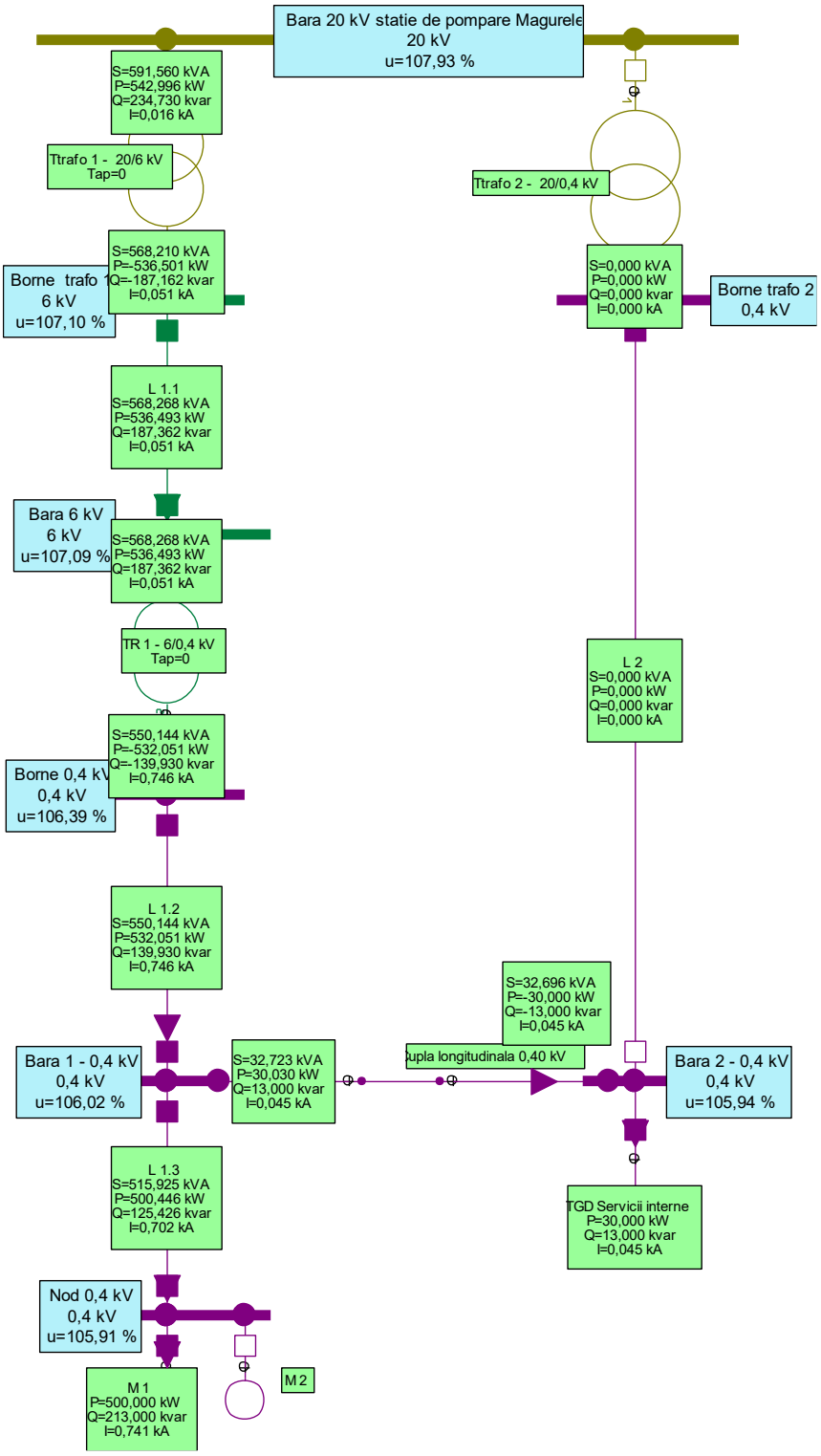

Fig. 4.34. Configuration 2 – Results in NEPLAN for Power Flow and Losses

Configuration 3

Fig. 4.36 illustrates the results obtained with the NEPLAN software for power circulation and losses in each component element of the power supply chain of the UP1 pumping unit and for internal services.

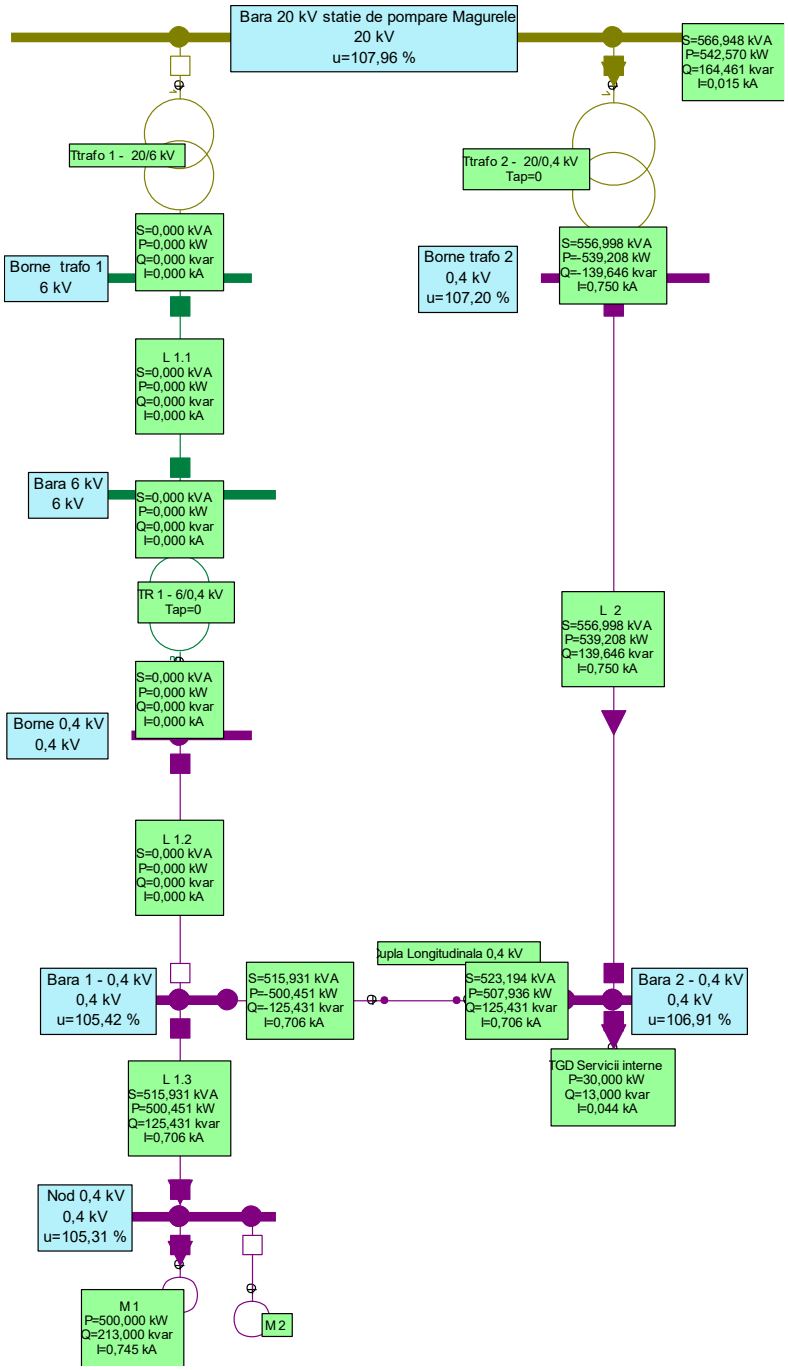

Fig. 4.36. Configuration 3 – Results in NEPLAN for Power Flow and Losses

Configuration 4

In Fig 4.37, the configuration is illustrated in which the power supply for the pumping unit and Internal Services is provided exclusively through Line II, with the bus-tie at the 0.4 kV bars closed, ensuring full system connectivity. The circuit breaker of transformer Tr1 is open, effectively disconnecting Line I from the power supply scheme. In this setup, a renewable energy source—specifically a photovoltaic generator (ACGENC-1077261555)—is integrated at the 0.4 kV bus, modeled within the NEPLAN platform.

This renewable source contributes to supplying local loads and enhances power continuity in the event of a failure of the main source, thereby improving the system's sustainability and reliability. The active power

generated was defined according to the technical specifications of the source, with the exact output value determined through simulation.

In Fig 4.38, the results obtained using NEPLAN are presented, showing the power flow and losses across each component of the power supply chain for pumping unit UP1 and Internal Services.

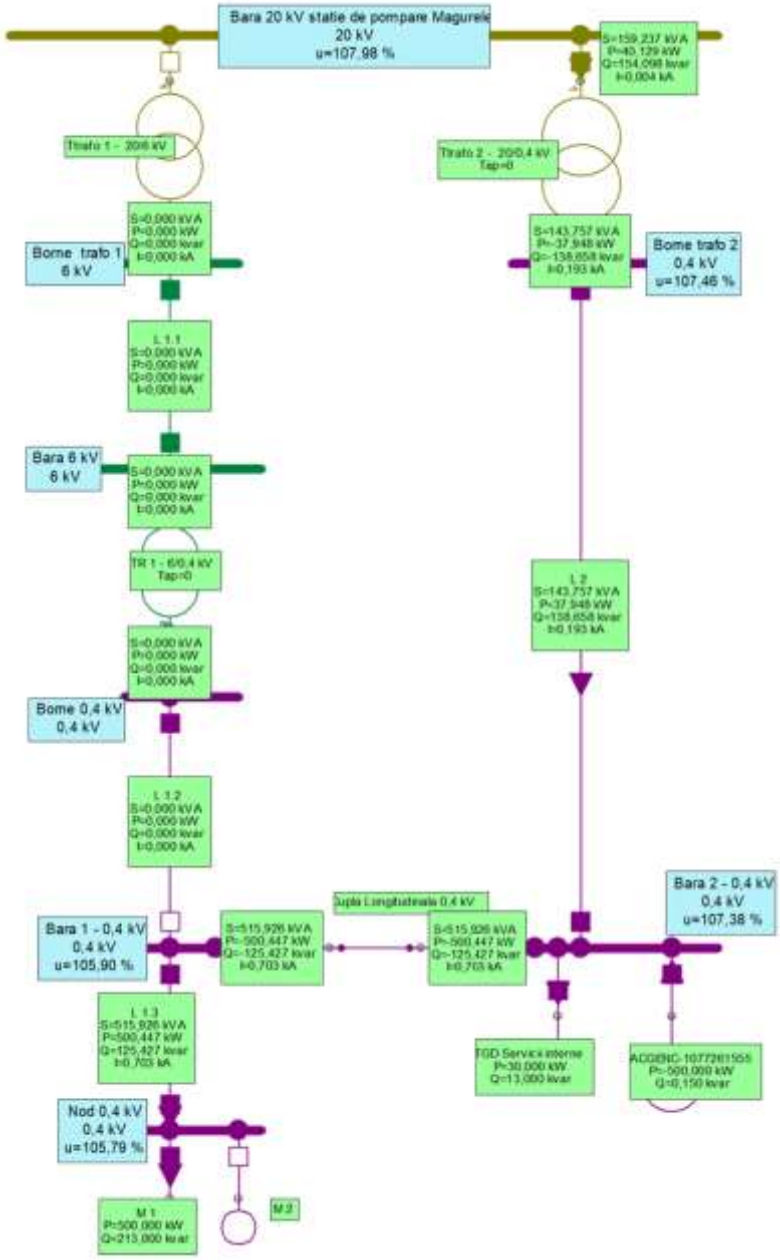

Fig. 4.38. Configuration 4 – Results in NEPLAN for Power Flow and Losses

4.5.3 Analysis and Recommendations

In Fig 4.32, 4.34, 4.36, and 4.38, the results obtained from NEPLAN simulations for the four configurations proposed in Section 4.5.1 are illustrated. These results highlight the electrical losses occurring in the transformers and supply lines feeding the pumping units UP1, UP2, and the internal services of the Măgurele Pumping Station.

Table 4.24 presents the consolidated values derived from the four simulation scenarios, emphasizing the key parameters related to energy consumption and losses for each proposed power supply configuration of the Măgurele Pumping Station.

Table 4.247. Numerical simulation results

Hourly Balance Components	Configuration 1	Configuration 2	Configuration 3	Configuration 4
20 kV Network Energy [kWh]	544,599	542,996	542,570	40,129
Renewable Energy Source [kWh]	0	0	0	500
Input Energy [kWh]	544,599	542,996	542,57	540,129
Transformer Losses [kWh]	12,746	10,937	6,362	2,181
Line Losses [kWh]	1,853	2,059	6,208	0
Renewable Source Losses [kWh]	0	0	0	7,948
Required Energy [kWh] (motors + internal services)	530	530	530	530

The comparative analysis of the four configurations for the power supply of the Măgurele Pumping Station reveals significant differences in terms of energy efficiency, loss distribution, and energy sourcing, all evaluated over a standardized one-hour operation period.

Configuration 1, supplied from the medium-voltage network via Line I and Line II through transformers Tr1–Tr3, incurs the highest transformer losses (12.746 kWh) and results in the lowest energy efficiency.

Configuration 2, in which both pumping units and auxiliary services are supplied exclusively from Line I via transformers Tr1 and Tr2, reduces transformer losses to 10.937 kWh. However, it slightly increases the distribution line losses to 2.059 kWh, yielding a marginal overall improvement in energy efficiency.

Configuration 3, which relies solely on Line II and transformer Tr3 for powering the entire installation, achieves the lowest transformer losses (6.362 kWh). Nonetheless, it leads to significantly higher line losses (6.208 kWh), primarily due to extended cable lengths and possible overload conditions.

Configuration 4, combining supply from Line II and transformer Tr3 with the integration of a 500 kW renewable energy source connected to the 0.4 kV busbar, significantly decreases grid dependency—drawing only 40.129 kWh from the network—and maintains a total input energy of 530 kWh. This setup registers the lowest transformer losses (2.181 kWh), zero line losses, and limited losses associated with the renewable energy system (7.948 kWh).

This final configuration stands out as the most energy-efficient and sustainable solution, substantially reducing reliance on the conventional grid while optimizing operational performance and minimizing technical energy losses.

A comparative representation of energy losses in lines and transformers is shown in Fig. 4.39:

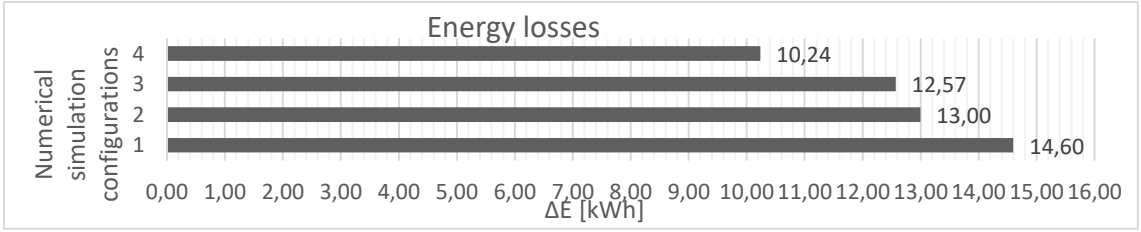

Fig. 4.39. Consolidated losses for the four numerically simulated configurations

The loss values decrease progressively from Configuration 1 (14.60 kWh) to Configuration 4 (10.24 kWh), indicating an improvement in energy efficiency as the network configuration is optimized and renewable energy sources are integrated. Configuration 4 exhibits the lowest total losses, thus representing the most energy-efficient solution. However, from the standpoint of technical feasibility and infrastructure

requirements, Configuration 3 emerges as the most easily implementable option, requiring minimal structural modifications.

Following the determination of specific hourly losses through simulations performed using NEPLAN, an estimated calculation of monthly and annual energy losses was conducted for each power supply configuration of the Măgurele Pumping Station. These values were derived by correlating hourly losses with the actual number of operational hours of pumping units UP1/UP2 during the year 2024, based on the aggregated data provided in Table 4.9. The resulting figures for each simulated operating regime are presented in Table 4.25:

Table 4.25. Estimated losses based on simulations in Neplan

Configuration	Operating hours	Hourly losses	Total losses [kWh]	Savings [kWh]
1	2428	14,60	35448,80	-
2		13,00	31564,00	3.884,80
3		12,57	30519,96	4.928,84
4		10,24	24862,72	10.586,08

Interpretation of the results obtained from the energy analysis of the four electrical supply configurations for the Măgurele Pumping Station reveals significant differences in total energy losses and in the potential energy savings associated with each configuration, considering an annual operational duration of 2,428 hours.

Configuration 1, used as the reference scenario, records the highest losses, totaling 35,448.80 kWh/year. In comparison, Configuration 3, based on exclusive supply via Line II through transformer Tr3, reduces losses to 30,519.96 kWh/year, resulting in a saving of 4,928.84 kWh. This option provides a favorable compromise between energy loss reduction and implementation requirements, as it entails minimal intervention on the existing infrastructure, and is therefore recommended for adoption in an initial phase.

In the long term, Configuration 4, which integrates a renewable energy source, enables a reduction in losses to 24,862.72 kWh/year, ensuring a total saving of 10,586.08 kWh compared to the reference scenario. This confirms the strategic potential of renewable sources in enhancing energy efficiency and reducing dependency on the conventional grid.

The results are based on numerical simulations and are to be interpreted as estimates. Further improvements in the energy efficiency of the Măgurele Pumping Station can be achieved through operational optimization, reduction of partial load conditions, implementation of predictive maintenance, and adoption of intelligent energy management strategies. Consequently, the adoption of Configuration 3 as an intermediate solution, followed by a transition to Configuration 4, may constitute a sustainable and energy-efficient long-term strategy.

4.6. Conclusions

The overall efficiency of the pumping unit is determined by the product of the efficiencies of its components—pump, electric motor, coupling, frequency converter, and transformer—typically ranging between 85% and 99%, depending on the specific equipment used.

The optimization of the energy conversion chain, through the implementation of high-efficiency motors, low-loss couplings, and variable frequency drives (VFDs), has resulted in a significant reduction in energy losses and a corresponding increase in energy efficiency by adapting the rotational speed to the hydraulic requirements.

The hourly energy balance for UP1 indicates that the useful energy accounts for 64.02% of the electrical energy input, with losses distributed as follows: 23.67% in the pump, 8.76% in the electric motor, and 2.64% in the supply infrastructure (cables and transformers).

The operational regime recorded in 2024 was characterized by an average monthly usage of 202.33 operating hours and 529.66 idle hours, indicating a substantial potential for optimizing operational scheduling.

During peak season, the energy intensity exceeded the thresholds recommended by European standards (0.6–1.6 kWh/m³) and the International Water Association (IWA), highlighting the necessity for upgrading installations and implementing advanced pressure control mechanisms.

Numerical simulations conducted using NEPLAN software supported several key measures, including adjusting pump operation to its optimal efficiency point, enhancing predictive maintenance strategies, replacing motors with IE3/IE4 efficiency class equipment (offering potential energy savings of up to 8.7%), and integrating renewable energy sources into the electrical supply scheme.

The conclusions underscore the importance of an integrated approach to the energy optimization of pumping systems and highlight the tangible impact of targeted interventions on the performance and sustainability of the water supply infrastructure.

5. Final Conclusions on the Research, Scientific Contributions, Applicability of Results, and Future Development Perspectives

5.1. Final Conclusions

This chapter presents the general conclusions derived from the research, highlighting the extent to which the thesis objectives have been achieved and the contribution made to the field of performance monitoring and control in urban drinking water supply systems. The conclusions synthesize the analyses conducted throughout each chapter, integrating technological, energy-related, and management aspects identified as essential for optimizing the operation of these systems in the context of the energy transition and sustainable development. The following sections detail the main conclusions corresponding to each stage of the research.

Chapter 2

The analysis conducted in Chapter 2 highlighted the essential role of urban drinking water supply systems in ensuring sustainable development, public health, and the efficient functioning of cities. These systems have evolved from rudimentary structures into integrated, automated, and digitized networks, responding to the current demands of urban environments.

The operation of such systems requires compliance with fundamental criteria: source security, water quality, service continuity, energy efficiency, risk resilience, and the integration of smart technologies. Today, they face major challenges, including infrastructure degradation, hydraulic losses, source pollution, accelerated urbanization, and the impact of climate change. These issues call for sustainable technological solutions and integrated management strategies.

The interdependence between water and energy consumption—commonly referred to as the Water-Energy Nexus—emphasizes the need for synergistic approaches that incorporate renewable sources, water–energy microgrids, and advanced analytical tools for optimizing resource use and reducing environmental impact.

Environmental policies and the ongoing energy transition support digitalization, recycling, and carbon footprint reduction, thus enhancing the resilience of critical infrastructures. SCADA technologies, IoT, and AI enable real-time monitoring, consumption optimization, and adaptive management under the dynamic conditions of urban settings.

Looking ahead, the adoption of an integrated governance framework and intersectoral cooperation is imperative, focusing on strategic planning, sustainable investment, and the application of circular economy principles in resource management.

Some of the conclusions of this study have been disseminated through relevant scientific publications, contributing to the advancement of knowledge in the field of urban water supply systems. In conclusion, the modernization of these systems requires a holistic approach grounded in sustainability, energy efficiency, and innovation to ensure resource security and improve the quality of urban life.

Chapter 3

Chapter 3 focuses on the analysis of modern solutions for monitoring, control, and performance evaluation of urban drinking water supply systems, with a particular emphasis on the use of specific performance indicators, the integration of SCADA technologies, the application of energy efficiency strategies, and the development of relevant applied studies.

The research highlights the need for an integrated framework based on continuous monitoring, intelligent control, and efficient energy management tailored to local operational conditions.

(1) The definition and use of a structured set of performance indicators (technical, operational, financial, and service quality) are essential for the objective assessment of urban water networks. The application of IWA standards supports benchmarking and informs strategic decision-making.

(2) The implementation of SCADA systems brings significant benefits, enabling continuous supervision, rapid intervention, and predictive maintenance. Integration with IoT technologies and analytical algorithms enhances the ability to anticipate malfunctions and optimize resource use.

(3) The chapter proposes a set of specific energy indicators (such as energy intensity, active power, and reactivity index), which facilitate the identification of loss sources and the optimization of energy consumption, contributing to carbon footprint reduction.

(4) The importance of a multidimensional approach that correlates technical, economic, social, and environmental performance is emphasized. Methods such as the Analytic Hierarchy Process (AHP) can be used to prioritize interventions based on their overall impact.

(5) The evaluation of the firefighting water supply network highlights the importance of continuous monitoring and rigorous maintenance. Proposed indicators (e.g., consumption levels, duration of use, and specific consumption) support the proper planning of emergency infrastructure.

(6) Case studies reinforce the conclusions: water quality analysis in Brașov confirms compliance with standards; evaluation of hydrant consumption reveals the need for seasonally adapted management; comparative analysis of pumping stations (with and without variable speed drives) demonstrates the superior energy efficiency of VSD technologies.

(7) The research findings have been disseminated in reputable scientific publications, underscoring the relevance and applicability of the conclusions drawn.

Overall, the chapter offers substantial contributions toward the implementation of integrated and sustainable management for urban water systems, emphasizing the essential roles of digitalization, energy efficiency, and infrastructure security in supporting sustainable development and urban resilience.

Chapter 4

Chapter 4 presents the practical contributions to increasing energy efficiency in pumping stations of urban water supply systems, based on analyses and calculations performed using real experimental data, partly provided by the network operator in the Brașov area and partly obtained through direct field measurements. These measurements were affected by technical and organizational difficulties, including limited access to infrastructure and equipment.

The main conclusions are:

(1) The energy flow analysis highlighted the central role of pumping stations in energy consumption, emphasizing that overall efficiency is determined by the performance of each component: transformer, motor, frequency converter, mechanical coupling, and pump. Their correct selection and configuration directly contributes to reducing energy consumption.

(2) The performance of centrifugal pumps is optimal at the peak efficiency point on their performance curve. Deviations from this point lead to hydraulic and electrical losses. Control through variable frequency drives (VFDs) has proven superior to traditional regulation methods, significantly reducing energy losses.

(3) Electricity quality measurements at the Măgurele station showed stable electrical parameters, but highlight the need for continuous monitoring, as fluctuations can affect equipment performance and durability.

(4) The case study carried out at the Măgurele station (which serves Poiana Brașov) showed that technological modernization through the introduction of high-efficiency pumps and soft-starter motors led to an increase in pumping height, a reduction in losses, and a decrease in specific energy consumption.

(5) Data collected through SCADA enabled the identification of areas with losses and underperformance, leading to concrete recommendations: replacement of obsolete equipment and use of intelligent flow and speed control.

(6) Studies on motors and converters demonstrated the advantages of IE3 and IE4 technologies, which offer considerable energy savings and reduced carbon emissions, supporting the strategic importance of modernization.

(7) Analysis of transformers indicated that, particularly in partial load conditions, losses become significant, recommending the use of efficient and well-sized transformers.

(8) The problems encountered during the measurements confirm the need for efficient data collection procedures and the implementation of automated monitoring systems to increase accuracy and facilitate operational decision-making.

In conclusion, the chapter confirms the strategic importance of technological modernization, high-performance equipment, and advanced monitoring for achieving sustainable energy consumption. The results provide a solid basis for replicating these interventions in other urban networks, promoting responsible and efficient management of energy resources in the water supply sector.

5.2. Scientific Contributions and Original Elements brought by the research

The original contributions of this PhD thesis are defined by an applied and integrated approach to the energy and functional optimization of urban water supply systems, with a particular focus on pumping station infrastructure. The main elements of originality include:

The central aspect of the research lies in the definition and application of an extended set of specific energy indicators, developed within the case study “Energy Efficiency and Specific Indicators”. These indicators enable a rigorous assessment of energy performance across infrastructure components. They contribute to quantifying energy consumption and identifying areas with optimization potential, supporting the transition toward more energy-efficient operations.

A significant original element is the formulation and implementation of a set of operational indicators for evaluating the performance of the external hydrant network, which is particularly relevant in emergency intervention contexts. These indicators allow for the assessment of specific water consumption for firefighting, the estimation of the theoretical usage time of hydrants, and the optimization of their spatial distribution.

An integrated methodological framework was developed for monitoring the performance of urban water supply systems, using standardized indicators in accordance with IWA methodology and WAREG regulations. This framework facilitates the correlation between technical, energy, economic, and social efficiency, and supports both strategic and operational decision-making processes.

A dynamic predictive model was proposed and validated to estimate energy consumption in pumping stations, specifically applied to the Măgurele station. The model integrates hydraulic, energy, and operational data, allowing the simulation of station behavior under variable operating regimes and the identification of optimal operational scenarios.

These contributions provide both theoretical advancements and practical tools for improving the energy performance and resilience of critical urban infrastructure.

A detailed assessment was carried out to quantify energy losses across the entire conversion chain—from the electrical power supply to the delivery of hydraulic energy. The analysis included losses in the electric

motor, frequency converter, mechanical coupling, and piping system, offering a comprehensive view of the critical points that require intervention to enhance overall efficiency.

Technical solutions were proposed for the modernization of pumping stations, including the replacement of existing equipment with higher-efficiency class alternatives and the integration of frequency converters. These allow pump speeds to be adjusted according to flow and pressure demand, thereby reducing energy losses and operational costs.

The SCADA system was integrated into the monitoring and control process, ensuring continuous recording of energy and hydraulic parameters, early anomaly detection, and proactive intervention in the event of malfunctions. This significantly contributes to improved reliability and operational safety.

Overall, the thesis enhances the performance of urban water supply systems within the context of the energy transition through a scientific approach grounded in systemic analysis, operational modeling, and digital technology integration. The objectives related to the characterization of critical infrastructure, advanced monitoring, energy efficiency improvement, and integrated management optimization are achieved through rigorous quantitative evaluations and representative case studies.

Through these contributions, the thesis provides relevant and applicable solutions in the fields of electrical engineering and critical infrastructure management, supporting energy optimization, increased resilience, and the promotion of sustainable development in urban water supply systems.

5.3 Valorization of Research Results

The outcomes of this research have been disseminated through scientific conferences and specialized publications, contributing to the expansion of knowledge in the field of sustainable water infrastructure management and to the promotion of technological innovation in essential public service systems.

5.4 Future Research Directions

This work opens significant avenues for future research, including: the integration of artificial intelligence and machine learning technologies into diagnostic processes and operational optimization, the correlation of SCADA data with spatial (GIS) information for risk management and infrastructure planning, the evaluation of climate change impacts on water system performance, and the extended integration of renewable energy sources into urban infrastructures, with the aim of reducing energy dependence and enhancing long-term sustainability

Selected papers from the reference list:

- Cojanu, V., & Helerea, E. (2021). From the history of urban water supply systems and future challenges. AGIR Bulletin, 1(2021), January-March. Retrieved from https://www.agir.ro/buletine/3209.pdf
- Cojanu, V., & Helerea, E. (2020, March). Applying the mathematical optimization model in water distribution management. In IOP Conference Series: Materials Science and Engineering (Vol. 789, No. 1, p. 012011). IOP Publishing
- Popov, A., Fratu, A., Lepadat, I., Helerea, E., & Cojanu, V. (2019). Monitoring the cost of energy for powering the railway electric traction system. In 8th International Conference on Modern Power Systems (MPS), Cluj-Napoca, Romania, pp. 1-6. https://doi.org/10.1109/MPS.2019.8759724
- Helerea, E., Cojanu, V., & Călin, M. D. (2022). Interconnectivity between energy and water supply systems. Journal of Engineering Sciences and Innovation, 7(2), 263-278. https://doi.org/10.56958/jesi.2022.7.2.263
- Cojanu, V., & Helerea, E. Considerations on the efficient functioning of urban water pumping stations. In IOP Conference Series: Materials Science and Engineering (Vol. 1138, No. 1, p. 012017). IOP Publishing
- Picazo, M. Á. P., & Tekinerdogan, B. (2024). Urban water distribution networks: Challenges and solution directions. In Management and Engineering of Critical Infrastructures (pp. 245-264). Academic Press
- United Nations. (2020). World water development report 2020: Water and climate change. UNESCO. https://www.unesco.org
- United Nations, Department of Economic and Social Affairs. (2019). World population prospects 2019, volume II. https://population.un.org/wpp/
- World Bank. (2018). The role of infrastructure in meeting water challenges. https://www.worldbank.org

- UNESCO. (2019). The United Nations world water development report 2019: Leaving no one behind. https://www.unesco.org
- IPCC. (2021). Climate change 2021: The physical science basis. https://www.ipcc.ch
- FAO. (2021). The state of food and agriculture 2021. https://www.fao.org
- WHO & UNICEF. (2021). Progress on drinking water, sanitation and hygiene: 2021 update and SDG baselines. https://www.who.int
- United Nations Water. (2020). Water and climate change. https://www.unwater.org
- Ritchie, H., & Roser, M. (2024). Water use and stress. Our World in Data. https://ourworldindata.org/water-use-stress
- Helerea, E., Calin, M. D., & Musuroi, C. (2023). Water-energy nexus and energy transition—A review. Energies, 16(4), 1879. https://doi.org/10.3390/en16041879
- Ahmad, S., Jia, H., Chen, Z., Li, Q., & Xu, C. (2020). Water-energy nexus and energy efficiency: A systematic analysis of urban water systems. Renewable and Sustainable Energy Reviews, 134, 110381
- Li, Q., Yu, S., Al-Sumaiti, A. S., & Turitsyn, K. (2019). Micro water–energy nexus: Optimal demand-side management and quasi-convex hull relaxation. IEEE Transactions on Control of Network Systems, 6(4), 1313-1322. https://doi.org/10.1109/TCNS.2019.2932915
- Yu, R., Wang, Y., Zhang, H., & Tang, S. (2018). A hybrid approach for water-energy nexus optimization in urban water distribution systems. Applied Energy, 230, 531-541. https://doi.org/10.1016/j.apenergy.2018.08.150
- IPCC. (2023). Climate change 2023: Synthesis report. https://www.ipcc.ch/report/ar6/syr/
- Dumitrescu, D. G., Horobeț, A., Tudor, C. D., & Belaşcu, L. (2023). Renewables and decarbonization: Implications for energy policy in the European Union. Amfiteatru Economic, 25(63), 345-361
- Adamos, G., et al. (2023). Exploring nexus policy insights for water-energy-food resilient communities. Sustainability Nexus Forum, 31(69–82). https://doi.org/10.1007/s00550-024-00534-0
- FAO. (2021). The state of food and agriculture: Making agri-food systems more resilient. https://www.fao.org/state-of-food-agriculture/en/
- World Economic Forum (WEF). (2022). The future of nature and business. https://www.weforum.org/reports/the-future-of-nature-and-business
- European Commission. (2021). Fit for 55: Delivering the EU's 2030 Climate Target on the Way to Climate Neutrality. https://ec.europa.eu/clima/eu-action/fit-55_en
- European Commission. (2020). A European Green Deal. https://ec.europa.eu/clima/eu-action/european-green-deal_en
- Lodge, J. W. (2024). Modelling the availability of water, energy, and food resources. UNSW Sydney
- Cornea, V. (2024). Sustainable Development. Presa Universitară Clujeană
- Aziz, K. M. A., et al. (2025). Integrating digital mapping technologies in urban development. Alexandria Engineering Journal, 116, 512–524. https://doi.org/10.1016/j.aej.2024.12.078
- Ramos, H. M., et al. (2024). Energy transition in urban water infrastructures. Water, 16(504). https://doi.org/10.3390/w16030504
- Wang, H., et al. (2024). Sustainable energy transition in cities. Sustainable Cities and Society, 107, 105434. https://doi.org/10.1016/j.scs.2024.105434
- Javan, K., et al. (2024). Water–energy–food nexus: Urban pollution perspective. Science of the Total Environment, 912, 169319. https://doi.org/10.1016/j.scitotenv.2023.169319
- IWA. (2016). Performance Indicators for Water Supply Services: Manual of Best Practice (3rd ed.). IWA Publishing
- WAREG. (2023a). Analysis of Water Efficiency KPIs in WAREG Member Countries
- WHO. (2017). Guidelines for Drinking-water Quality: Fourth Edition Incorporating the First Addendum
- EEA. (2019). Water Resources Across Europe - Confronting Water Stress: An Updated Assessment
- Nowtricity. (n.d.). Romania electricity profile. https://www.nowtricity.com/country/romania/
- Cherdantseva, Y., et al. (2016). A review of cybersecurity risk assessment methods for SCADA systems. Computers & Security, 56, 1-27
- Nogueira, M., et al. (2020). A review of SCADA systems: State of the art, challenges, and possible solutions. IEEE Access, 8, 159358-159376
- El-Seidy, M. M., et al. (2021). A comprehensive review of SCADA systems. IEEE Access, 9, 13287-13305
- Georgescu, S.-C., & Georgescu, A.-M. (2014). EPANET Manual. Bucharest: Printech Publishing
- Chitale, S. K., et al. (2021). Parameters affecting efficiency of centrifugal pumps: A review. IJSRST, 8(6), 49–58. https://doi.org/10.32628/IJSRST21857